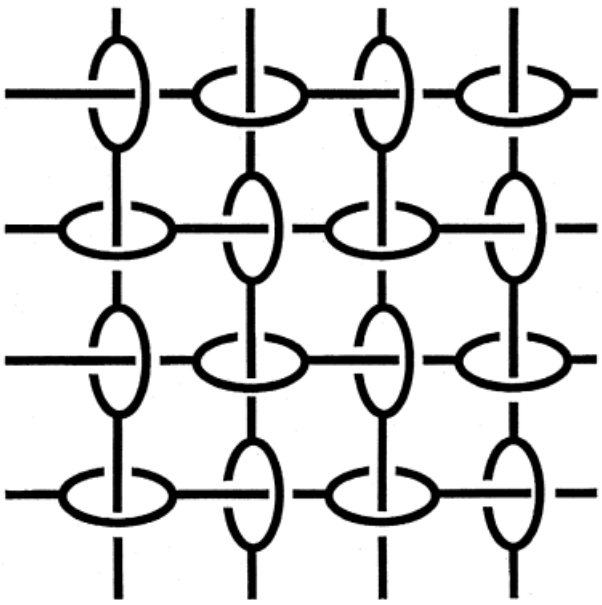

one-dimensional

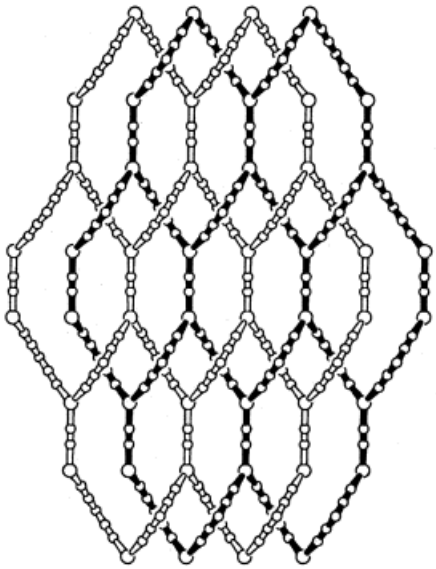

two-dimensional
parallel

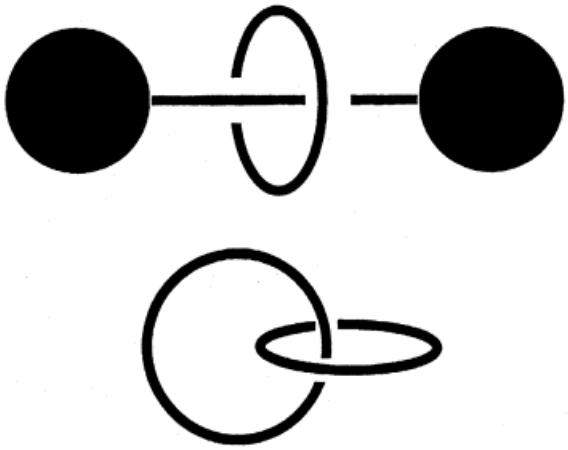

zero-dimensional

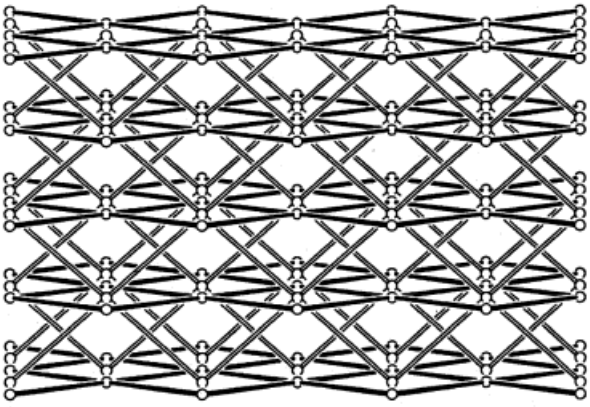

two-dimensional
inclined

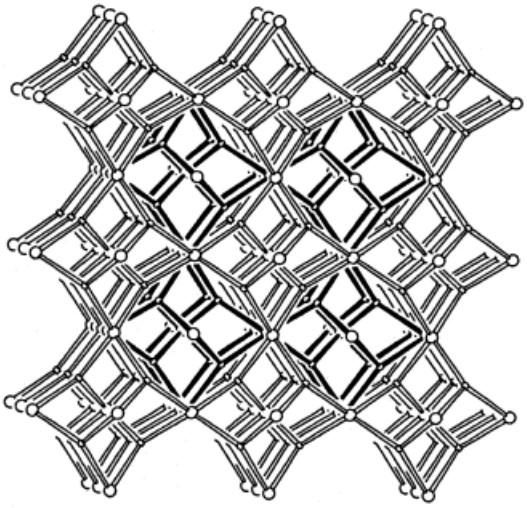

three-dimensional

Interpenetrating Nets: Ordered, Periodic Entanglement

Stuart R. Batten and Richard Robson*

Taking inspiration from the examples biology provides for the organization of simple units into a vast range of intricate and beautiful structures with complex and wonderfully efficient functions, many chemists have been turning their attention to the deliberate design of self-assembling aggregates of molecular building blocks with some specific structural or functional purpose in mind. This is supramolecular chemistry. It embraces systems ranging upwards in size and complexity to include infinite solid arrays. Molecular entanglement is common in biology. Entanglement that is inextricable, in the sense that disentanglement can be achieved only by breaking internal connections, has been one of the major themes of supramolecular chemistry. Such inextricable entanglements—as seen in catenanes, rotaxanes, and molecular knots—have provided a long-standing fascination for chemists, and many beautiful examples of ingenious design have been constructed. In the area of solids, the deliberate control of structure, and therefore properties and function, is a long-term objective being vigorously pursued by numerous groups. Increasingly, solid structures are being invented and created rather than discovered. The potential for technologically useful electronic, optical, electrochemical, and catalytic applications is an obvious driving force for much of this work, but the area is also of great fundamental structural interest and importance. Framework solids, which are often accessible by self-assembly under exceedingly mild conditions, are particularly attractive in this context because of their chemical and structural diversity and aesthetic appeal and because of the control potentially achievable in their construction. One aspect of framework solids which becomes increasingly apparent as more of them are discovered or invented is their tendency to form entangled structures in which two or more independent infinite networks interpenetrate each other. Polycatenane or polyrotaxane associations are an inherent feature of these structures. Examples of interpenetration were relatively rare until recently, but they are now being reported with increasing frequency. This is an opportune time to review this expanding area.

Keywords: coordination polymers · interpenetrating structures · crystal engineering · hydrogen bonds · supramolecular chemistry

1. Introduction

1.1. Framework Structures

The synthesis and characterization of infinite two- and three-dimensional networks has been an area of rapid growth in recent years.[1–3] The motivation behind much of this activity has been provided by the prospect of generating, by deliberate design, a wide range of purpose-built materials with predetermined structures and useful properties, for example electronic, magnetic, optical, and catalytic. Implicit or explicit in much of this work has been the idea of *self-assembly of specifically designed building blocks*. There is still a long way to go in the development of this field before it will be possible to say that these ambitious objectives have been fully realized. Nevertheless, great opportunities for exciting advances are provided by the enormous sweep of chemistry embracing coordination, organic, and main group chemistry, which is at our disposal for creative use in the planned construction of frameworks.

[*] Dr. R. Robson, Dr. S. R. Batten[+]
School of Chemistry, University of Melbourne
Parkville, Victoria 3052 (Australia)
Fax: (+61) 3-9347-5180
E-mail: richard_robson@muwayf.unimelb.edu.au

[+] New address:
Chemistry Department, Monash University
Clayton, Victoria 3168 (Australia)
Fax: (+61) 3-9905-4597

1.2. The Net-Based Approach to Framework Construction

One conceptual approach to building frameworks is based on the idea of a net. In essence, nets are abstract mathematical entities consisting of a collection of points or nodes with some clearly defined connectivity or topology. A very useful catalogue of nets of relevance to chemistry was compiled by

  1433-7851/98/3711-1461 $ 17.50+.50/0

Wells over twenty years ago.[4] Examples of simple, infinite 2D nets are those given the symbols (6,3) and (4,4) shown in Figures 1 and 2, respectively. One way to represent the

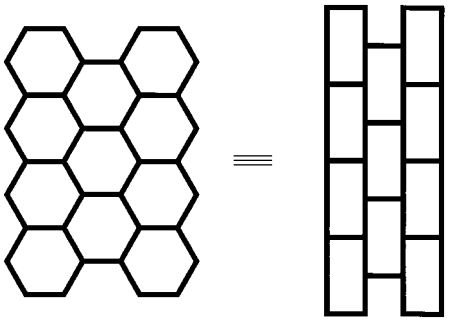

Figure 1. Two geometrically different forms of the (6,3) net.

topology or connectivity of a given net is in terms of the general symbol (n,p), where p is the number of connections to neighboring nodes that radiate from any center or node, and n is the number of nodes in the smallest closed circuits in the net. Thus, the number 6 in the symbol (6,3) indicates that the smallest complete circuits in the net are hexagons, and the number 3 indicates that each node is connected to three other nodes. The (n,p) notation applies strictly only to nets in which all $p(p-1)/2$ shortest circuits originating from any node are n-gons; otherwise the more complete Schläfli notation $n^{p(p-1)/2}$ should be used. Two of the six shortest circuits around any node in the net shown in Figure 2, whose representation as (4,4) is not strictly correct, in fact involve six nodes, and the complete Schläfli notation should be $4^4 6^2$; this was simplified by Wells to 4^4 or (4,4) by arbitrarily excluding circuits involving colinear connections.

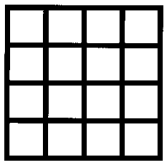

Figure 2. The (4,4) net.

Figure 1 shows two versions of the (6,3) net which are geometrically different but topologically identical. This example illustrates the general point that nets may be geometrically deformed to any extent and yet, provided no connections are broken, the topology is considered to remain unchanged. Some examples of simple, infinite 3D nets are

- the α-polonium (or NaCl) net with six-connected, octahedral nodes,
- the diamond, lonsdalite, quartz, feldspar-related, and zeolite-related nets, all of which have four-connected, essentially tetrahedral nodes,
- the NbO net, which has square-planar nodes with a 90° twist along every connection,[5]
- a variety of intriguing and little-known three-connected nets described by Wells,[4]
- a number of nets containing more than one type of node, such as the PtS net which contains equal numbers of tetrahedral and square-planar nodes, the rutile net containing octahedral and trigonal nodes, the "Pt_3O_4" net with square-planar and trigonal nodes, and the Ge_3N_4 net with tetrahedral and trigonal nodes. All of these nets provide realistic targets for crystal engineers.

One approach to building frameworks is based on the expectation that if molecular building blocks with a chemical functionality and a stereochemistry appropriate to one of the above target nets can be devised, then simply allowing these specifically organized components to react together in the correct proportions may lead to the spontaneous assembly of the intended network.[1, 6] Thus, for the sake of illustration, if we had set our sights on a Ge_3N_4-type net, we would require building blocks with tetrahedral and trigonal dispositions of complementary functional groups. This approach has met with some success—for example, in generating diamond,[6–8] PtS,[9, 10] and α-polonium[11, 12] nets by design—but outcomes of such attempts to build frameworks are often determined by a very fine balance of complex and subtle effects. Predicting such outcomes simply on the basis of the reactants present in the reaction mixture constitutes a major challenge for the theoretician. In the meantime, the empirical, experimental

Richard Robson, born and raised in Yorkshire (UK), received his B.A. and D.Phil. degrees from the University of Oxford. After postdoctoral work at the California Institute of Technology and Stanford University (USA) he joined the Chemistry School at the University of Melbourne (Australia). His research interests have centered around the imposition by design of organization at the molecular level. Earlier work concerned with complexes derived from ligands designed to bind pairs, quartets, and sextuplets of metal centers has been extended in recent years to infinite 2D and 3D coordination networks.

Stuart Batten was born and raised in Moyhu. After school he obtained a B.Sc. (Hons) (1990) and a Ph.D. (1996) in chemistry at the University of Melbourne. His Ph.D. research was performed under the supervision of Richard Robson and Bernard Hoskins, and involved the synthesis and characterization by X-ray crystallography of coordination polymers, with a view to predetermining their topology by judicious choice of ligand and metal ion. Particular attention was paid to the trigonal ligands tcm and tpt. Following postdoctoral positions at both the University of Bristol and Monash University, he is currently employed in Richard Robson's group on work related to his Ph.D. research.

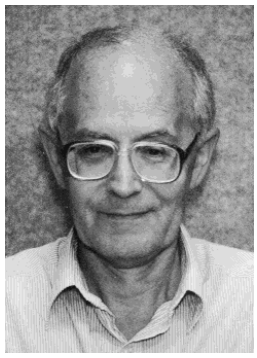

R. Robson

S. R. Batten

approach, based largely on sensible design and chemical intuition, has a great deal to offer. It has already revealed much new chemistry, including several unprecedented structural types, and there is every indication that it will continue to do so.

The idea of *topological equivalence* is useful in describing networks. For example the 2D network formed when large numbers of benzene-1,3,5-tricarboxylic acid (trimesic acid) molecules associate through hydrogen bonds of the type seen for acetic acid dimers (Figure 3) is said to be topologically

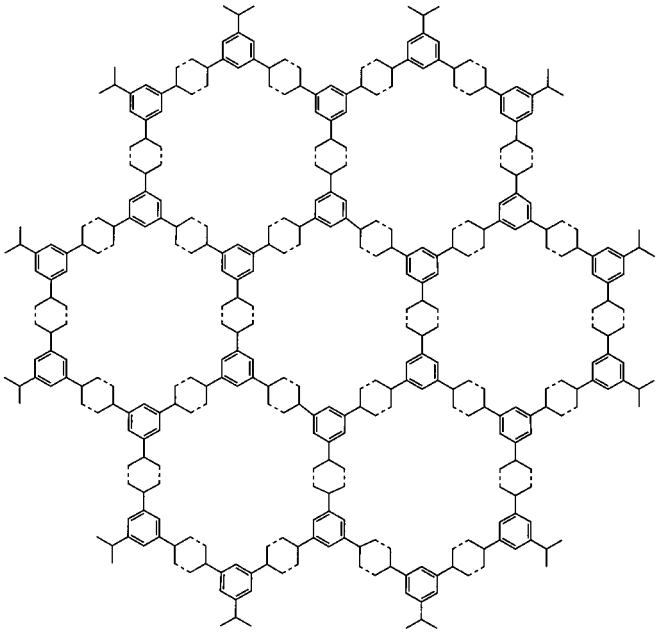

Figure 3. A hydrogen-bonded sheet of trimesic acid molecules with the (6,3) topology.

equivalent to or to have the topology of the (6,3) net.[13] Nodes within a net do not necessarily have to coincide with a particular atom, and in the trimesic acid sheets they are located at the centers of the benzene rings. The imaginary process of reducing a real chemical structure to the essence of its connectivity is useful for clarifying this fundamental aspect of its nature: It is particularly useful in understanding and interrelating modes of interpenetration, as we shall see below.

1.3. Voids, Interpenetration, and the Scope of This Review

Examination of models of a range of framework structures constructed from molecular building blocks that might realistically be employed in practice leads to the realization that, for many simple nets, connecting units with rodlike character need not be very long to provide structures with relatively large channels, cavities, and windows. In recent years large numbers of framework solids have been structurally characterized; the vast majority make use of either hydrogen bonding[3] or ligand-to-metal coordinative bonding[2] to link the individual components. In some cases the frameworks do generate spacious voids, cavities, and channels, which may account for more than half the volume of the crystal.[6, 7, 10, 14] These large spaces are usually occupied by highly disordered, essentially liquid solvent. In other cases remarkable interpenetrating structures are formed in which the voids associated with one framework are occupied by one or more independent frameworks; an inherent feature of such entangled structures is that they can be disentangled only by breaking internal connections.

These interpenetrating framework structures are the subject of this article; until recently examples were rare,[15] but they are now being reported with ever increasing frequency. We have restricted the scope of this review to interpenetrating structures in which the building blocks within the individual infinite networks or chains are linked together through either metal-to-ligand bonds or hydrogen bonds. A further restriction is that only ordered, structurally regular, and crystallographically characterized systems will be covered. The interpenetrating polymer networks (IPNs),[16] which are noncrystalline materials with rubberlike and plastic properties, are therefore not included.

1.4. Molecular Entanglement

Infinite interpenetrating structures constitute a subgroup within a broader class of entangled systems, which are the subject of intensive current research.[17] A familiar example is provided by the entangled strands in the DNA double helix. This and other helical biological molecules have provided the inspiration for a rapidly expanding range of double- and triple-helical coordination compounds.[18] Dendrimers are another class of tangled compounds of great current interest.[19] Catenanes, rotaxanes, and molecular knots,[20] however, occupy positions of special importance in the area of molecular entanglement, because they can be disentangled only by breaking connections (in contrast, for example, to the DNA double helix, for which it is not necessary to disrupt the individual strands in order to disentangle them). Catenanes consist of independent rings that are locked together (Figure 4a) In rotaxanes a ring component encircles the shank of an

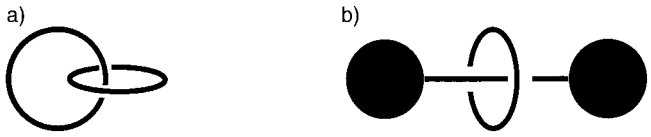

Figure 4. Schematic representation of a) a catenane and b) a rotaxane.

independent dumbell-like component (Figure 4b). The two "stops" at the ends of the dumbell-like component prevent the ring from escaping. In pseudorotaxanes one or more rings are threaded onto a molecular "string", but the stops present in true rotaxanes are lacking. Molecular knots are characterized by self-entanglement.

1.5. Some General Points about Interpenetration

Some general points about interpenetrating networks can be illustrated by considering the example of zinc cyanide, whose structure was determined over half a century ago.[6, 21, 22] It consists of two independent infinite frameworks, each with diamondlike topology. The point symbol for the diamond net is 6^6-a; the superscript indicates the number of different pairs of connections radiating from one node to its neighbors (i.e., $(4 \times 3)/2$). The smallest circuits in which each pair participates are hexagons, which is indicated by the main, nonsuperscripted symbol. The −a indicates that this is the most symmetrical of a number of different possible 6^6 nets. In $[Zn(CN)_2]$ the metal centers provide the tetrahedral nodes, and the cyanide groups act as linear bridges between the metal atoms. A characteristic structural motif within the diamond net is the "adamantane unit" (Figure 5a). The two independent networks interpenetrate in such a way that every

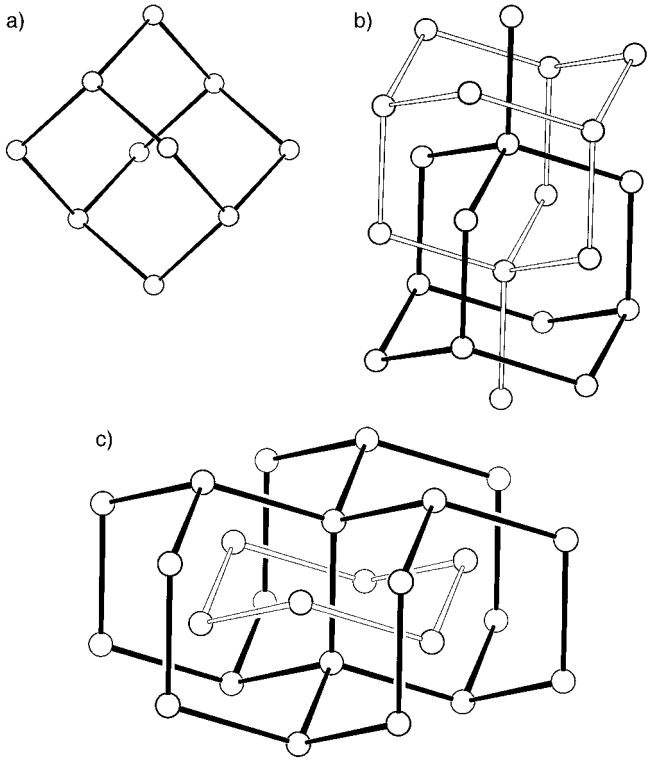

Figure 5. a) An adamantane unit of a diamondlike net. b) Interlocked adamantane units of two independent diamondlike nets. c) A cyclohexane-like ring of one net with a rod of the other passing through it; the rod is part of six different hexagons.

tetrahedral node is found at the center of an adamantane unit of the other framework, and the four connections to nearest neighbors project through the four cyclohexane-like windows of the surrounding adamantane unit (Figure 5b). We shall refer to connections between nodes within nets in general as rods. Each rod in $[Zn(CN)_2]$ forms part of six distinguishable cyclohexane-like rings and is exclusively associated with one particular cyclohexane-like ring of the other framework through which it passes (Figure 5c). This is catenation on the grand scale. Clearly, the two frameworks can be disentangled only by wholesale breaking of connections. The regions of closest contact between the two independent frameworks are at the midpoint of every cyanide unit, and the closest parts of the other framework are the midpoints of the six equivalent cyanide units that surround it.

In this review we shall use the term *n*-fold interpenetration to describe systems with *n* independent nets; for example, $[Zn(CN)_2]$ displays twofold interpenetration.

All interpenetrating network structures can be regarded as infinite, ordered polycatenanes or polyrotaxanes. One of their characteristic features is the repeated, orderly appearance of rings belonging to one framework or chain, through which independent components are inextricably entangled. The very interesting possibility, presently unrealized, in which the individual rings in an infinite polycatenane are themselves finite and molecular would not fall in the category of interpenetrating frameworks as we define it here because the units participating in interpenetration are not infinite.

Another example of a structure involving infinite entanglement which nevertheless does not fall in the category of an interpenetrating structure is the material of composition $[IAuP(C_6H_5)_2(CH_2)_6P(C_6H_5)_2AuI]_n$. This contains 1D zigzag polymeric chains in which neutral digold monomers are linked together through weak gold–gold interactions.[23] These chains are then interwoven like warp and weft to generate a clothlike 2D sheet in which every chain passes alternately over and then under an infinite number of other chains (Figure 6). This interesting structure is not interpenetrating in the sense we have reserved for the term because it is

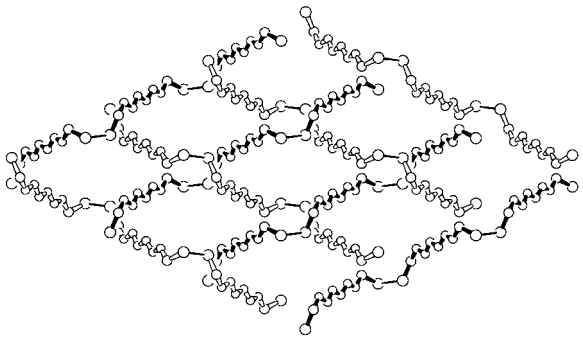

Figure 6. Warp-and-weft structure of $[IAuP(C_6H_5)_2(CH_2)_6P(C_6H_5)_2AuI]_n$. The circles represent in order of decreasing size Au, P, and C atoms. Phenyl groups and iodine atoms have been omitted for clarity.

not necessary, in principle, to break any links within the independent chains in order to disentangle them, nor do the components contain rings through which other components can project and become entangled. For similar reasons we exclude from the general class of interpenetrating frameworks microporous structures with linear polymers trapped in their channels.

2. Interpenetrating One-Dimensional Polymers

We know of only two examples that can be assigned to this category. Ligand **1** affords a coordination polymer of compo-

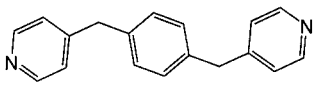

1

sition $[Cd_2(\mathbf{1})_3(NO_3)_4]$, which contains infinite, 1D, ladderlike chains of the type shown in Figure 7.[24] From the topological point of view each cadmium atom acts as a T-type three-connected center; its seven-coordinate environment is completed by two bidentate nitrate ligands which are pendant, that is, not an essential part of the connectivity of the network. Each ladderlike chain contains an infinite number of rings, all equivalent, defined by two ladder "rungs" and segments of two ladder "uprights". In the interpenetration shown in Figure 7 the uprights of four separate ladders pass through each such ring.

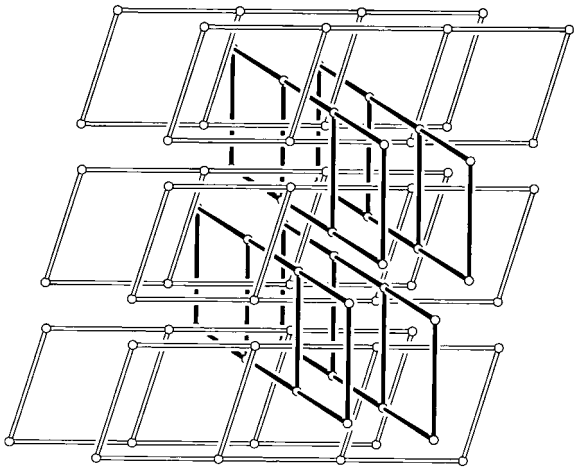

Figure 7. Interpenetrating ladderlike chains in $[Cd_2(\mathbf{1})_3](NO_3)_4$. The T-type three-connected centers represent Cd atoms. Every ring has the uprights of four separate ladders passing through it.

Ligand **2** gives a coordination polymer of composition $[Ag_2(\mathbf{2})_3](NO_3)_2$ which contains 1D chains of the type shown

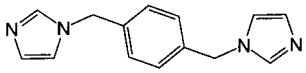

2

in Figure 8.[25] We shall later encounter examples of interpenetrating structures which can correctly be described either as polyrotaxanes or as polycatenanes; deciding which is the better description is not easy. The mode of interpenetration in $[Ag_2(\mathbf{2})_3](NO_3)_2$ (shown schematically in Figure 8c), however, is unquestionably of the polyrotaxane type, and catenane associations are simply not present. Each individual chain is interlocked with an infinite number of others by multiple rotaxane associations in which every one of its rodlike segments passes through a ring of another chain and every one of its rings encircles a rod of another chain (Figure 8c).

In the first example, $[Cd_2(\mathbf{1})_3(NO_3)_4]$, the interpenetration produces a 3D interlocked structure, whereas in $[Ag_2(\mathbf{2})_3](NO_3)_2$ a 2D interlocked structure results.

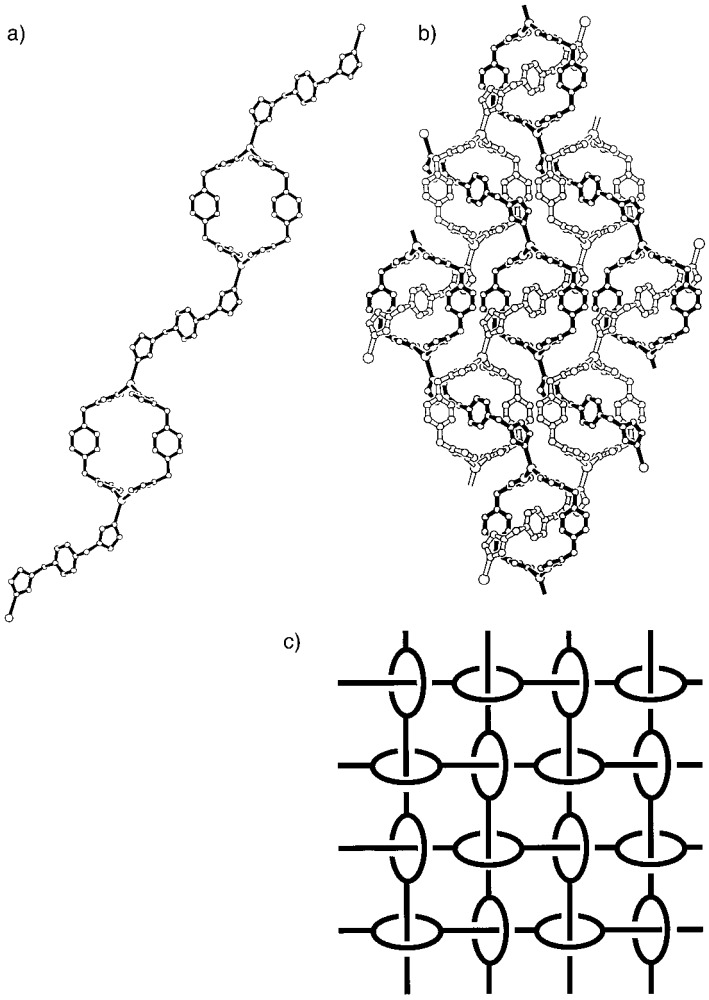

Figure 8. a) A single chain in $[Ag_2(\mathbf{2})_3](NO_3)_2$. The large circles represent Ag atoms, and the smaller circles C and N atoms. b) A polyrotaxane sheet in $[Ag_2(\mathbf{2})_3](NO_3)_2$. c) Schematic representation of the multiple rotaxane associations.

3. Interpenetrating Two-Dimensional Networks

Two major categories of interpenetrating 2D networks can be discerned: One we shall call "parallel interpenetration" and the other "inclined interpenetration".

For parallel interpenetration to be possible, the individual 2D networks must be corrugated or possess some appropriate element of undulation. Usually two such undulating sheets, but occasionally more, are arranged with their average planes parallel—this is indeed the case in all presently known examples—so that each is able to pass through the other an infinite number of times (shown schematically in Figure 9).

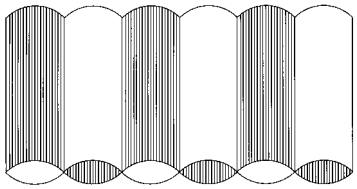

Figure 9. Parallel interpenetration of undulating sheets.

The composite structure resulting from this form of interpenetration is itself two-dimensional, and these composite sheets are then stacked one on top of another.

In inclined interpenetration there are two stacks of sheets, one stack inclined, often perpendicular, to the other (Figure 10). Any particular 2D network layer then has an infinite

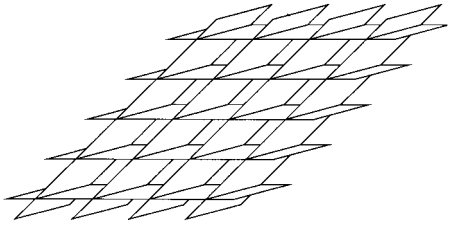

Figure 10. Inclined interpenetration of sheets.

number of inclined layers passing through it. In contrast to parallel interpenetration, each sheet passes through an inclined one just once along a line of intersection of the two planes. Also in contrast to parallel interpenetration, the product of inclined interpenetration is a 3D interlocked structure. With only one exception the individual networks involved in 2D interpenetration, whether of the parallel or inclined types, are based on either the (4,4) or the (6,3) topology.

3.1. Parallel Interpenetration of Two-Dimensional Frameworks

3.1.1. Two Parallel, Interpenetrating Nets Based on the (6,3) Topology

Four topologically different modes of (6,3) parallel interpenetration which are crystallographically regular and within which all rings are equivalent are shown in Figure 11. By topologically different we mean that one could be transformed into another only by breaking connections and making new ones. If we relax the restriction that all rings be equivalent (e.g., if we allow some rings to have no part of the other net passing through them) then clearly an infinite number of modes of interpenetration become possible.

[Ag(tcm)] ($tcm^- =$ tricyanomethanide, $C(CN)_3^-$) contains (6,3) nets whose three-connected nodes are provided by alternating central carbon atoms of the tcm ions and three-coordinate Ag^I centers.[26, 27] The two independent and identical (6,3) networks are corrugated so that each is able to pass through the other an infinite number of times (Figure 12). This is topologically identical to the interpenetration mode shown in Figure 11a. The corrugations in the sheets which make the interpenetration possible arise from a combination of a distinctly nonplanar, pyramidal geometry at the silver centers and a significant bending at the nitrogen centers.

It is possible to make derivatives of [Ag(tcm)] which retain the parallel, interpenetrating, double-sheet structure. [Ag(tcm)(CH_3CN)] has basically the same composite layer structure as [Ag(tcm)], but the acetonitrile molecule is now

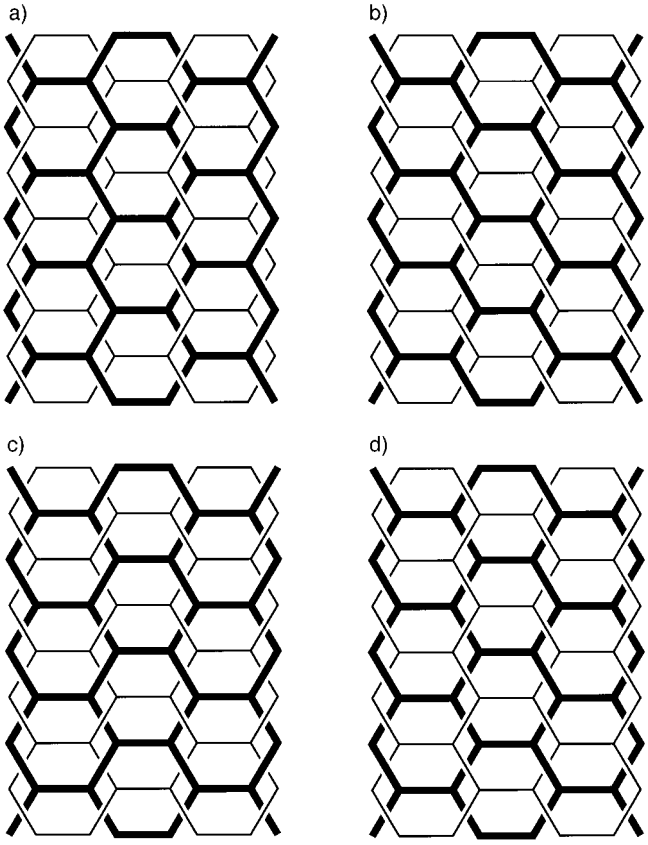

Figure 11. a) – d) Four topologically different modes of parallel interpenetration of (6,3) nets.

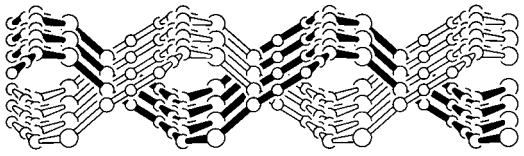

Figure 12. Interpenetrating undulating (6,3) nets in the structure of [Ag(tcm)]. The circles represent in order of decreasing size Ag, N, and C atoms.

coordinated to the metal, which acquires thereby a tetrahedral geometry.[28] The acetonitrile methyl groups are directed generally away from the center of the composite sheet and towards the neighboring sheets, causing an increase in the separation between composite layers. In [Ag(tcm)($L)_{1/2}$] (L = phenazine) almost the same double-interpenetrating [Ag(tcm)] layers are present, but they are now connected together through phenazine molecules that bridge silver atoms in one composite sheet to those in a neighboring composite sheet.[27] Two independent but interpenetrating 3D networks are thus formed.

Two examples that involve the interpenetration of 3D nets are described at this point because of the close structural relationship, elaborated below, to the tcm compounds above. [Ag{$C(CN)_2NO$}] contains (6,3) nets in the form of undulating sheets, closely analogous to those in [Ag(tcm)], in which the two nitrile nitrogen atoms and the nitroso oxygen atom of each ligand form dative bonds to the silver atom.[29] These undulating sheets participate in twofold parallel interpenetration in a fashion almost identical to that seen in [Ag(tcm)].

Dative bonds between the nitroso nitrogen atoms in one composite sheet and silver atoms in an adjacent composite sheet then produce two interpenetrating 3D networks (Figure 13).

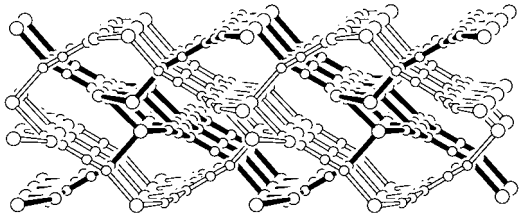

Figure 13. Structure of $[Ag\{C(CN)_2NO\}]$ in which parallel interpenetrating (6,3) nets are joined together into a 3D structure through bonds between Ag atoms in one sheet and the nitroso N atoms of another. The circles represent in order of decreasing size Ag, O, and C/N atoms.

The series of compounds with variable composition $[Cu(NH_3)(py)Ag_{3-x}Cu_x(CN)_5]\cdot py$ (py = pyridine) form layers of two (6,3) sheets that interpenetrate in the fashion shown in Figure 11 a.[30] The three-connected nodes of the sheets are formed by alternating Cu^{II} centers (which also coordinate to pendant pyridine and ammonia groups to give a five-coordinate center) and Ag^I centers, and are connected through CN^- and $Ag(CN)_2^-$ bridges. The three-connected Ag^I atoms and the Ag^I atom in one of the two crystallographically independent $Ag(CN)_2^-$ links are partially substituted by Cu^I. Again, there are links between the layers. Each set made up of a trigonally coordinated Ag^I/Cu^I atom and a carbon atom connected to it has a centrosymmetric dimeric partnership with a corresponding pair of atoms in an adjoining layer. The tetrahedral coordination geometry of the metal atom is completed by a carbon atom in the adjoining layer; short metal–metal contacts are seen (2.641(1) and 2.791(3) Å in the two phases studied). These interactions produce two interpenetrating 3D nets with a similar topology to that seen in $[Ag(tcm)(L)_{1/2}]$ (L = phenazine).

$[Ag\{CH_3COCH_2C(CN)_2C(CN)_2\}]$, produced by the unexpected reaction of tetracyanoethylene with $[Ag(CF_3SO_3)]$ in H_2O/Me_2CO, has layers of two interpenetrating (6,3) nets in which each ligand is coordinated through three of the nitrile nitrogen atoms to three-connected silver atoms.[31] The interpenetration of the sheets is topologically identical to that shown in Figure 11 a.

The semiconductor θ-(BEDT-TTF)$_2[Cu_2(CN)\{N(CN)_2\}_2]$ (BEDT-TTF = bis(ethylenedithio)tetrathiafulvalene) contains anionic $[Cu_2^I(CN)\{N(CN)_2\}_2]^-$ layers with intercalated $[(BEDT\text{-}TTF)_2]^+$ ions.[32] The anionic layers consist of two independent and interpenetrating (6,3) nets in which Cu^I provides the three-connected nodes and CN^- and $N(CN)_2^-$ act as two-connectors. A pronounced bend at the central nitrogen atom in $N(CN)_2^-$ provides the undulating character to each individual sheet that makes the interpenetration possible (Figure 14). This mode of interpenetration is topologically identical to that represented schematically in Figure 11 b, and is intrinsically different from that observed in the previous examples.

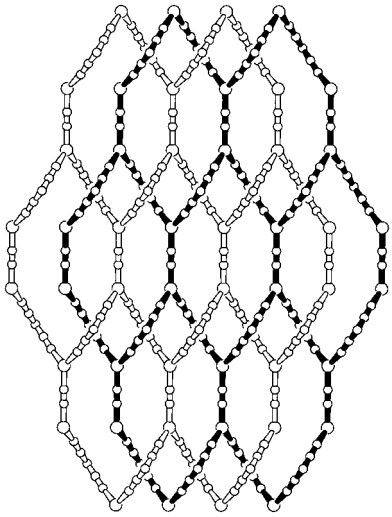

Figure 14. The parallel interpenetration of (6,3) nets in the $[Cu_2(CN)\{N(CN)_2\}_2]^-$ polyanion, which is topologically identical to that shown in Figure 11 b. The large circles represent Cu atoms, and small circles C and N atoms.

The bis(imidazole) ligand **2** combines with zinc nitrate to give a coordination polymer of composition $[Zn(\mathbf{2})_2](NO_3)_2\cdot 4.5\,H_2O$, which contains layers comprising two independent 2D nets that interpenetrate in the parallel manner;[33] the individual nets, represented schematically in Figure 15 a, are

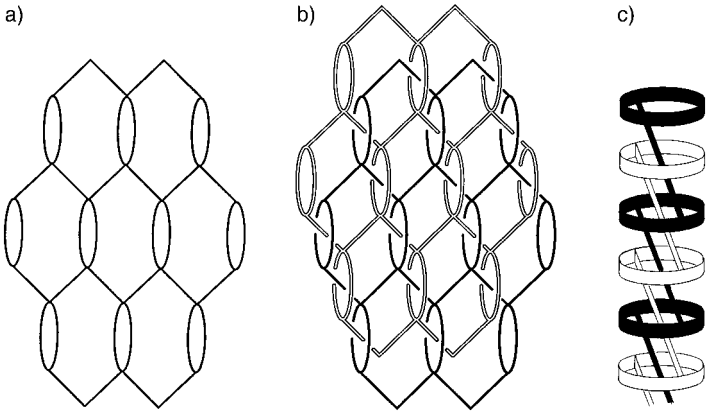

Figure 15. a) Schematic representation of a single 2D net in $[Zn(\mathbf{2})_2](NO_3)_2\cdot 4.5\,H_2O$. Zn atoms provide the four-connected nodes, and molecules of **2** the connections between nodes. b) Schematic representation of the two interpenetrating nets in $[Zn(\mathbf{2})_2](NO_3)_2\cdot 4.5\,H_2O$. c) Schematic representation of the polyrotaxane columns.

based on the (6,3) topology, but a second bridging ligand is present within certain pairs of zinc nodes. The zinc atoms thus become four-coordinate. Two such nets then interpenetrate in the manner represented schematically in Figure 15 b to generate polyrotaxane columns (Figure 15 c). This structure is closely related to that of $[Ag_2(\mathbf{2})_3](NO_3)_2$ (Figure 8), which unquestionably is a polyrotaxane. However, $[Zn(\mathbf{2})_2](NO_3)_2\cdot 4.5\,H_2O$ could equally well be considered as a polycatenane, because the smallest rings of one net are involved in catenane associations with the second-smallest rings (Zn_6) of the other net. There is little to be gained by argument as to which

description should take precedence; the structure has both polyrotaxane and polycatenane character.

3.1.2. Two Parallel Interpenetrating Nets Based on the (4,4) Topology

A close analogue of the mode of interpenetration seen in [Ag(tcm)] is provided by $[Cd(4\text{-pic})_2\{Ag(CN)_2\}_2](4\text{-pic})$ (4-pic = 4-methylpyridine), which involves two corrugated (4,4) nets (Figure 16) rather than the two (6,3) nets in [Ag(tcm)]

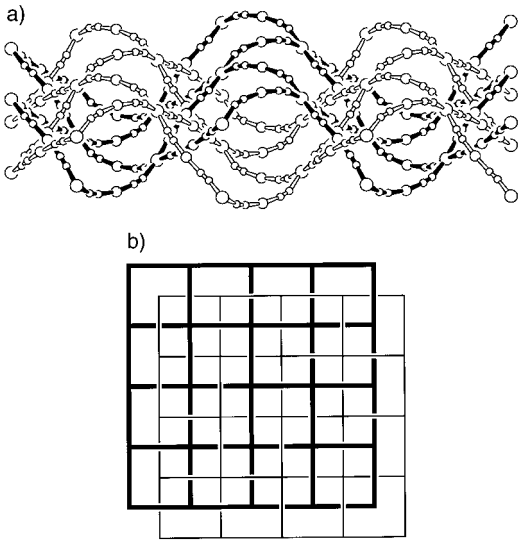

Figure 16. a) Parallel interpenetrating (4,4) nets in the structure of $[Cd(4\text{-pic})_2\{Ag(CN)_2\}_2](4\text{-pic})$ (4-pic = 4-methylpyridine). The pendant 4-pic molecule is omitted. Therefore, the six-coordinate Cd atoms appear to be four-connected. Each Cd atom is connected to four others through bridging $Ag(CN)_2^-$ units. The circles represent in order of decreasing size Cd, Ag, and C/N atoms. b) Schematic representation of the mode of interpenetration.

(Figure 12).[34] The cadmium centers, all of which are equivalent, are four-connected nodes; they are coordinated by two mutually *trans* picoline molecules, which can be regarded as mere appendages to the 2D net, and by a roughly square-planar set of nitrogen atoms from four two-connected $Ag(CN)_2^-$ units. Each (4,4) net is corrugated with its troughs and crests parallel with one diagonal of the Cd_4 rhombuses within the net. Two nets then interpenetrate as shown in Figure 16.

A topologically different mode of parallel interpenetration of two (4,4) nets is found in [Cu(tcm)(bipy)] (bipy = 4,4′-bipyridine), in which the tcm ligands act as bent two-connected units (Figure 17).[28]

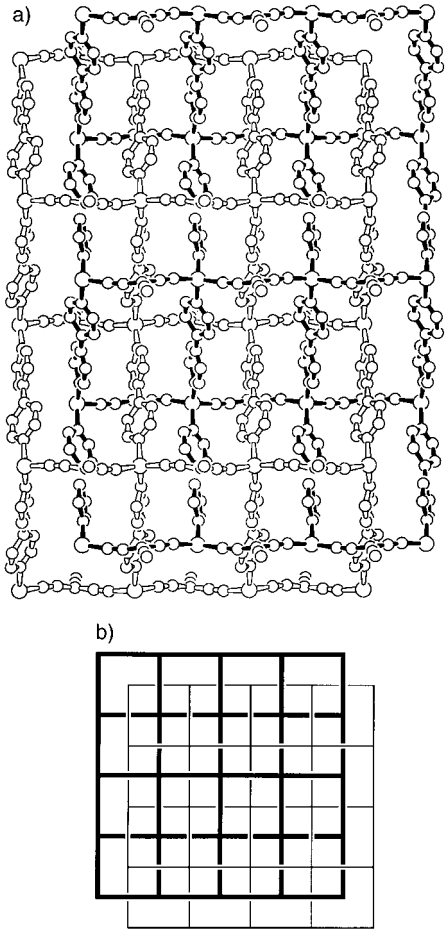

Figure 17. a) Two parallel interpenetrating (4,4) nets in the structure of [Cu(tcm)(bipy)]. The large circles represent Cu atoms, and the small circles C and N atoms. b) Schematic representation of the mode of interpenetration.

Clusters of composition $[Re_4(CO)_{12}(OH)_4]$, which have a cubanelike arrangement of four $Re(CO)_3$ units and four μ_3-OH groups at alternating cube corners, cocrystallize with 4,4′-bipyridine to yield crystals of composition $Z \cdot 2\,bipy \cdot 2\,MeOH$ ($Z = [Re_4(CO)_{12}(OH)_4]$) containing hydrogen-bonded (4,4) nets.[35] The four-connected nodes of the net are provided by Z units, which are connected to one another through their OH groups by the hydrogen-bonded system $Z(OH)/CH_3OH/bipy/(HO)Z$. Two such (4,4) nets interpenetrate in the manner shown schematically in Figure 18. This mode of interpenetration is topologically different from that in $[Cd(4\text{-pic})_2\{Ag(CN)_2\}_2](4\text{-pic})$ and [Cu(tcm)(bipy)], as can be appreciated by comparison of Figure 18 with Figures 16b and 17b; in all of these Figures the structure has been reduced to its topological essence. Answers to questions concerning the number of different ways two (4,4) nets could theoretically interpenetrate in the parallel fashion must await systematic mathematical treatment of the topology of interpenetration. Such an investigation is highly desirable, not only with regard to (4,4) nets, but in general.

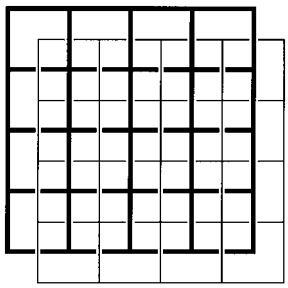

Figure 18. Schematic representation of the two parallel interpenetrating hydrogen-bonded (4,4) nets in the structure of $[Re_4(CO)_{12}(OH)_4] \cdot 2\,bipy \cdot 2\,MeOH$. The four-connected nodes shown represent the centers of the Re_4 clusters.

4,4′-Sulfonyldiphenol crystallizes to give hydrogen-bonded (4,4) nets that interpenetrate in the parallel manner shown in Figure 19.[36] This mode of interpenetration is topologically identical to that in [Cu(tcm)(bipy)] (Figure 17).

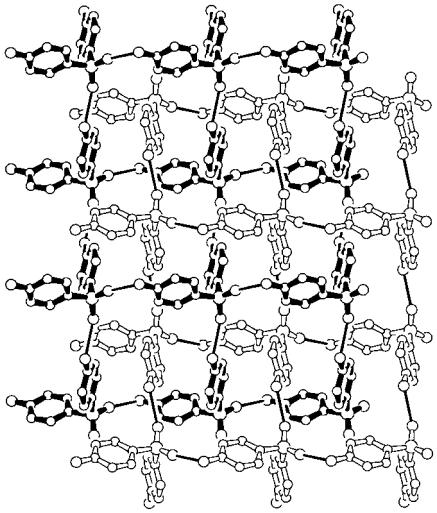

Figure 19. Two parallel interpenetrating hydrogen-bonded (4,4) nets in the structure of 4,4′-sulfonyldiphenol. The circles represent in order of decreasing size S,O, and C atoms. The thin lines represent hydrogen bonds.

The coordination polymer formed by the ligand *N*,*N*′-*p*-phenylenedimethylenebis(pyridin-4-one) (**3**) of composition $[Mn(\mathbf{3})_3](ClO_4)_2$ consists of two (4,4)-based nets that interpenetrate in the parallel fashion.[37] As in the case of

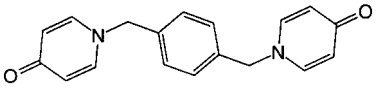

3

$[Zn(\mathbf{2})_2](NO_3)_2 \cdot 4.5\,H_2O$ considered in Section 3.1.1, a second bridging ligand is present between certain Mn nodes, whereby $Mn_2(\mathbf{3})_2$ rings are formed and the metal centers become six-connected. A schematic representation of the polyrotaxane/polycatenane fashion in which they interpenetrate is shown in Figure 20. Compounds $[Ag_2(\mathbf{2})_3](NO_3)_2$, $[Zn(\mathbf{2})](NO_3)_2 \cdot 4.5\,H_2O$, and $[Mn(\mathbf{3})_3](ClO_4)_2$ can be considered as members of a progression in which the connectivity of the metal center increases from three to four to six; in all cases $(metal)_2(ligand)_2$ rings participate in rotaxane interactions.

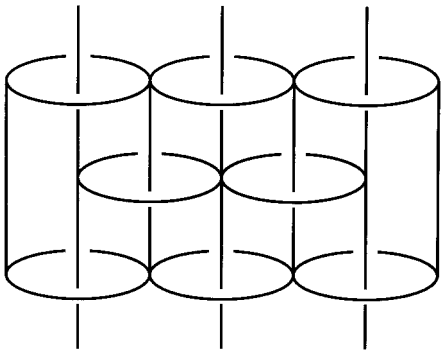

Figure 20. Schematic representation of the two parallel interpenetrating (4,4) nets in $[Mn(\mathbf{3})_3](ClO_4)_2$ showing the polyrotaxane/polycatenane associations. Six-connected nodes are provided by six-coordinate Mn, and connections between the nodes by ligand **3**.

3.1.3. Two Interpenetrating Two-Dimensional $8^2 10$ Nets: Hittorf's Phosphorus

The allotrope of phosphorus known as Hittorf's phosphorus is the only example of 2D parallel interpenetration involving nets other those based on (6,3) and (4,4) topologies. Two 2D $8^2 10$ nets interpenetrate in the manner represented schematically in Figure 21 a.[38] The three-connected nodes of the net

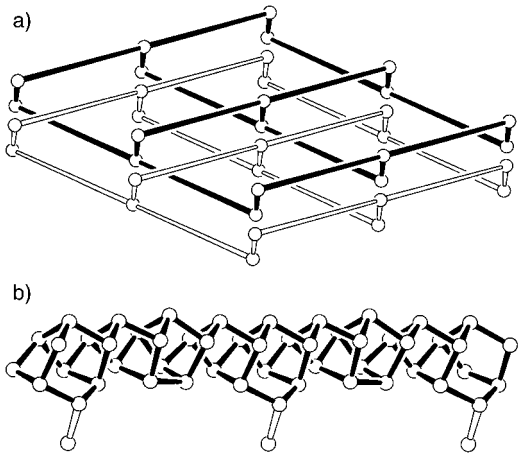

Figure 21. a) Schematic representation of the interpenetration of two 2D $8^2 10$ nets in Hittorf's phosphorus. b) Representation of the columnar rods which constitute the long connections between three-connected phosphorus nodes in a). The open bonds in b) represent direct P – P covalent bonds between the three-connected phosphorus nodes of the rod shown to three adjoining rods running at right angles.

are located at particular phosphorus atoms. All such nodes are equivalent, and each is connected to one other node through a direct P – P bond (the short node-to-node connections in Figure 21 a) and to two other nodes through columnar rods with a roughly pentagonal cross-section (Figure 21 b).

3.1.4. Three Parallel Interpenetrating Two-Dimensional Nets

There is of course no reason why parallel interpenetration should be restricted to two independent nets. A number of examples of threefold parallel interpenetration are known at present, all of which involve (6,3) nets.

Trimesic acid cocrystallizes with 4,4′-bipyridine to form hydrogen-bonded (6,3) networks with voids so large that three identical but independent networks of this type form a structure with parallel interpenetration (Figure 22).[39] This mode of threefold interpenetration is closely related to the hypothetical mode of twofold interpenetration shown in Figure 11 c. This can be imagined by removing any one of the three nets in Figure 22, which leaves a twofold interpenetrating system topologically identical to that in Figure 11 c.

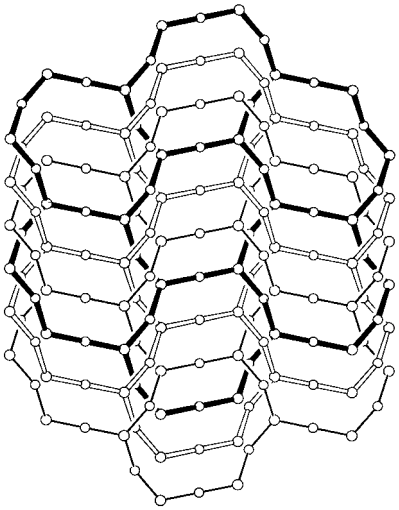

Figure 22. Schematic representation of the threefold parallel interpenetration of (6,3) nets in the cocrystal of trimesic acid and bipy. Three-connected nodes represent the centers of trimesic acid molecules, while the two-connected nodes represent the midpoints of the bipy ligands.

$[Cd_2(\mathbf{4})_3(NO_3)_4]$ contains three independent (6,3) nets in which the three-connected nodes are provided by cadmium atoms that are bridged by ligand **4**.[24] Every $Cd_6(\mathbf{4})_6$ ring has a rod from each of the other two nets passing through it (Figure 23). This interpenetration mode is a very close analogue of the twofold interpenetration shown by [Ag(tcm)], as comparison of Figure 23 with Figures 12 and 11a will reveal. Indeed, removal of any one of the three nets in Figure 23 leaves a twofold interpenetrated system topologically identical to that in Figures 12 and 11a.

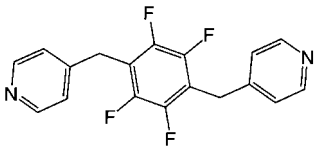

4

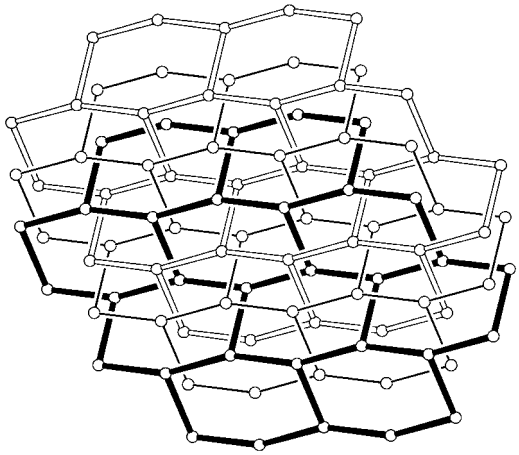

Figure 23. Three parallel interpenetrating (6,3) nets in the structure of $[Cd_2(\mathbf{4})_3(NO_3)_4]$. The three-connected nodes are provided by Cd atoms, and ligand **4** forms the connections between the nodes.

The crystal structure of **5** contains three interpenetrating (6,3) nets; the nodes of the nets are the centers of the two isophthalic acid groups in each molecule.[40] One of the links from any three-connected node represents the covalent

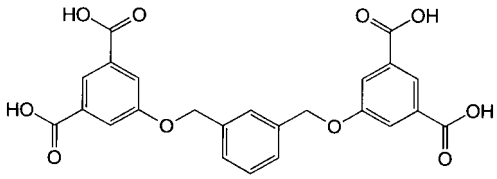

5

spacer between the two isophthalic acid groups of each molecule, and the other two links represent hydrogen-bonding associations with adjacent molecules. The interpenetration is shown schematically in Figure 24; a comparison of Figures 23 and 24 shows that the mode of interpenetration is identical to that in $[Cd_2(\mathbf{4})_3(NO_3)_4]$.

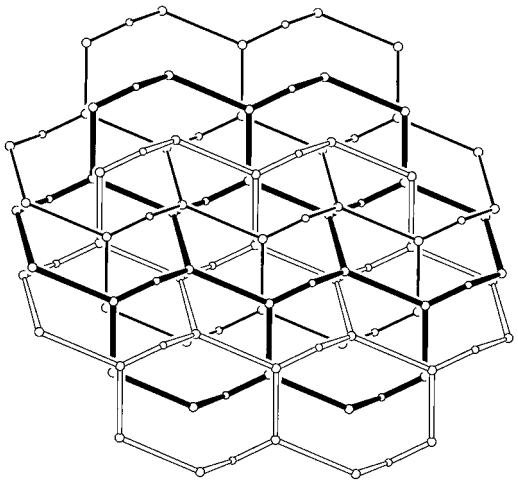

Figure 24. Schematic representation of the three parallel interpenetrating (6,3) nets in the crystal structure of **5**. The three-connected centers represent the centers of the isophthalic acid groups of **5**, while the smaller two-connected centers represent the midpoint of the central C_6 ring of **5**.

Similarly, $\mathbf{6}\cdot 2L$ (L = 1,4-benzoquinone) has three interpenetrating (6,3) sheets in which the three-connected nodes are the centers of the resorcinol groups of the ligand.[41] One link from each node represents the covalent bridging of the resorcinol groups through the anthracene unit, and the other two links represent hydrogen-bonding interactions in which resorcinol groups of two different molecules are bridged by bifunctional 1,4-benzoquinone molecules. This interpenetration is shown schematically in Figure 25. Removal of any one net would leave a system of two interpenetrating nets topologically identical to that shown in Figure 11c.

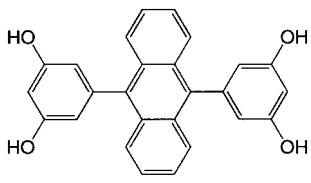

6

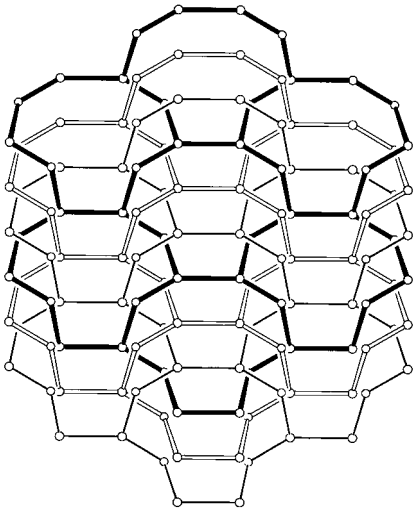

Figure 25. Schematic representation of the three parallel interpenetrating (6,3) nets in the crystal structure of **6**·2L (L = 1,4-benzoquinone). The larger three-connected circles represent the resorcinol groups on **6**, and smaller two-connected circles represent the midpoints of the 1,4-benzoquinone molecules.

3.1.5. Six Parallel Interpenetrating Two-Dimensional Nets

Six parallel interpenetrating (6,3) sheets are seen in the structure of solvated $[Ag(teb)CF_3SO_3]$ (teb = 1,3,5-tris(4-ethynylbenzonitrile)benzene, **7**).[42] The three-connected nodes are defined by alternating ligand and silver centers. The

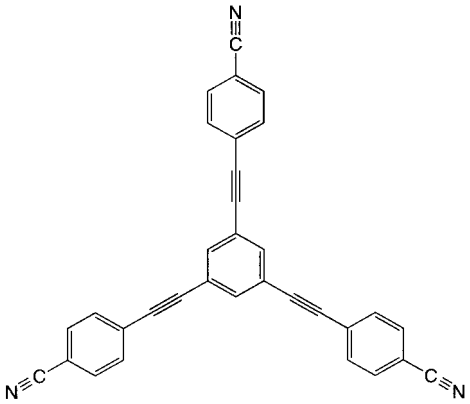

7

silver atoms are also coordinated to pendant triflate ions, and hence have tetrahedral geometry. The nets interpenetrate such that any two nets have the same topological relationship as that shown in Figure 11 a.

3.2. Inclined Interpenetration of Two-Dimensional Frameworks

In the inclined mode of interpenetration of 2D frameworks any one sheet has an infinite number of others passing through it (see Figure 10). As mentioned earlier, inclined interpenetration of 2D sheets produces an interlocked 3D structure; this is in contrast to parallel interpenetration, which yields a composite 2D product. Any pair of inclined sheets pierce each other only along the line of intersection of the two planes. In some cases each ring of a sheet has only one rod of an inclined sheet passing through it, but there are examples in which the rings are large enough and the rods slim enough to allow more than one sheet to pass through each ring. All known cases of inclined interpenetration of 2D sheets involve either (4,4) or (6,3) nets.

3.2.1. Inclined Interpenetration of (4,4) Nets

Crystalline compounds of composition $[M(bipy)_2(H_2O)_2](SiF_6)$ (M = Zn, Cd, Cu) and $[Cd(bipy)_2(H_2O)(OH)](PF_6)$ have the interlocked, perpendicular, square-grid structure shown in Figure 26.[43, 44] The bridging bipy ligands are

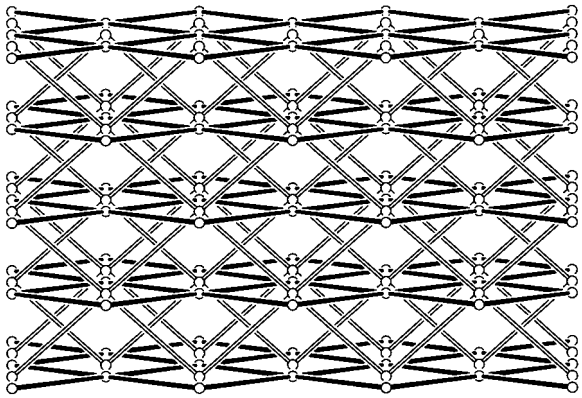

Figure 26. Inclined interpenetration (actually perpendicular) of two (4,4) nets in $[M(bipy)_2(H_2O)_2](SiF_6)$. Four-connected nodes are provided by M atoms, which have two pendant *trans* H_2O ligands not shown here.

arranged around the metal atom in a square-planar fashion, and two water ligands (or, in the Cd/PF_6 case, one water and one hydroxide ligand) on opposite sides of that plane complete an octahedral coordination environment. The $Cd(PF_6)_2$/bipy system is interesting in that the use of solvent mixtures only slightly different from those used to obtain the interpenetrating $[Cd(bipy)_2(H_2O)(OH)](PF_6)$ structure yields noninterpenetrating $[Cd(bipy)_2(H_2O)_2](PF_6)_2 \cdot 4H_2O \cdot 2$bipy,[44] which contains very similar square-grid sheets in which each corrallike ring encloses two uncoordinated bipy molecules. This example demonstrates how fine a balance may dictate whether an interpenetrating structure is formed or not.

$[Fe(bpe)_2(NCS)_2] \cdot CH_3OH$ (bpe is the "extended" bipy analogue *trans*-1,2-di-(4-pyridyl)ethene) has a structure that is geometrically very similar and topologically identical to that in Figure 26; bipy has been replaced by bpe, and the two *trans* water ligands have been replaced by thiocyanate ligands.[45]

A bipy analogue that is even more extended than bpe, 1,4-bis(4-pyridyl)butadiyne (bpb), gives crystals of the composition $[M_2(OH)(bpb)_4](BF_4)_3 \cdot H_2O \cdot EtOH$ (M = Cd, Cu) containing "doubled-up" square-grid sheets which interpenetrate each other (Figure 27). The manner of interpenetration is closely analogous, and in fact topologically identical, to that represented in Figure 26.[46]

$[Cd(NH_3)_2\{Ag(CN)_2\}_2]$ also has an interpenetrating sheet structure which is topologically identical to that in Figure 26;

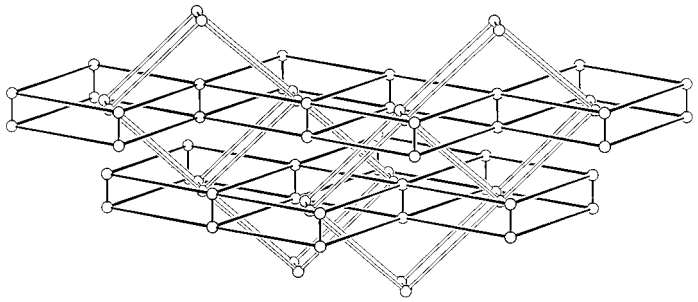

Figure 27. Inclined interpenetrating doubled-up sheets in the structure of $[M_2(OH)(bpb)_4](BF_4)_3 \cdot H_2O \cdot EtOH$ (bpb = 1,4-bis(4-pyridyl)butadiyne). The circles represent M atoms. "Short" connections here are provided by μ_2-OH^- and "long" connections by μ_2-bpb ligands. The overall topology of the doubled-up sheets is (4,4), and the nodes are located at the midpoints of the short connections.

there are $Ag(CN)_2^-$ bridging ligands in place of bipy and two *trans* amine ligands in place of the two water ligands.[47]

A second, chemically realistic way in which two inclined (4,4) nets could be imagined to interpenetrate is shown in Figure 28. The only example of this mode of interpenetration

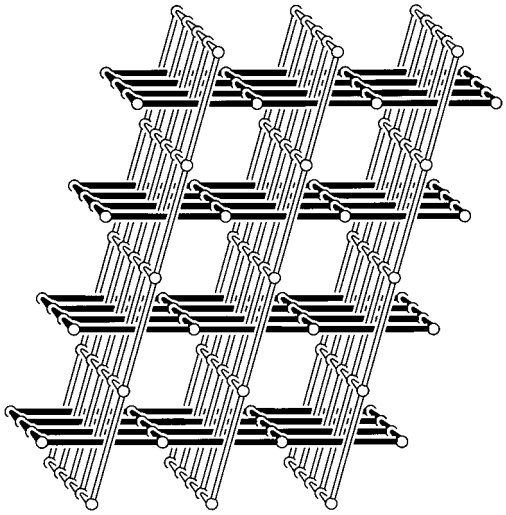

Figure 28. An alternative mode of inclined interpenetration of two (4,4) nets.

exists in the structure of $[Cd(4\text{-ampy})_2\{Ag(CN)_2\}_2] \cdot [Cd(mea)(4\text{-ampy})\{Ag(CN)_2\}_2]_2$ (4-ampy = 4-aminopyridine, mea = 2-aminoethanol).[48] This structure contains (4,4) 2D sheets that are composed of octahedrally coordinated cadmium atoms bound to terminal 4-ampy ligands and bridged by linear $Ag(CN)_2^-$ moieties. A second type of sheet exists in the structure which contains linear chains of cadmium atoms bridged by $Ag(CN)_2^-$ groups. These chains are linked to one another through hydrogen bonds between the uncoordinated nitrogen atoms of monodentate $Ag(CN)_2^-$ ligands, which are also bound to the cadmium atoms, and the oxygen atoms of the mea ligands, which are coordinated to cadmium atoms of adjacent chains (Figure 29).

A particularly interesting feature of this structure is that the windows of the two types of sheets have different numbers of

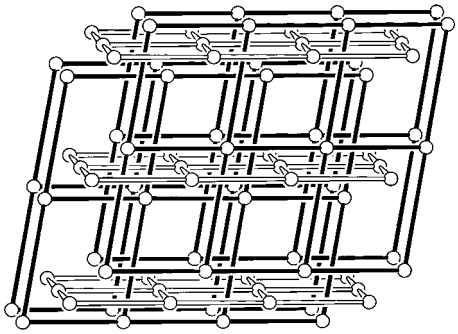

Figure 29. Schematic representation of the 2D inclined interpenetration of (4,4) sheets in the structure of $[Cd(4\text{-ampy})_2\{Ag(CN)_2\}_2] \cdot [\{Cd(mea)(4\text{-ampy})\{Ag(CN)_2\}_2]$ (4-ampy = 4-aminopyridine, mea = 2-aminoethanol). The open bonds represent the coordination polymer nets of composition $[Cd(4\text{-ampy})_2\{Ag(CN)_2\}_2]$, while the black bonds represent the sheets formed by cross-linking of coordination polymer chains of composition $[Cd(mea)(4\text{-ampy})\{Ag(CN)_2\}_2]$ through hydrogen bonds. The hydrogen bonds are represented by the almost vertical black bonds. The circles represent Cd atoms.

nets passing through them. In the first type of net two sheets of the second type pass through any given window, while in the second type only one net of the first type passes through any given window.

The structure of solvated $[Cd(py)_2\{Ag(CN)_2\}_2]$ (py = pyridine) contains (4,4) sheets composed of octahedrally coordinated cadmiums which are bound to pendant pyridine ligands and bridged by linear $Ag(CN)_2^-$ units.[49] Every ring of any sheet contains parts of two others passing through it (Figure 30). The mode of interpenetration is unrelated to the two previous modes discussed for (4,4) nets (Figures 26 and 28).

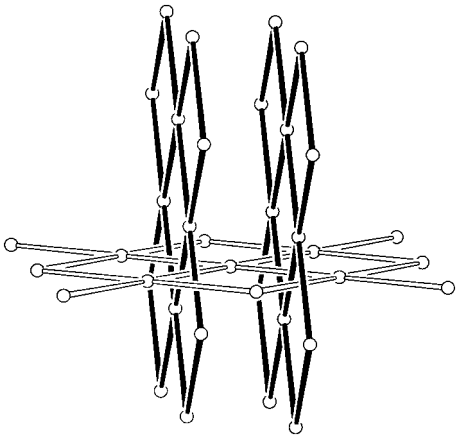

Figure 30. Schematic representation of the 2D inclined interpenetration of (4,4) sheets in the structure of $[Cd(py)_2\{Ag(CN)_2\}_2]$ (py = pyridine). Each window of each sheet, all of which are equivalent, has parts of two other sheets passing through it. The circles represent Cd atoms.

In principle, inclined interpenetration of (4,4) nets in three mutually perpendicular planes is possible (Figure 31), but no examples of this are known at present.

3.2.2. Inclined Interpenetration of (6,3) Nets

Two topologically different ways in which two inclined (6,3) nets can interpenetrate are shown in Figure 32. $[Cu_2(pz)_3]$-

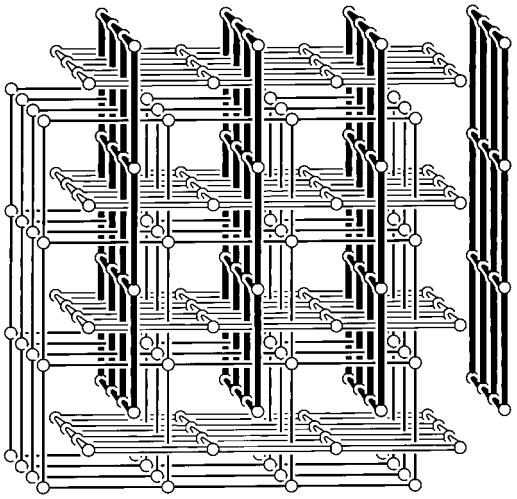

Figure 31. Hypothetical mode of interpenetration of (4,4) nets in three mutually perpendicular planes.

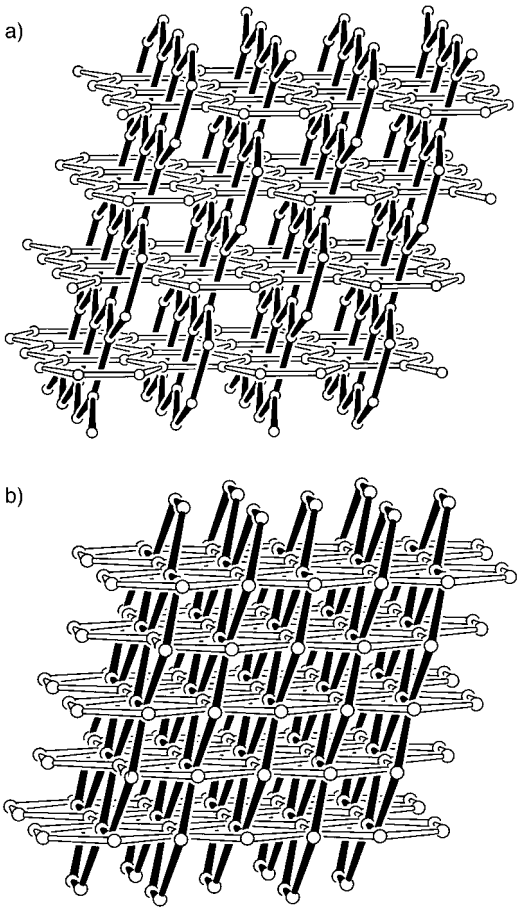

Figure 32. Two topologically different ways inclined (6,3) nets may interpenetrate.

(SiF_6) (pz = pyrazine) contains (6,3) nets in which the three-connected nodes are provided by Cu^I centers, which are each connected to three neighboring Cu^I centers through pyrazine bridges. The mode of interpenetration, shown in Figure 33, is topologically identical to that represented schematically in Figure 32a.[50]

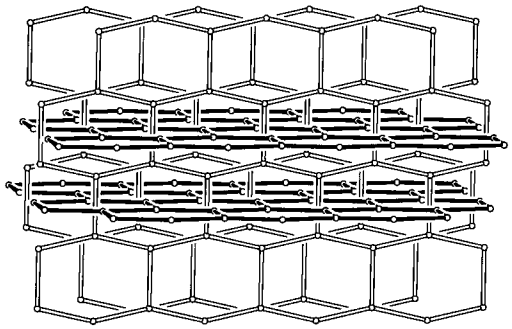

Figure 33. Inclined interpenetration of (6,3) nets in the structure of $[Cu_2(pz)_3](SiF_6)$ (pz = pyrazine). The circles represent Cu atoms.

The anionic complex $[Cu^{II}(opba)]^{2-}$ (**8**, opba = *o*-phenylenebis(oxamate)) can itself act as a bridging unit. With Mn^{II} ions this yields a (6,3) net of composition $[Mn^{II}_2(\mathbf{8})_3]^{2-}$ in which the triply chelated Mn^{II} center acts as the three-connected node. The negative charge on the 2D network is counterbalanced by the organic radical cation 2-(4-*N*-methylpyridinium)-4,4,5,5-tetramethylimidazolin-1-oxyl-3-oxide. Each (6,3) net has an infinite number of identical sheets passing through it, inclined at 72.7°, with one rod from an inclined sheet passing through every hexagon: The essential nature of the interpenetration is that represented schematically in Figure 32a. The radical cations play an important role in the overall structure, since they provide weak "axial" dative bonds through their oxygen atoms to copper centers in independent inclined sheets and thus act as weak bridging agents between sheets. There are three different paramagnetic centers present, namely, the radical cation, the copper ions, and the manganese ions; the couplings are such that the material acts as a magnet below 22.5 K.[51]

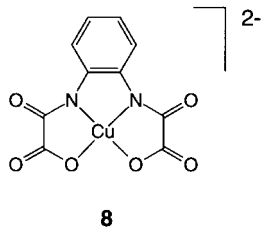

8

One example was reported recently in which every ring has components of two independent inclined (6,3) nets passing through it;[52] in this case the three-connected nodes are provided by Ag^I ions which are linked by units of **9**. This beautiful structure is an example of a 2D polyrotaxane in

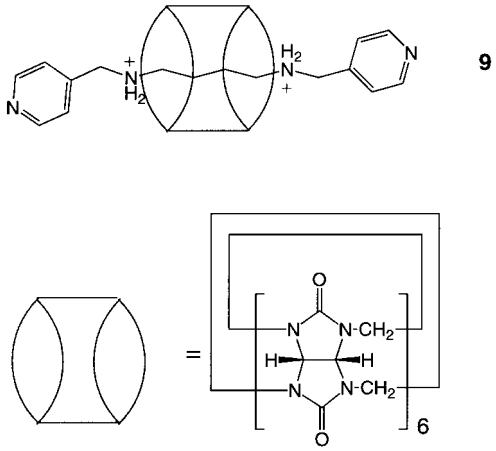

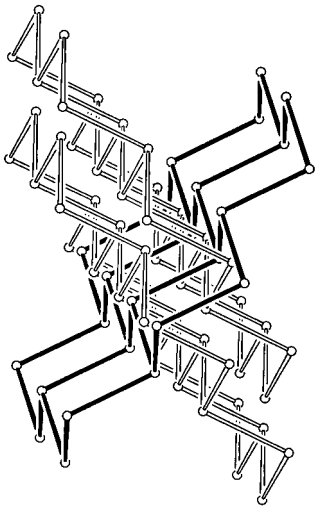

Figure 34. Representation of the interpenetration in the network of composition $[Ag_2^I(\mathbf{9})_3]$. Every hexagon has components of *two* inclined (6,3) nets passing through it. The circles represent Ag atoms.

which the beadlike component encircling the diprotonated diamine in **9** in rotaxane fashion is furnished by cucurbituril (Figure 34). All rings are equivalent, and every ring has a rod from each of two inclined sheets passing through it.

Various forms and derivatives of benzene-1,3,5-tricarboxylic acid (trimesic acid) contain hydrogen-bonded (6,3) nets of the type shown in Figure 3, which interpenetrate so that every hexagonal ring has components of three inclined sheets passing through it.[13] The essential character of the interpenetration, which is related to that in Figure 32a, is represented in Figure 35.

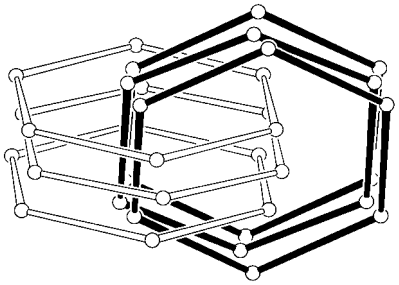

Figure 35. Schematic representation of the mode of inclined (6,3) interpenetration seen in various derivatives of trimesic acid. Every hexagon has components of three inclined independent nets passing through it in the manner shown in Figure 32a. The circles represent the midpoints of the central C_6 rings of the trimesic acid molecules.

Another example of inclined (6,3) interpenetration in which every ring has components of three independent inclined sheets passing through it is [Cu(bipy)X] (X = Cl, Br, I).[53, 54] Binuclear halide-bridged $(CuX)_2$ units play the role of the three-connected nodes; each is connected to a neighboring $(CuX)_2$ node by two side-by-side bipy ligands and to two other neighbors through single bipy units (Figure 36, the connections consisting of side-by-side bipy units are represented by two parallel lines). This example is of particular interest from the topological point of view because one of the three independent sheets, the central one, passing through any one ring adopts the interpenetration mode represented in Figure 32b, whilst the other two, which are equivalent, adopt a different mode.

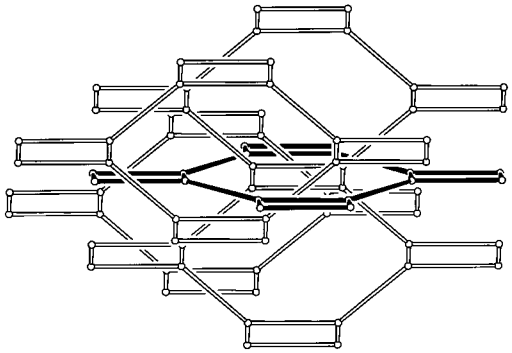

Figure 36. Structure of [Cu(bipy)X] (X = Cl, Br, I). The circles represent Cu atoms. Each "short" connection shown here is provided by two μ_2-X^- bridges. "Long" connections are provided by bipy ligands, some of which are present in close side-by-side pairs. The three-connected nodes of the (6,3) net are located at the midpoints of the $Cu(X)_2Cu$ rectangles (i.e., at the midpoints of the "short" connections shown here).

4. Interpenetrating Three-Dimensional Nets

An infinite number of different 3D nets are theoretically possible. Nevertheless, the individual 3D nets involved in interpenetration, as far as is presently known, belong to a restricted number of topological classes with only a few exceptions. This situation may of course change radically in the near future. The diamond net is by far the most common type currently known to participate in interpenetration. We classify the modes of 3D interpenetration below in terms of the topologies of the individual nets.

4.1. Interpenetrating Three-Connected Three-Dimensional Nets

All known examples of interpenetrating three-connected 3D nets are of either the (10,3)-a type or the (10,3)-b type; there is one exception of the (8,3)-c type. In view of the large number of three-connected 3D nets that are possible—no fewer than thirty topologically uniform examples were listed by Wells[4]—it is surprising that so few types are represented in real cases. However these are early days in the generation of framework structures, and perhaps this situation will change as a result of further work in the area.

4.1.1. Interpenetrating (10,3)-a Nets

Figure 37 shows a representation of the (10,3)-a net (sometimes referred to as the $SrSi_2$-related net) in its most regular form possible. It should be recalled that any net, however much it may be geometrically distorted, is considered to retain its topological identity provided connections are not broken. The net is shown in Figure 37 in its geometrically most symmetrical form (cubic), and every node shows a trigonal-planar environment with 120° angles. A characteristic feature of the (10,3)-a net is the presence of fourfold helices, all of the same handedness, running parallel with the three cubic axes (Figure 37). The net as a whole is therefore chiral. In the discussion that follows we shall refer to (10,3)-a nets contain-

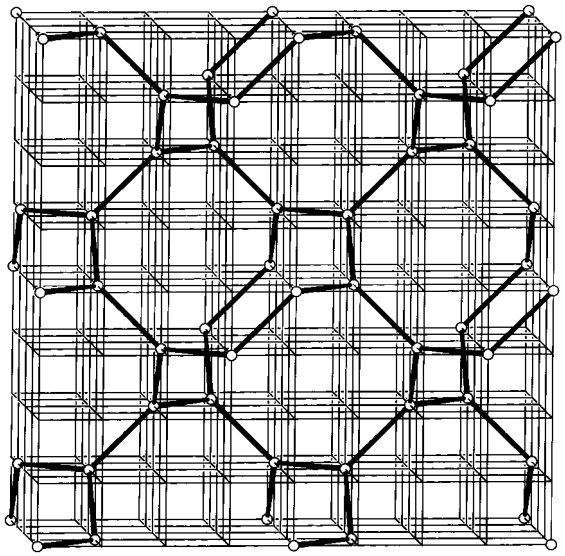

Figure 37. The (10,3)-a net in its most symmetrical form, cubic, displayed on a cubic grid.

ing right-handed fourfold helices simply as "right-handed nets".

Showing remarkable insight, Wells suggested,[4] well before real examples were discovered, that the (10,3)-a net is in principle capable of interpenetrating not only an identical net of the same handedness, but also a net of the opposite handedness. In the latter case "a three-dimensional racemate", as he referred to it, is generated that at the time was purely hypothetical. The crystal structure of cyanamide NH_2CN (Figure 38) can be regarded, because of the simplicity

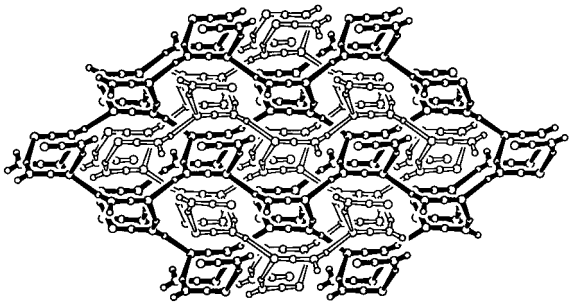

Figure 38. Two enantiomorphic interpenetrating (10,3)-a nets in the crystal structure of cyanamide NH_2CN. The circles represent in order of decreasing size N, C, and H atoms.

of its components, as the prototype for this sort of racemic interpenetration.[55] The two types of nitrogen centers provide the three-connected nodes for the hydrogen-bonded (10,3)-a net. Two such nets of opposite handedness then interpenetrate in the manner shown in Figure 38. $[Ag_2(2,3\text{-}Me_2pz)_3](SbF_6)_2$, in which the silver atoms provide the three-connected nodes, is topologically identical.[56]

Both modes of interpenetration proposed by Wells, interpenetration of a given (10,3)-a net by nets of the same handedness and by nets of the opposite handedness, are simultaneously displayed in cubic crystals of composition $[Zn(tpt)_{2/3}(SiF_6)(H_2O)_2(CH_3OH)]$ (tpt = 2,4,6-tris(4-pyridyl)-1,3,5-triazine, **10**).[57] The three-connected nodes are provided by triazine molecules. The zinc centers—with a coordination environment consisting of two *trans* tpt-pyridine donors, one SiF_6^{2-} ion bound through one F atom, two water ligands, and one methanol ligand—effectively act as linear two-connected units. Figure 39a shows one of the eight (10,3)-a nets that are present. Inspection will reveal that this is left-handed; also present are three other left-handed and four right-handed nets. Any net is related to the three others of the same handedness by half-cell translations parallel to the three cubic axes. Helices consequently appear in pairs sharing the same helical axis, an example of which is shown in Figure 39b. Each double helix makes multiple close triazine – triazine π contacts with four double helices of the opposite handedness, all with their helical axes parallel; a pair of double helices connected by such π interactions is shown in Figure 39c. The tpt units appear in close, centrosymmetrically related pairs (indicated in Figure 39c by arrows).

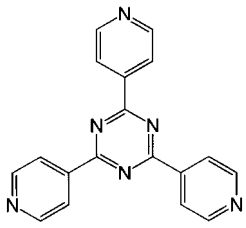

10

The mineral eglestonite of composition $[(Hg_2)_3O_2H]Cl_3$ has been described as consisting of four $[(Hg_2)_3O_2^{2+}]_n$ nets with the (10,3)-a topology.[58, 59] The oxide centers act as the three-connected nodes, and the mercurous units act as two-connected nodes that link one oxide to another. The O···O···O angles of 102.1° are close to the tetrahedral angle. This observation led us to the realization that it is possible to construct strain-free (10,3)-a nets using pyramidal three-connected nodes, provided these retain a threefold axis of symmetry, which, like the "parent" (10,3)-a net with trigonal nodes, also have cubic symmetry (indeed, the structure of H_2O_2 can be described in terms of a (10,3)-a topology with pseudo-tetrahedral centers, and $SrSi_2$ itself displays slight pyramidal distortion at each three-connected node).[4] Such a net consisting of pyramidal nodes with tetrahedral angles of 109.45° is shown in Figure 40. For ease of description, (10,3)-a nets comprising trigonal or pyramidal nodes will be referred below to as "trigonal " and "pyramidal nets", respectively. As can be seen by comparing Figures 37 and 40, the trigonal and pyramidal (10,3)-a nets differ considerably in appearance and geometry. One consequence of substituting the planar-trigonal centers by pyramidal ones is that the fourfold helices become markedly flattened. Some of these flattened helices can be seen in Figure 40; their axes are roughly perpendicular to the plane of the page, and, since the structure has cubic symmetry, equivalent flattened helices also run from left to right and from top to bottom. The (10,3)-a nets present in eglestonite, two right-handed and two left-handed (Figure 41), are very similar to the idealized net shown in Figure 40. The flattened helices of two nets of the same handedness share a common axis, and they can be related by a translation along this shared axis of half the helical period combined with a 90° rotation (Figure 41). Two pyramidal nets of the same handedness can be derived from a single trigonal net of the same handedness by distorting each individual node into a pyramidal geometry in the appropriate direction along

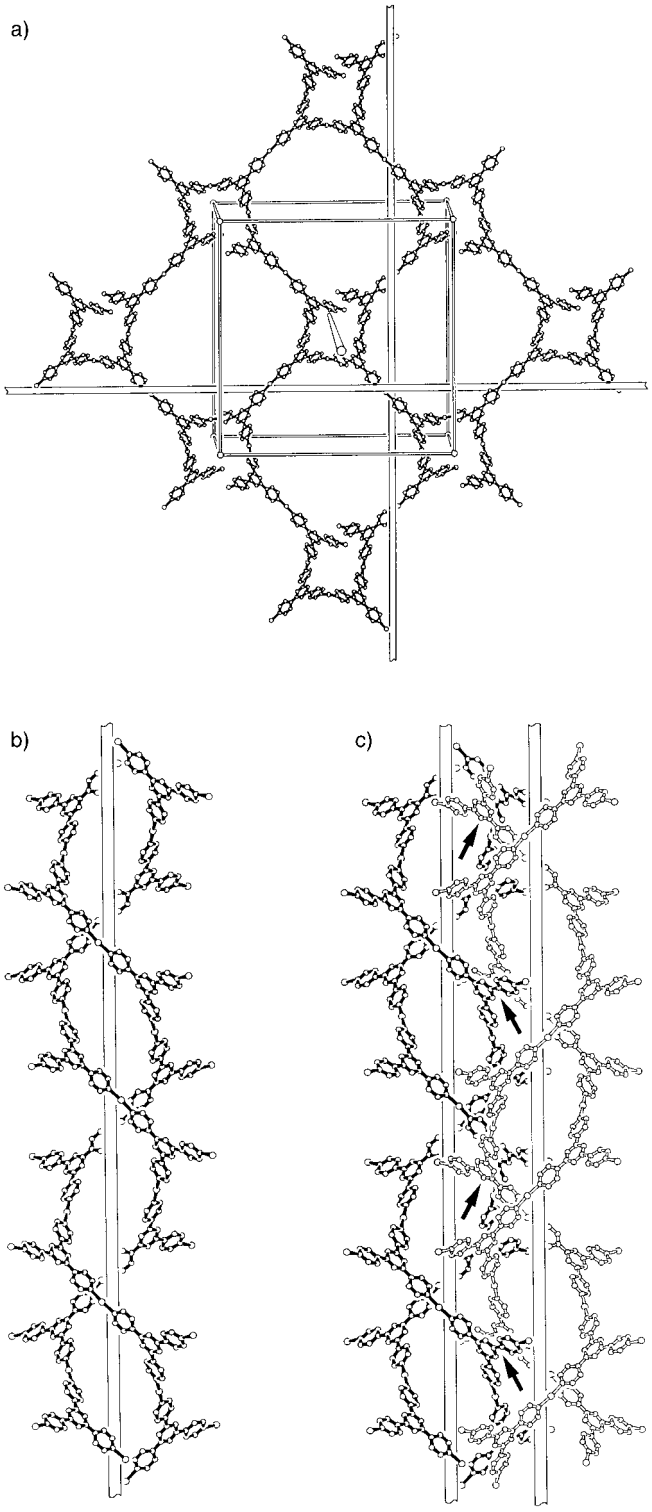

Figure 39. a) One of the eight (10,3)-a nets present in $[Zn(tpt)_{2/3}(SiF_6)(H_2O)_2(CH_3OH)]$ (tpt = **10**). The larger circles represent Zn atoms, and the smaller circles C and N atoms. b) A double helix. c) A π-contacting pair of double helices of opposite handedness. The arrows indicate centrosymmetrically related π-contacting pairs.

the normal to the trigonal plane (Figure 42); two directions of distortion are possible, hence the existence of two derived pyramidal nets. Conversely, the trigonal net can be derived from the two pyramidal nets by placing a trigonal node at the

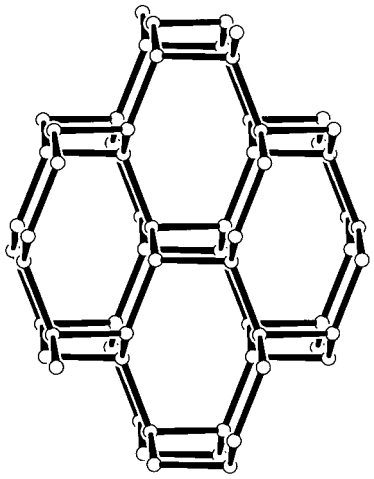

Figure 40. A (10,3)-a net constructed from pyramidal nodes with tetrahedral angles.

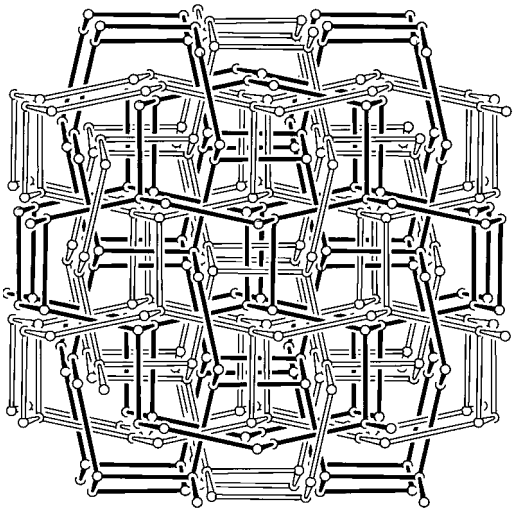

Figure 41. Four "pyramidal" (10,3)-a nets, two right-handed and two left-handed, in eglestonite. The circles represent O atoms.

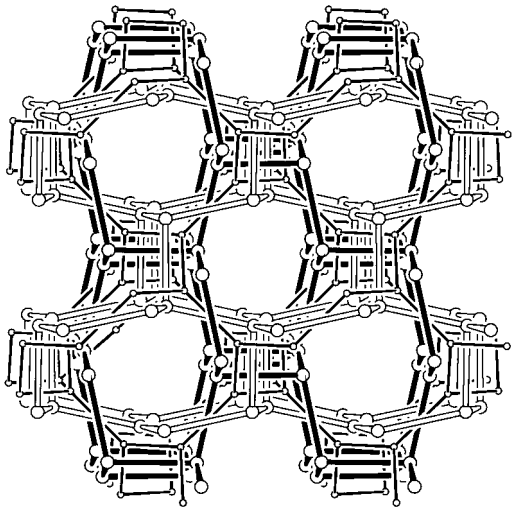

Figure 42. Relationship between a "trigonal" (10,3)-a net and the two possible derived "pyramidal" (10,3)-a nets.

midpoint between two directly neighboring pyramidal nodes of independent nets that share the same threefold axis, as can also be seen in Figure 42. In eglestonite the helices of the second pair of nets with handedness opposite to that of the first pair are then located in the channels generated by the first pair (Figure 41).

In many of the structures discussed here it is debatable how independent the various nets are. It is convenient to describe the structure of eglestonite in terms of four "independent" (10,3)-a nets, as we have done above (and as others have done previously, although not in the detail presented here). However, the fact is that the pyramidal oxygen centers from adjacent nets form short hydrogen bonds ($O \cdots O \approx 2.5$ Å;[58] note the presence of one proton per two oxides in the composition).

In cubic $RhBi_4$ all Rh centers are equivalent and provide the nodes for a four-connected 3D net.[60] Bi_2 units connect Rh atoms, and every Rh is immediately surrounded by four Bi_2 pairs. The four-connected net thus formed has previously and correctly been described as possessing the $3^2 10^4$ topology, which in fact is chiral. In $RhBi_4$ two such nets of opposite handedness interpenetrate, as shown in Figure 43. The units

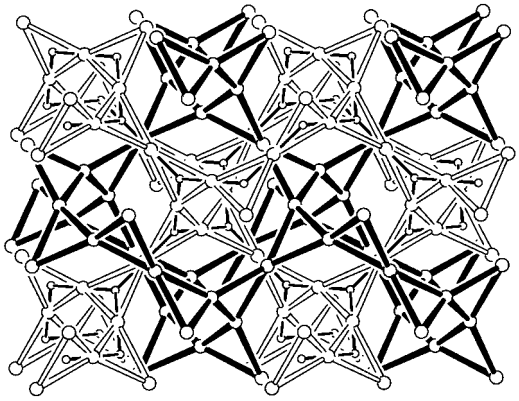

Figure 43. Two interpenetrating $3^2 \cdot 10^4$ nets of opposite handedness in the structure of $RhBi_4$. The circles represent Rh atoms. The midpoints of the Rh_3 triangles within a particular $3^2 \cdot 10^4$ net form a (10,3)-a net. The (10,3)-a net derived from the $3^2 \cdot 10^4$ net represented here by "open" connections is indicated by fine lines and smaller circles. For clarity the (10,3)-a net derived from the other net is omitted.

linked together are triangular Rh_3 groups; each triangle is linked to three others through shared Rh vertices. It is helpful to conceptually simplify these nets to the (10,3)-a form in which the midpoints of the Rh_3 triangles now provide the three-connected nodes (Figure 43). $RhBi_4$, which has the same space group as eglestonite (*Ia3d*), can thus be seen as yet another example of the type of 3D racemate predicted by Wells.

4.1.2. Interpenetrating (10,3)-b Nets

The (10,3)-b net (sometimes referred to as the $ThSi_2$-related net) is tetragonal in its most symmetrical form (Figure 44). As in (10,3)-a nets, the nodes have 120° angles. Each node is connected to two neighbors in a 1D planar zigzag strip. The third connection at every node is to a node belonging to a

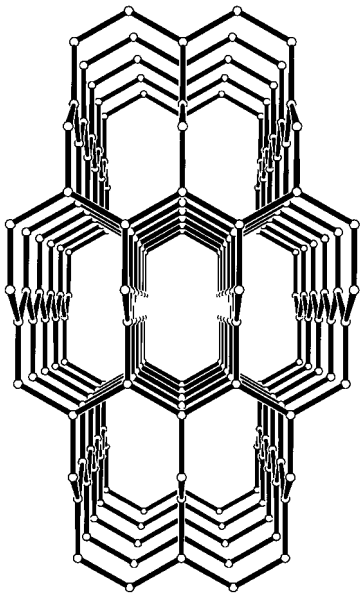

Figure 44. The (10,3)-b net in its most symmetrical form (tetragonal).

zigzag strip running perpendicular to the first. Alternate nodes within a strip are connected to a strip above it, then a strip below it, and so on. An interesting feature of this net is that it can be "collapsed" by concerted rotation around the strip–strip connections of all the strips in one direction relative to all those in the other direction. This collapse does not interfere with the trigonal geometry of the individual nodes; it merely reduces the angle between connected zigzag strips. This collapse is seen in real cases to extents that vary so as to achieve optimum packing.

A characteristic structural motif in the (10,3)-b net that parallels the adamantane motif in the diamond net is the cagelike unit shown in Figure 45a. Indeed, the (10,3)-b net

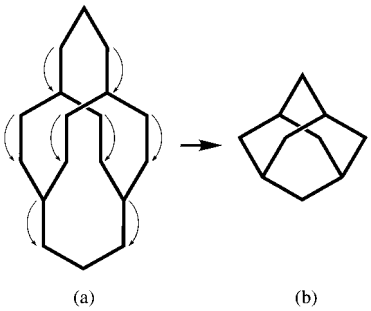

Figure 45. The imaginary contraction and fusion process relating a "(10,3)-b cage" (a) of the (10,3)-b net to an adamantane cage (b) of the diamondlike net.

and the diamond net are very closely related, in that the former can be converted into the latter by contraction of the links between the zigzag strips (i.e., the links aligned with the tetragonal axis in the most symmetrical form of the (10,3)-b net) to the point where the two three-connected nodes fuse together to become a single four-connected node. Figure 45 illustrates this imaginary conversion of a (10,3)-b cage into an adamantane cage. Just as the nature of the interpenetration of

diamond nets can most simply be understood by focussing on the way one adamantane unit is interpenetrated by others (as we saw in the example of $[Zn(CN)_2]$ in Section 1.5 and as we shall see in more complicated examples in Section 4.2.1), the nature of the interpenetration of (10,3)-b nets can be best appreciated by looking at the way one (10,3)-b cage is interpenetrated by others.

Examples are known in which two, three, and six independent (10,3)-b nets interpenetrate. The mineral neptunite, $M^I_4M^{II}_2(TiO)_2Si_8O_{22}$ ($M^{II} = Fe^{II}$, Mg^{II}, Mn^{II}; M^I = alkali metal), contains two infinite polysilicate (10,3)-b nets, one of which is shown in Figure 46a, that interpenetrate in the manner depicted in Figure 46b.[61] The three-connected nodes are provided by SiO_4 tetrahedra that each carry one terminal, nonbridging SiO^- unit and are represented as Si^3 below. Present in equal numbers are two-connected SiO_4 tetrahedra, each carrying two terminal SiO^- groups (represented as Si^2 below). The zigzag planar strips that are characteristic of the (10,3)-b net consist in neptunite of alternating long and short bonds between three-connected nodes. The the short bonds consist of direct connections between Si^3 centers, and the long bonds have two Si^2 centers interposed between Si^3 nodes to produce the sequence $\cdots Si^3Si^3Si^2Si^2Si^3Si^3Si^2Si^2\cdots$ within a strip (Figure 46a). Zigzag strips of this type run from top right to bottom left and also from top left to bottom right. Also apparent in Figure 46a are channels running perpendicular to the plane of the page, that is, parallel to what would have been the tetragonal axis if the net had not been deformed. The interpenetration is such that the connections between zigzag strips within one net are located along the centers of these channels in the other net (Figure 46b).

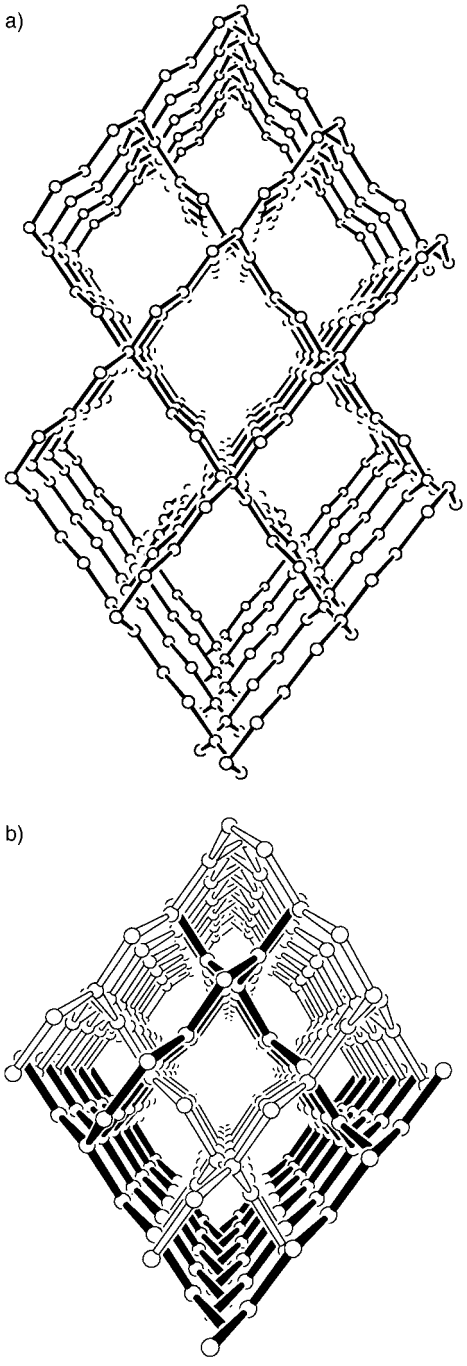

Figure 46. a) A single (10,3)-b net in neptunite. The circles represent Si atoms. b) Two interpenetrating nets in neptunite.

Two interpenetrating (10,3)-b nets are present in crystals of solvated $[(ZnCl_2)_3(tpt)_2]$ (tpt = **10**).[28] The three-connected nodes are provided by the triazine molecules. The zinc centers have an approximately tetrahedral coordination environment consisting of two tpt-pyridine and two chloro ligands, and therefore act as angular two-connectors. As a consequence, the resulting (10,3)-b net (Figure 47a) is considerably distorted. Figure 47b shows the two interpenetrating (10,3)-b nets.

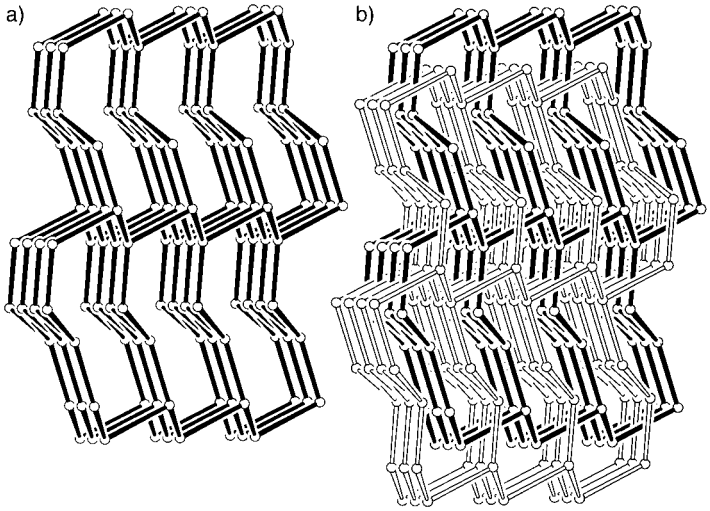

Figure 47. a) One of the two (10,3)-b nets in the structure of $[(ZnCl_2)_3(tpt)_2]$ (tpt = **10**). The circles represent the centers of triazine rings. b) Two interpenetrating (10,3)-b nets.

Three independent, identical, and interpenetrating (10,3)-b nets are seen in $[Ag_2(pz)_3](BF_4)_2$.[62] Silver atoms provide the three-connected nodes, which are linked together through bridging pyrazine units. The nets are collapsed, so that the angle between zigzag strips is 55.4°. Figure 48a shows three unit cells stacked along the *a* direction. One net can be generated from another by a (1,0,0) translation; but a shorter translation (1/2, 1/2, 0) also relates one net to another. Every decagon has one rod from each of the other two nets passing

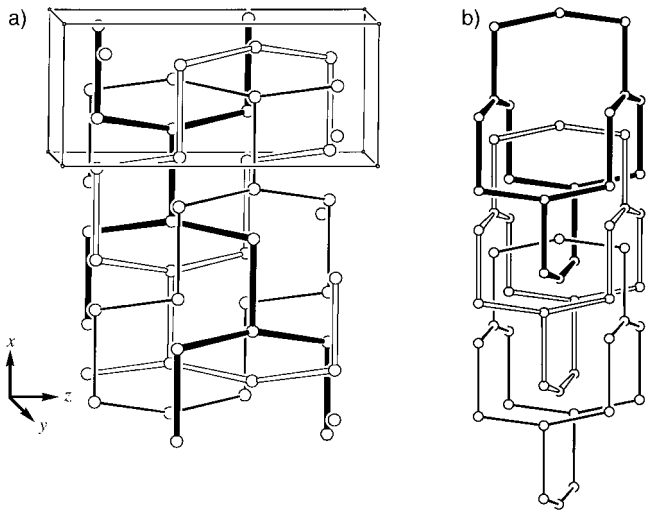

Figure 48. a) Three unit cells in the structure of $[Ag_2(pz)_3](BF_4)_2$. The circles represent Ag atoms. b) Three interpenetrating "(10,3)-b cages" from separate nets.

through it. Three interpenetrating (10,3)-b cages from separate nets are shown in Figure 48b.

With regard to the general question concerning the circumstances under which an interpenetrating structure or a noninterpenetrating alternative form, it is interesting that out of the same reaction mixture a second type of crystal can be obtained with the same $[Ag_2(pz)_3]^{2+}$ framework composition but with a different and noninterpenetrating structure: the 2D (6,3) net. This can be viewed as consisting of the same zigzag strips joined together in a coplanar fashion to give the 2D structure, rather than joined together at an angle to give the 3D (10,3)-b net.

A second example of threefold interpenetration of (10,3)-b nets is provided by a material of composition $[CrP_3S_{9+x}]$ ($x \approx 0.25$),[63] which consists of Cr^{III} centers interconnected through bridging $P_2S_6^{2-}$ ligands (**11**), a small fraction of which (approximately 1 in 12) have been replaced by $P_2S_8^{2-}$ (**12**). Both ligands act as bidentate chelating agents at both ends. The Cr^{III} centers are therefore in a triply chelated pseudo-octahedral coordination environment of six sulfur atoms and provide the three-connected, essentially trigonal nodes for the (10,3)-b nets. The three independent nets interpenetrate in a manner topologically identical to that described above for $[Ag_2(pz)_3](BF_4)_2$.

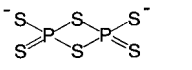

11

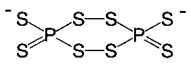

12

Another system that has been described in terms of three interpenetrating three-connected nets, which we have noticed have the (10,3)-b topology, is $[Ag(bipy)]NO_3$.[64] Linear polymeric chains consisting of alternating bridging bipy units and linearly coordinated silver centers are cross-linked through Ag–Ag interactions at a distance of 2.977(1) Å to give the 3D (10,3)-b net in which the three-connected nodes are the T-shaped metal centers. Three such nets then interpenetrate (Figure 49a). Three (10,3)-b nets that interpenetrate in a manner topologically identical to that observed for $[Ag(bipy)]NO_3$ are shown in their idealized, most symmetrical form in Figure 49b. This figure was constructed to facilitate comparison with Figure 48b; the two modes of threefold interpenetration are clearly topologically different.

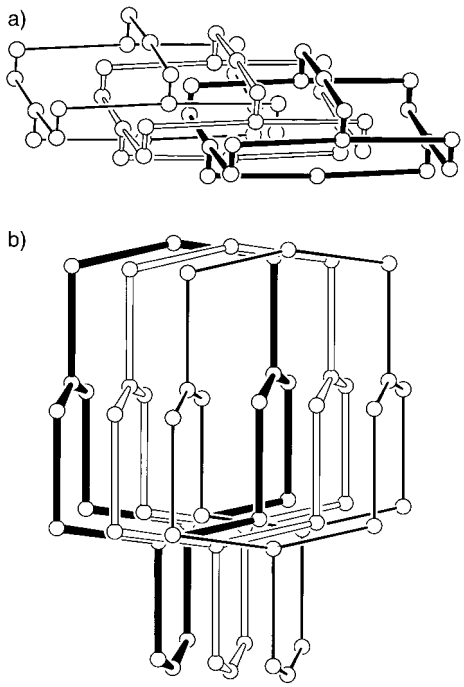

Figure 49. a) Three interpenetrating (10,3)-b nets with T-shaped three-connected nodes in the structure of $[Ag(bipy)]NO_3$. The circles represent Ag atoms. "Long" connections represent bridging bipy units, and "short" connections are direct Ag···Ag interactions. b) An idealized version of the mode of interpenetration of three (10,3)-b nets, of the type seen in $[Ag(bipy)]NO_3$.

Two examples are known of sixfold (10,3)-b interpenetration. One of these is solvated $[Ag(teb)]CF_3SO_3$ (teb = **7**),[65] which contains two types of three-connected nodes provided by alternating **7** and silver centers. Figure 50 shows a representation of the way in which (10,3)-b cages from five other independent nets interpenetrate a given (10,3)-b cage. The central C_6 rings of units of **7** from independent nets are stacked (with minor deviations) along the direction AB shown in Figure 50 (which corresponds to the crystallographic *a* axis). It is worth noting that this structure is a polymorph of an earlier structure discussed which has six parallel interpenetrating (6,3) 2D nets.

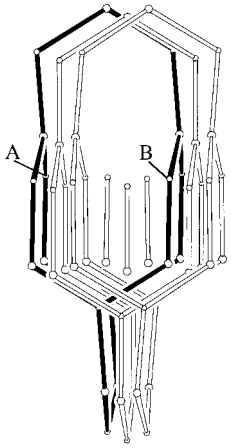

Figure 50. Representation of six independent interpenetrating (10,3)-b cages in $[Ag(teb)]CF_3SO_3$ (teb = **7**). The smaller circles represent centers of ligands **7**, and the larger circles represent Ag atoms. Analogous ligand nodes of independent nets are stacked (with minor deviations) along the line AB. For clarity only a single rod of three of the nets is shown.

The second example of sixfold interpenetration of (10,3)-b nets, $[Cu_2(bipy)_3](NO_3)_2 \cdot 2.5\,H_2O$,[66] differs from the one just described in that all the three-connected nodes are of the same type: Cu^I ions. The topology of interpenetration is distinctly different, as can be seen in

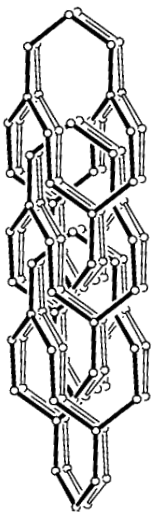

Figure 51. Six interpenetrating "(10,3)-b cages" from separate nets in the structure of $[Cu_2(bipy)_3](NO_3)_2 \cdot 2.5\,H_2O$. The circles represent Cu atoms.

Figure 51, which shows (10,3)-b cages from six independent nets. The nets are present in closely spaced pairs, and each pair is interpenetrated by the two other pairs in much the same way as a single (10,3)-b cage was interpenetrated by two other single (10,3)-b cages in the examples of threefold interpenetrating in Figure 48b. The comparison between sixfold interpenetration in $[Cu_2(bipy)_3](NO_3)_2 \cdot 2.5\,H_2O$ and threefold interpenetration in $[Ag_2(pz)_3](BF_4)_2$ is interesting, because both contain trigonal metal nodes that are linked through linear bridging ligands of very similar girth, but the longer bipy units allow a much greater degree of interpenetration.

4.1.3. Interpenetrating (8,3)-c Nets

Figure 52 shows a representation of the (8,3)-c net in its most symmetrical form, which has a hexagonal unit cell. All nodes, of which there are two types, have 120° angles. The plane of one type of node is normal to the hexagonal axis, and the second type of node, of which there are three times as many, forms planar zigzag strips that run parallel with the hexagonal axis. It has previously not been appreciated that $Na[Ti_2(PS_4)_3]$[67] contains

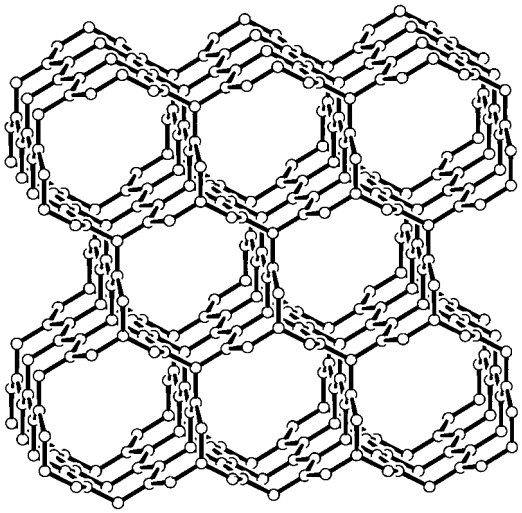

Figure 52. The (8,3)-c net in its geometrically most symmetrical form (hexagonal).

(8,3)-c nets. The Ti^{IV} centers are chelated by three bidentate PS_4^{3-} ligands, which in turn act as μ_2 ligands and bind two metals each by a bidentate interaction. The metal centers thus provide the trigonal nodes for the (8,3)-c net. Two nets of this type then interpenetrate as shown in Figure 53. An important feature is that the nodes normal to the hexagonal axis from the two nets are arranged in a colinear and equidistant fashion. If the nets were in their most symmetrical form, this interpenetration mode would lead to aclash between the zigzag strips from the two nets. Deformation of the nets depicted in Figure 53 allows the zigzag strips to avoid each other.

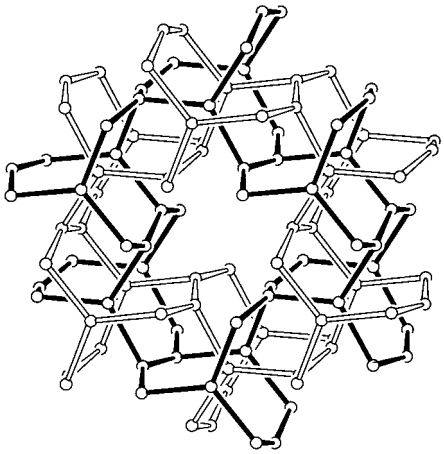

Figure 53. Two interpenetrating (8,3)-c nets in the structure of $Na[Ti_2(PS_4)_3]$. Three-connected nodes are located at the Ti centers, represented here by circles. PS_4^{3-} ions act as μ_2-bis-bidentate bridging ligands connecting the Ti nodes.

4.2. Interpenetrating Three-Dimensional Four-Connected Nets

4.2.1. Interpenetrating Diamondlike Nets

By far, the largest class of interpenetrating structures involves diamond-related nets. The twofold interpenetrating structure of $[Zn(CN)_2]$ has already been described in Section 1.5.[6, 21, 22] Examples are known of degrees of interpenetration ranging from two- to ninefold (Table 1). With, to the best of our knowledge, only one exception which is discussed below, the modes of interpenetration in all these examples are closely related. In an undeformed (cubic) diamondlike net each adamantane unit possesses three orthogonal twofold rotation axes aligned parallel with the cubic axes. One of these twofold axes running from top to bottom is shown in Figure 54. The common interpenetration mode is such that the nodes of independent nets are aligned and equally spaced along one of these twofold axes. To illustrate this common *n*-fold interpenetration mode, we show in Figure 55 a representation of a ninefold interpenetrating system in which the nodes of eight other nets are arranged equally spaced between the top-most and bottom-most extremities of an adamantane unit of the "first" net.[68] As can be seen here, and as is often the case, the individual nets are distorted so as to elongate the adamantane units along the

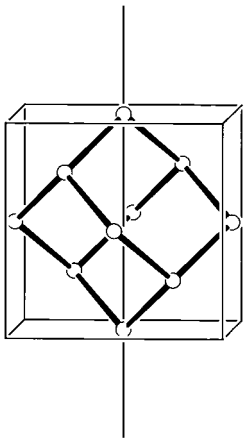

Figure 54. One of the twofold rotation axes in an adamantane component of a diamond-related net.

Table 1. Interpenetrating diamond-related nets; n = number of nets.

Compound[a]	n	Comments	Ref.
Various organic polymers	2 or 3		[81]
Two lipid – water phases	2		[82]
M_2O (M = Cu, Ag, Pb)	2		[59, 84, 85]
$CaWO_4$ (scheelite) and related structures (e.g. $[NH_4][ReO_4]$), $ZrSiO_4$ (zircon) and related structures	2	Diamond nets can be constructed.	[85 – 87]
$MO \cdot 2B_2O_3$, (M = Li_2, Mg, Zn, Cd, Mn, Fe, Co, Ni, Hg), α-$Na_2O \cdot 3B_2O_3$, $MO \cdot 4B_2O_3$ (M = Ag_2, Na_2, Ba), $MO \cdot 5B_2O_3$ (M = K_2 (α and β forms), Rb_2, Tl_2), $Cs_2O \cdot 9B_2O_3$	2	Diamond nets are constructed from borate frameworks, and the clusters within these frameworks act as the tetrahedral nodes. Intercalated M atoms link the nets through M – O interactions in many cases.	[88]
$K_2[PdSe_{10}]$	2	Each net has a different composition.	[80]
Some high-pressure forms of ice (ice VII and VIII)	2	Ice VII is orientationally disordered, whereas ice VIII is not.	[89]
2,6-Dimethylideneadamantane-1,3,5,7-tetracarboxylic acid		Hydrogen-bonded; four structures with different guests.	[71]
$[M_2(C_6H_2O_4)_3] \cdot 24H_2O$ (M = lanthanide, Y)	2	Diamond net with one link being a hydrogen-bonded water cluster; hydrogen bonding between nets.	[79]
$K_2[M\{NC_5H_3(CO_2)_2\}_2]$ (M = Mn, Zn)	2		[78]
$[HN(CH_3)_3]_2[Sn_5S_9O_2]$	2	Tetrahedral $Sn_{10}S_{20}O_4$ clusters linked through S atoms.	[90]
$[Si(NCN)_2]$	2		[91]
$CBr_4 \cdot$ hmta	2	Nets containing N – Br interactions.	[92]
$[Si(C_5H_4NO)_4]$	2	Hydrogen-bonded nets containing various guests.	[72, 73]
$[M(CO)_3(\mu_3\text{-}OH)]_4 \cdot 2L$ (M = Mn, Re; L = hydrogen-bonding, bridging ligand)	2, 3, or 4	Hydrogen bonds between tetrahedral clusters.	[8, 93]
$[SCd_8\{SCH(CH_3)C_2H_5\}_{12}(CN)_2]$	2	Clusters form the nodes of the nets.	[94]
$[Cd_{17}S_4(SCH_2CH_2OH)_{26}]$	2	Clusters form the nodes of the nets.	[95]
$[M(CN)_2]$ (M = Zn, Cd)	2		[6, 21, 22, 76]
$[Cu(L)_2](ClO_4)$ (L = 4-cyanopyridine)	2		[96]
[Cd(en)Cd(CN)$_4$]	2	Net with four-connected nodes, which can be related to a diamond net where the nodes are $Cd(CN)_4$ squares.	[71, 97]
$Li_5B_7S_{13}$, $Li_9B_{19}S_{33}$	2	Nodes are boron sulfide clusters.	[98]
Tetrasodium 1,3,5,7-adamantanetetracarboxylate tetrahydrate	3	Hydrogen-bonded.	[99]
2,6-Dioxoadamantane-1,3,5,7-tetracarboxylic acid (hydrate)	3	Hydrogen-bonded; contains acetic acid guests.	[70]
3,3-Bis(carboxymethyl) glutaric acid ("methanetetraacetic acid")	3	Hydrogen-bonded.	[87]
All-*trans*-cyclobutane-1,2,3,4-tetracarboxylic acid	3	Hydrogen-bonded.	[71]
4,4′,4″,4‴-Tetraphenylmethanecarboxylic acid	3	Hydrogen-bonded.	[100]
[Cu(CN)(L)] (L = 4-cyanopyridine)	3		[101]
$[Ag_2\{OOC(CH_2)_2COO\}]$	3	Ag_4 clusters bridged by chelating bridges.	[102]
$[Cd(mea)(dahxn)\{Ni(CN)_4\}] \cdot H_2O$	3		[103]
$[Cu(dmtpn)_2](X)(dmtpn)(THF)$ (X = BF_4, ClO_4)	3		[104]
Disodium and dipotassium dihydrogen 1,3,5,7-adamantanetetracarboxylate	4	Hydrogen-bonded.	[99]
$[Cu(Hcmp)_4](X)$ (X = PF_6, CF_3SO_3)	4	Nets with hydrogen bonding between CuL_4 molecules.	[105]
$[Cu(bipy)_2(PF_6)]$	4		[50, 106]
$[M(bipy)_2](CF_3SO_3)$ (M = Ag, Cu)	4		[107]
$[Ag(L)_2](BF_4)$ (L = 4-cyanopyridine)	4		[107]
Adamantane-1,3,5,7-tetracarboxylic acid	5	Hydrogen-bonded; different mode of interpenetration.	[69]
$[Cu(L)_2](BF_4)$ (L = 1,4-dicyanobenzene)	5		[44]
$[Cu\{bpe\}_2](BF_4)$	5	CH_3CN or CH_2Cl_2 guest molecules.	[54, 108]
$[Zn(L)_2](ClO_4)_2$ (L = $^-O_2CCH_2CH_2N^+(CH_2CH_2)_3N^+$-$CH_2CH_2CO_2^-$	6		[109]
$[Cu\{NC(CH_2)_4CN\}_2](NO_3)$	6		[110]
$[Cu(bpb)_2](X)$ (X = ClO_4, BF_4)	6		[46]
$[Cu(R^1,R^3\text{-dcnqi})_2]$ and deuterated derivatives (R^1,R^3 = CH_3, CH_3O, Cl, Br, I)	7	With Li or Ag in place of Cu: isomorphous; with Na, K, NH_4, Rb, or Tl in place of Cu: very closely related structures (but no longer separate, interpenetrating frameworks).	[83]
$[C(C_6H_5CCC_5H_4NO)_4]$	7	Hydrogen-bonding nets containing various guests.	[73, 74]
$[Si(C_6H_5CCC_5H_4NO)_4] \cdot 2G$ (G = valeric acid)	8	Hydrogen-bonded	[73, 75]
$[Ag(4,4'\text{-}NCC_6H_4C_6H_4CN)](XF_6)$ (X = P, As, Sb)	9		[68]

[a] Abbrivations used: hmta = hexamethylenetetramine; en = ethylenediamine; mea = 2-aminoethanol; dahxn = 1,6-diaminohexane; dmtpn = 2,3-dimethylterephthalonitrile; bipy = 4,4′-bipyridine; Hcmp = 3-cyano-6-methyl-2(1*H*)-pyridinone; bpe = *trans*-1,2-bis(4-pyridyl)ethene; bpb = 1,4-bis(4-pyridyl)-butadiyne; dcnqi = N,N′-dicyanoquinodiimine.

shared twofold axis. In the general n-fold interpenetrating case, the translation of $1/n$ times the length of the adamantane unit along the direction of the shared twofold axis corresponds to one of the unit cell dimensions (generally the shortest).

The only exception to this general pattern is seen in the unusual fivefold mode of interpenetration shown by crystalline adamantane-1,3,5,7-tetracarboxylic acid.[69] The structure is contrasted in Figure 56 with that of the "normal" mode of fivefold interpenetration. In this exceptional case the inde-

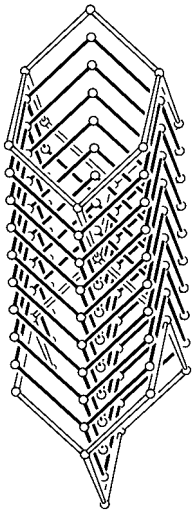

Figure 55. Representation of the structure of $[Ag(L)_2](PF_6)$ (L = 4,4′-biphenyldicarbonitrile) consisting of nine interpenetrating diamondlike nets. The circles represent Ag atoms. The dinitrile ligand links Ag atoms to each other.

pendent nets are related not by the usual translation of $1/n$ (i.e., 1/5) of the distance across an adamantane unit along a shared twofold axis (Figure 56a), but rather by the translation indicated in Figure 56b.

Interpenetration can be regarded as a space-filling device, but in some cases relatively large intraframework spaces remain even after "optimum" interpenetration has taken place; this is true of the normal mode of diamondlike interpenetration. Figure 57 shows an example of a normal fivefold interpenetrating system, the structure of $[Cu(L)_2]BF_4$ (L = 1,4-dicyanobenzene),[44] viewed slightly displaced from the shared twofold axis. As can be seen, channels of rhombic cross-section running parallel with the twofold axis are generated. In $Cu[(L)_2]BF_4$ (L = 1,4-dicyanobenzene) these channels are occupied by the BF_4^- ions, but in cases where the networks are electrically neutral the channels may be occupied by significant quantities of solvent.[70–75]

In many of the examples presented in Table 1 the four-connected nodes of the diamondlike nets are to be found at the midpoints of complex clusters of atoms. A detailed discussion is precluded here by space restrictions.

$[Cd(CN)_2]$ derivatives, besides adopting a wide range of framework structures which are interesting in their own right, are important in the context of interpenetration because they demonstrate how interpenetration can be prevented by the inclusion of guests. $[Cd(CN)_2]$ itself is isostructural with $[Zn(CN)_2]$, consisting of two interpenetrating diamondlike nets.[6, 22, 76] However, when it is crystallized in the presence of certain organic solvents, such as chlorinated solvents, the crystals contain a *single* diamondlike framework with guest solvent molecules occupying the spaces where the second network is found in the parent structure.[22, 77] $[Me_4N][CuZn(CN)_4]$, whose structure was truly crystal-engineered, contains a single diamond-related anionic $[CuZn(CN)_4]^-$ network with NMe_4^+ counter cations occupying half the adamantane cavities thereby preventing interpenetration.[6] In relation to the general question of whether interpenetration will or will not occur in a particular case, the example of heavily solvated $[Cu^I\{(4\text{-}NCC_6H_4)_4C\}](BF_4)$ is interesting: Despite the fact that the framework occupies only about a third of the volume of the crystal and that there is ample space for a second network to interpenetrate, this does not occur.[6, 7]

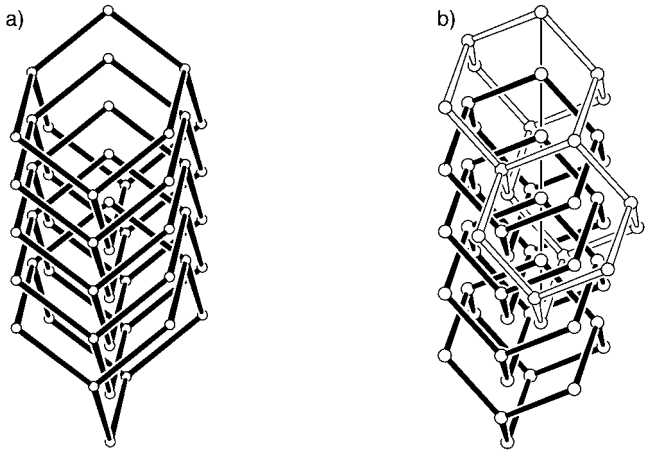

Figure 56. a) The "normal" mode of fivefold interpenetration of diamondlike nets, as seen in $[Cu(L)_2]BF_4$ (L = 1,4-dicyanobenzene). The circles represent Cu atoms. b) The "abnormal" mode of fivefold interpenetration, as seen in adamantane-1,3,5,7-tetracarboxylic acid, showing the translational relationship between independent nets. Two adamantane units of one of the nets fused together by one shared rod are represented here with open connections. Nodes of the remaining four nets are then equally spaced along the vector indicated here by a fine line joining the top-most node to the bottom-most node of the pair of adamantane units in the first net. The circles represent the centers of the molecules.

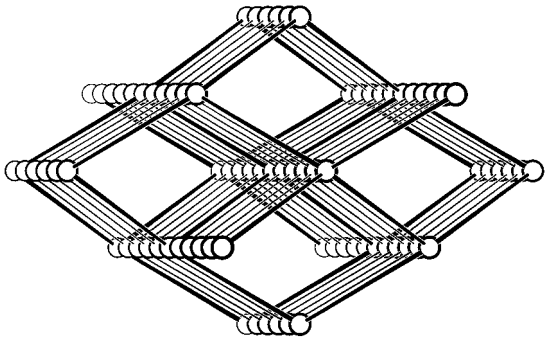

Figure 57. The fivefold interpenetrating diamondlike framework system in $[Cu(1,4\text{-dicyanobenzene})_2]BF_4$; the view is slightly displaced from the shared twofold axis. The circles represent Cu atoms.

Crystals of composition $K_2[M(L)_2]$ (M = Zn, Mn; L = pyridine-2,3-dicarboxylate) are noteworthy because they contain two chiral interpenetrating diamondlike nets with opposite handedness.[78] The ligands bridge between metal centers by chelating to one and binding to the second through the 3-carboxylate donor. Every metal center has a coordination environment consisting of two N,O chelating units and two monodentate carboxylate donors which are *cis* to each other. In one net all metals have the *Λ* configuration, whilst in the other net all are Δ.

The networks in most of the systems listed in Table 1 are formed with either hydrogen bonds or metal–ligand bonds. Both types of interactions are present in the two diamondlike networks in $[Ce_2^{III}(dhbq)_3]\cdot 24H_2O$ ($dhbq^{2-}$ = dianion of 2,5-dihydroxy-1,4-benzoquinone H_2dhbq).[79] This is yet another example for which the degree of independence of the two nets is debatable, because there is evidence of hydrogen bonding between the nets.

$K_2[PdSe_{10}]$, which will be discussed in Section 4.5.1, is unusual in that it contains two *different* diamondlike nets that interpenetrate.[80]

Two- and threefold interpenetrating diamondlike structures have been proposed for certain organic polymers,[81] and a "structure" based on twofold interpenetration of diamond-related nets has been suggested for two lipid/water phases.[82]

A series of compounds of composition $[Cu\{R^1,R^2\text{-dcnqi}\}_2]$ (dcnqi = *N*,*N*′-dicyanoquinonediimine; R^1, $R^2 = CH_3, CH_3O$, Cl, Br, I) consist of seven interpenetrating diamondlike nets.[83] As a result of the interpenetration, the planar aromatic rings form infinite stacks showing close $\pi-\pi$ contacts, which are thought to be responsible for the metallike electrical conductivity. These are significant examples that point to the potential of interpenetration as a source of interesting or useful physical properties.

4.2.2. Interpenetrating Quartzlike Nets

The structures of $[M\{Au(CN)_2\}_2]$ (M = Zn,[111] Co[112]) consist of six interpenetrating 3D nets with the same connectivity as quartz, which, like the NbO net discussed below, has a 6^48^2 topology (Wells designates the NbO net as 6^48^2-a and the quartz net as 6^48^2-b). The structure of a single, chiral net is shown in Figure 58a, and the way the six nets, all of the same handedness, interpenetrate is shown in Figure 58b. The metal centers provide the four-connected pseudo-tetrahedral nodes, and the links between them are provided by approximately linear $Au(CN)_2^-$ bridges whose considerable length combined with small girth make possible the relatively high degree of interpenetration. Based on the number of examples known at present, there is an apparent marked preference of interpenetrating four-connected nets with essentially tetrahedral nodes to adopt the topology of diamond rather than that of quartz. This may arise from the fact that the idealized quartz net with linear connecting rods requires considerable distortion from regular tetrahedral geometry at the four-connected nodes, whereas in the diamond case linear rods and regular tetrahedral nodes are exactly suited to each other. When the rods are appropriately bent this situation may be reversed; for example, the bent connecting rod provided by the angular two-connected oxygen atom in SiO_2 may be an important factor contributing to the preference for the quartz topology in this case at low temperature. The reason why the quartz topology is preferred in $[M\{Au(CN)_2\}_2]$ is not known, but significant Au ··· Au interaction between nets may play a part.

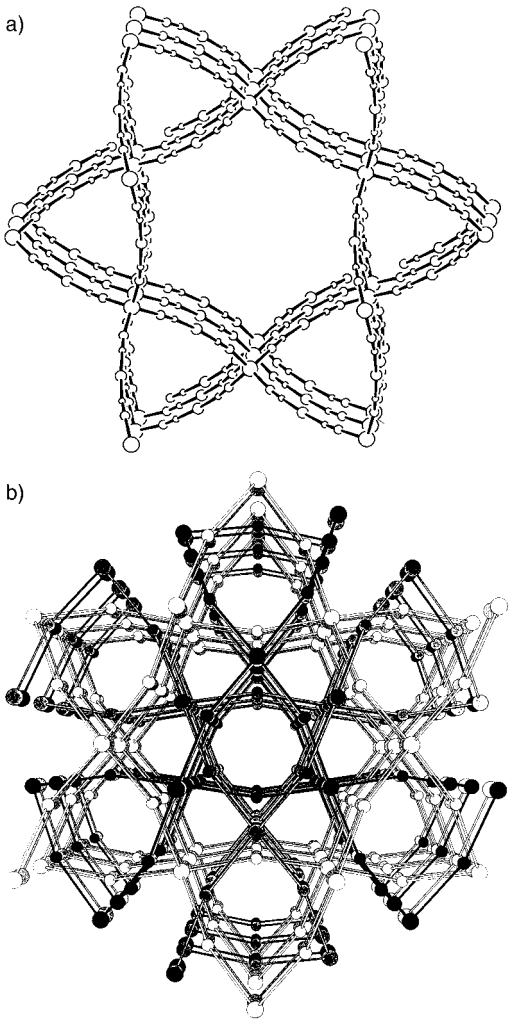

Figure 58. a) A single quartzlike net in the structure of $[Zn\{Au(CN)_2\}_2]$. The circles represent in order of decreasing size Zn, Au, N, and C atoms. b) Six interpenetrating quartzlike nets in $[Zn\{Au(CN)_2\}_2]$. Only Zn (large circles) and Au centers (small circles) are shown.

4.2.3. Interpenetrating NbO-Like Nets

From the purely topological point of view, the NbO net (6^48^2-a) is fundamentally important for it is a very simple four-connected net. In its most symmetrical (cubic) form, it consists of square-planar nodes that are each connected to four equivalent neighbors with a 90° twist along every connection. It has received little attention from chemists for the good reason that few examples are known. We noticed that the structure reported for the 1:1 co-crystal formed by cyanuric acid (**13**) and biuret (**14**) consists of two hydrogen-bonded interpenetrating NbO-like nets.[113] Every cyanuric acid molecule, all of which are equivalent, is hydrogen-bonded to four others either directly or through two-connected biuret molecules to generate a somewhat distorted NbO-like net. The nodes of the net are found at the centers of the cyanuric acid molecules. Two independent nets interpenetrate as shown in Figure 59.

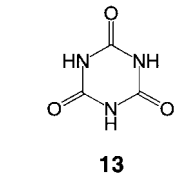

13

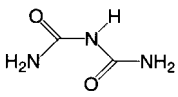

14

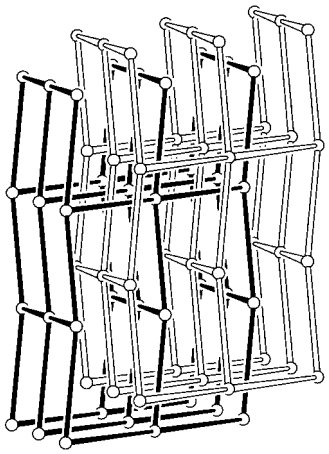

Figure 59. Two interpenetrating NbO-like nets in the hydrogen-bonded structure of cocrystals of cyanuric acid and biuret. The circles represent the four-connected nodes located at the centers of the cyanuric acid molecule.

4.2.4. Interpenetrating $4^2 8^4$ Nets

A simple way in which equal numbers of tetrahedral and square-planar centers can be combined to give an infinite 3D net is shown by PtS, which thus provides a convenient label for the net. Every node is connected to four nodes of the other type, as can be seen in Figure 60, to give a $4^2 8^4$ net which, in its most symmetrical form, has a tetragonal unit cell.

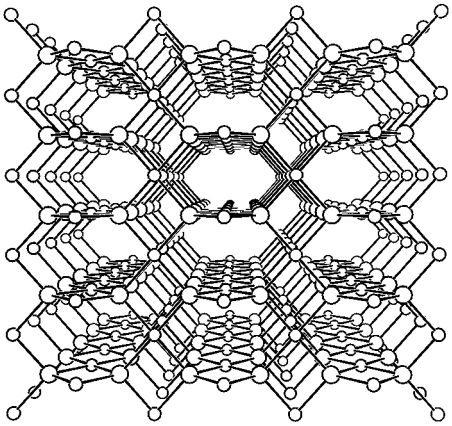

Figure 60. The PtS-like net.

When the porphyrin derivatives **15a** and **15b**, which were intended to play the role of the square-planar component of a PtS-like net, were allowed to react with Cu^I, which was intended to act as the tetrahedral component, PtS-like nets did indeed spontaneously assemble.[10] In the case of the pyridyl-substituted derivative **15a** a single, noninterpenetrating network is formed, whereas derivative **15b**, with somewhat longer 4-cyanophenyl substituents attached to the porphyrin, gives a twofold interpenetrating structure (Figure 61). Yet again, interactions between the nets are clearly present, and the porphyrin molecules appear in close centrosymmetrically related pairs, one from each net. Large, solvent-filled intraframework spaces, accounting for well over 50% of the volume of the crystal, are present in the noninterpenetrating network formed by **15a**. However, even in the interpenetrating structure in Figure 61 the two independent nets hug each other so tightly that, despite the interpenetration, very large solvent-filled spaces still remain.

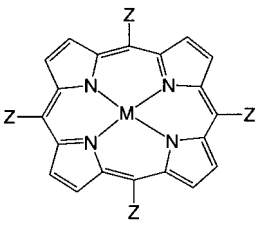

15a, Z = 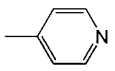

15b, Z = 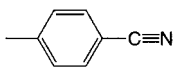

It has been noted [114] that [Ag(tcnq)] (tcnq = tetracyanoquinodimethane)[115] consists of two interpenetrating PtS-related nets.

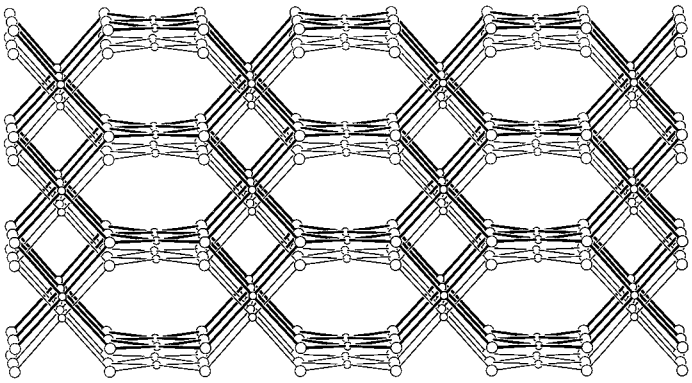

Figure 61. Two interpenetrating PtS-like nets in the structure of solvated $[Cu^I(\mathbf{15b})](BF_4)$. Tetrahedral centers represent Cu^I atoms, and square-planar centers represent the Cu^{II} atoms at the centers of the **15b** ligands ($M = Cu^{II}$).

The diol **16** gives on crystallization from benzene $(\mathbf{16})_4 \cdot C_6H_6$.[116] The OH groups of four separate diols are hydrogen-bonded together to give $(O{-}H\cdots)_4$ rings. From the topological point of view, it is convenient to consider these rings as providing four-connected nodes, the nodes being located at the centers of the rings. Molecule **16** therefore acts as a two-connect or that links nodes into the unusual four-connected net (Figure 62a). Like the PtS net,

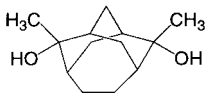

16

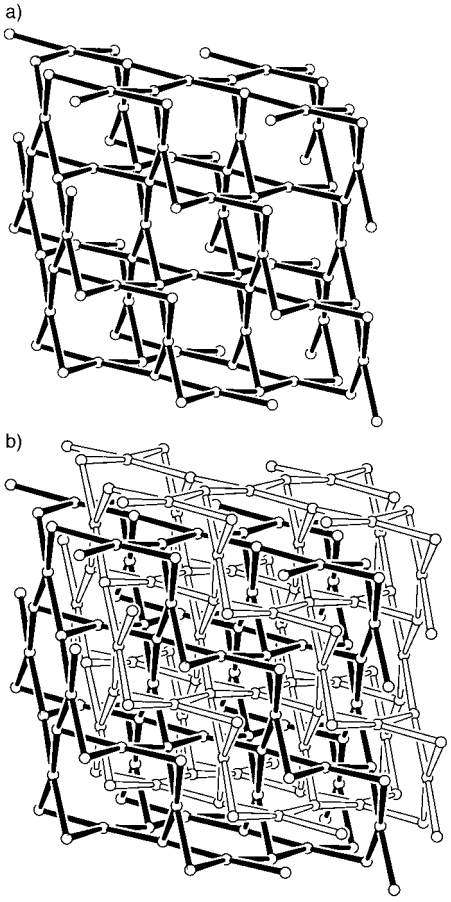

Figure 62. a) A single net of the unusual $4^2 8^4$ type present in $(\mathbf{16})_4 \cdot C_6H_6$. The circles represent the four-connected nodes located at the centers of the $(O{-}H\cdots)_4$ rings. b) Two interpenetrating $4^2 8^4$ nets in the structure of $(\mathbf{16})_4 \cdot C_6H_6$.

this net has the $4^2 8^4$ point symbol, but is geometrically and topologically quite different. Two nets of this type that are related by an inversion center then interpenetrate as shown in Figure 62b. This structure has also been described in terms of interpenetrating diamond nets, where the nodes of the net represent the centers of the four-membered rings in Figure 62.[70]

4.3. Interpenetrating Six-Connected Nets

All bar one of the known examples of interpenetrating six-connected nets are of the α-polonium-related ($4^{12}6^3$) topology. In its most symmetrical form this net consists of nodes with an octahedral geometry and has a primitive cubic unit cell, as in α-polonium itself.

4.3.1. Interpenetrating α-Polonium-Like Nets

Examples of two- and threefold interpenetrating α-polonium nets are known. Nb_6F_{15} contains Nb_6F_{12} clusters made up of niobium centers at the apices of a regular octahedron with angular μ_2-bridging fluoride ions along the twelve edges of the octahedron.[117] Each cluster is linked to six others by additional linear μ_2-bridging fluoride ions to give an α-polonium network of composition $(Nb_6F_{12})(\mu_2\text{-}F)_{6/2}$ (Figure 63a). The six-connected nodes are located at the centers of the Nb_6 octahedra. Two independent nets of this type then interpenetrate, as shown in Figure 63b, so that the nodes of one net are located at the centers of the cubes formed by the other net. The structures of $Zr_6Cl_{15}M$,[118] ($M = Li_2Mn$, LiFe, Co, Ni) and $Th_6Br_{15}M$[119] ($M = H_7$,[120] Mn, Fe, Co, Ni) are essentially the same, with guest metal atoms trapped inside M_6X_{12} clusters.

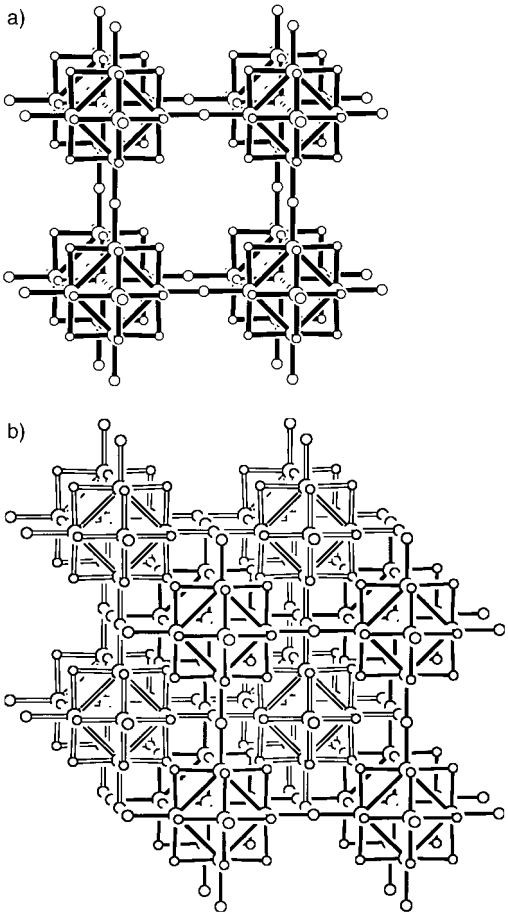

Figure 63. a) A single α-polonium-related net in the structure of Nb_6F_{15}. The circles represent in order of decreasing size Nb atoms, cluster-bridging F atoms, and other F atoms. b) Two interpenetrating nets in Nb_6F_{15}.

Solvated $[Cu_3(tpt)_4](ClO_4)_3$ (tpt = **10**) has essentially the same twofold interpenetrating α-polonium net structure as Nb_6F_{15} despite its very different constitution.[121] In this case cuprous centers are located at the apices of a regular octahedron, and μ_3-bridging tpt ligands are found in alternate faces of the octahedron; the other faces are vacant. Every copper center is shared by two octahedra, and thus links them together (Figure 64a). In this way every $Cu_6(tpt)_4$ octahedron

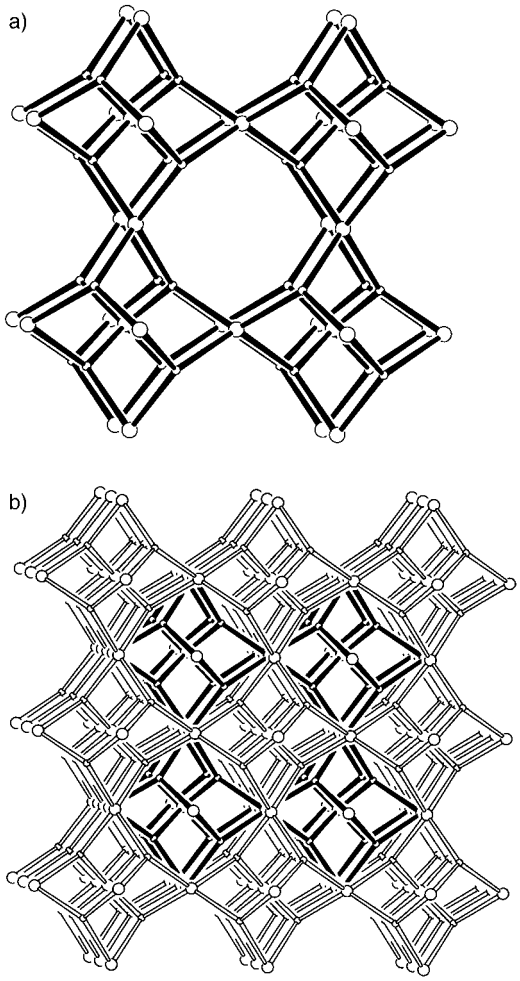

Figure 64. a) A single α-polonium-related net in the structure of solvated $[Cu_3(tpt)_4](ClO_4)_3$ (tpt = **10**). The larger circles represent Cu atoms, and the smaller circles represent the centers of the tpt ligands. b) Two interpenetrating nets.

is attached through shared copper apices to six others to generate an α-polonium net whose nodes are located at the centers of the octahedra. Two independent nets of this type then interpenetrate as shown in Figure 64b, which is essentially as in Nb_6F_{15}. An additional feature is that tpt units from independent nets are brought into close π contact in

centrosymmetrically related pairs. This is yet another example in which interactions between nets are probably decisive for the structure adopted.

Another highly symmetrical cubic coordination polymer of tpt that exhibits a mode of twofold interpenetration closely related to those described above is solvated $[Zn(CN)(NO_3)(tpt)_{2/3}]$.[122] A single net of this compound is represented in Figure 65a. This, as well as the aforementioned $[Cu_3(tpt)_4](ClO_4)_3$, can be regarded as a net with three- and four-

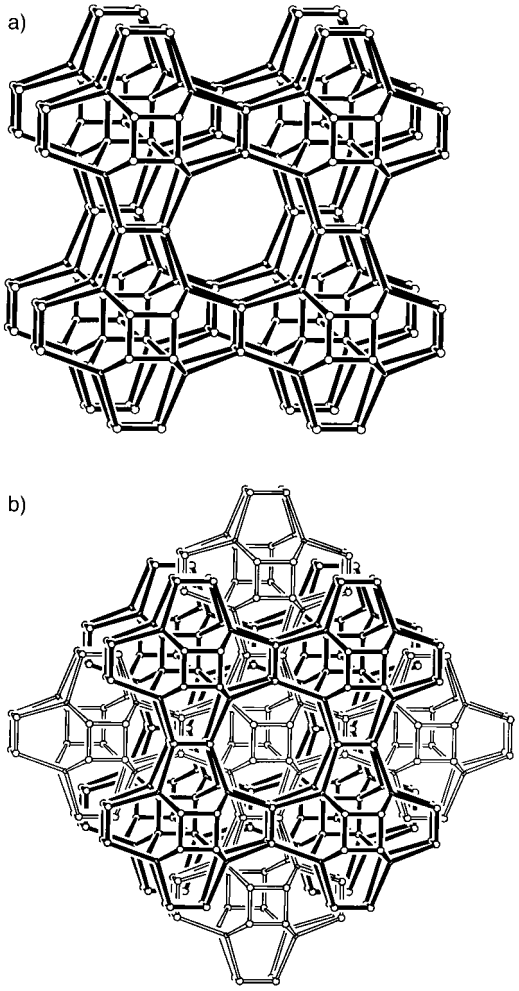

Figure 65. a) A single α-polonium-related net in the structure of solvated $[Zn(CN)(NO_3)(tpt)_{2/3}]$ (tpt = **10**). The larger circles represent Zn atoms, and the smaller circles represent the centers of the tpt ligands. Short Zn···Zn connections represent ZnCNZn groups. b) Representation of two interpenetrating nets in $[Zn(CN)(NO_3)(tpt)_{2/3}]$. The chambers of the "white" net projecting through the front and back faces of the "black" net have been omitted for clarity.

connected nodes. However, when the focus is on the nature of the interpenetration, it is useful to reduce it conceptually to an α-polonium net in which the six-connected nodes are at the centers of the large cavities. The two nets viewed in these terms then interpenetrate in a manner topologically identical to that seen above in Nb_6F_{15} and solvated $[Cu_3(tpt)_4](ClO_4)_3$ (Figure 65b). The tpt units from independent nets thus make close π contact in centrosymmetrically related pairs similar to those seen in $[Cu_3(tpt)_4](ClO_4)_3$.

One of the high-pressure forms of ice, ice VI,[123] consists of two independent hydrogen-bonded networks that are usefully described as α-polonium-like nets interpenetrating in a manner closely analogous to that described above. Two sorts of four-connected oxygen centers are present; those of the first sort are connected to three other oxygen atoms in one cluster and to one oxygen atom in another, whereas those of the second sort are connected to two oxygen atoms in one cluster and to two oxygen atoms in another. As is apparent in Figure 66 the individual nets have tetragonal symmetry and have the same topology as the aluminosilicate net in the mineral edingtonite.[59] If one considers the centers of each

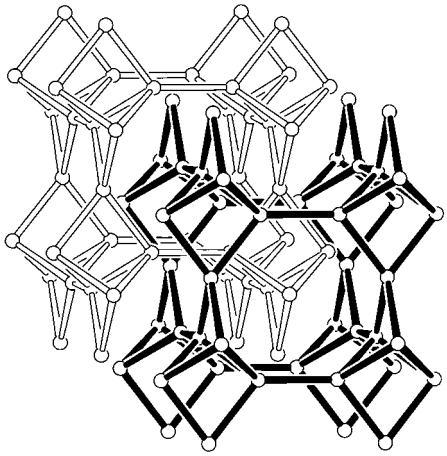

Figure 66. Two interpenetrating α-polnium-related nets in the structure of ice VI. The circles represent O atoms. The six-connected nodes of the net are located at the centers of the $(H_2O)_6$ clusters.

$(H_2O)_6$ cluster to constitute a six-connected node, the individual nets can then be regarded as tetragonally distorted α-polonium nets. At the center of each tetragonally distorted cube of one net is a six-connected node of the other net.

$[Co(Hdcbpy)_3]$ ($Hdcbpy^-$ = monoanion of 2,2′-bipyridyl-5,5′-dicarboxylic acid H_2dcbpy) forms a crystalline hydrate in which metal complex molecules are hydrogen-bonded into an α-polonium network; two such nets interpenetrate as in the preceding examples.[124] The water of crystallization forms a third hydrogen-bonded network between the two nets.

Another example of the same type of twofold interpenetrating α-polonium-related nets is provided by the compound obtained from $Mn^{II}(BF_4)_2$ and the two-connected ligand *N*,*N*′-butylenebis(imidazole).[125]

The structure of β-quinol, discovered by Powell almost half a century ago, is one of the classic examples of twofold interpenetration.[126] The phenolic OH groups from six separate 1,4-dihydroxybenzene molecules are hydrogen-bonded to produce hexagonal $(O-H\cdots)_6$ rings (Figure 67a). Every one of these rings is linked through C_6H_4 bridges to six others, three on one side and three on the other, in a pseudo-octahedral fashion to give an infinite 3D net which can be regarded as possessing the α-polonium topology; the centers of the rings constitute the six-connected nodes. Two such α-polonium nets then interpenetrate in the usual manner, with the nodes of one net located at the centers of the "cubes"

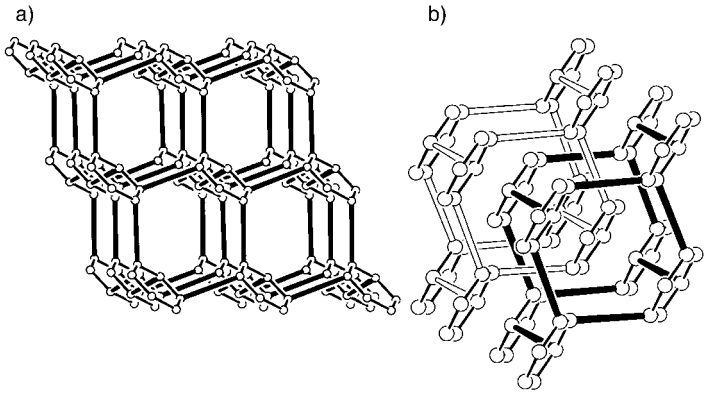

Figure 67. a) A single α-polonium-related net in the structure of β-quinol. The circles represent O atoms. The O–H···O hydrogen bonds are represented by thin lines, and the OC_6H_4O bridges are represented by thick lines. Six-connected nodes of the net are located at the centers of the $(O)_6$ rings. b) The two interpenetrating nets.

(actually rhombohedra) formed by the nodes of the other (Figure 67b). Guest molecules are incorporated into the spaces formed between the $(O–H\cdots)_6$ rings of separate nets.

Several examples of threefold interpenetrating α-polonium nets are provided by cyanometallate derivatives of the types $[A_3M(CN)_6]$ (A = Ag and M = Co^{III},[127] Cr^{III},[128], Cr^{III}/Co^{III}[128] or A = H and M = Co^{III},[127, 129], Fe^{III}[129]) and K[Co{$Au(CN)_2$}$_3$],[130] Rb[Cd{$Ag(CN)_2$}$_3$],[11] K[Cd{$Ag(CN)_2$}$_3$],[114] and K[Cd{$Au(CN)_2$}$_3$].[114] These nets comprise octahedral M centers linked together by essentially linear rods of the form M–NC–A–CN–M or M–CN–H–NC–M, which are sufficiently long and thin to permit threefold interpenetration of the type shown in Figure 68. These systems are often distorted

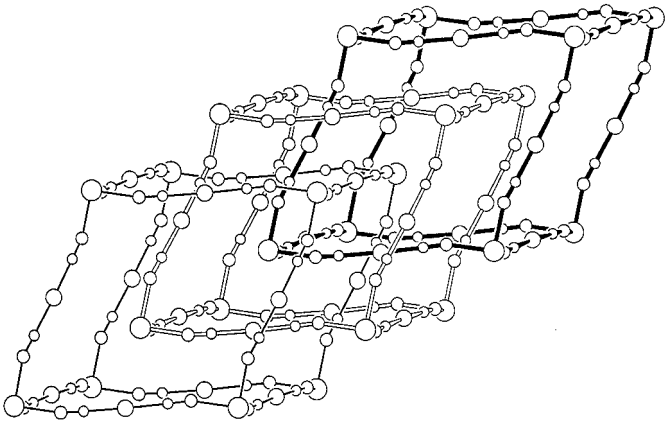

Figure 68. Threefold interpenetration of α-polonium-related nets in the structure of Rb[Cd{$Ag(CN)_2$}$_3$]. The circles represent in order of decreasing size Cd, Ag, N, and C atoms. Intercalated Rb atoms are omitted for clarity.

so as to become rhombohedral, and the essence of the interpenetration is that nodes of the second and third nets are located, equally spaced, along the rhombohedral "solid diagonal" of a distorted cube of the first net. Each square or rhombic "window" has a rod from each of the other two nets passing through it. In the case of the alkali metal derivatives listed above, for which the octahedral metal center is in oxidation state II, the alkali metal counterions occupy interframework void space. Related α-polonium-based nets belonging to the Prussian blue family, consisting of octahedral metal nodes linked through only cyanide ions, do not participate in the interpenetration. It is interesting that whilst six-membered rings of the $M_6(CN)_6$ type found, for example, in $[Zn(CN)_2]$ are large enough to allow a rod of an independent network to pass through, corresponding four-membered $M_4(CN)_4$ rings of the type found in the Prussian blue family are not.

Combining the bis(imidazole) ligand **2** with cadmium perchlorate gives a cationic coordination polymer of composition $[Cd(\mathbf{2})_3]^{2+}$ in which the cadmium atom is octahedrally coordinated by imidazole donors from six separate bridging ligands generating an α-polonium-related network. Three of the ligands interpenetrate in a manner topologically identical to that described above for the cyanometallates.[131]

$[Cd(pz)\{Ag_2(CN)_3\}\{Ag(CN)_2\}]$ shows threefold interpenetration of α-polonium nets in which octahedral Cd^{II} centers are linked together by three different types of rods: pyrazine, $Ag(CN)_2^-$, and $Ag_2(CN)_3^-$.[132]

4.3.2. Interpenetrating Six-Connected Nets Unrelated to α-Polonium

Just as six-connected nodes with octahedral geometry link in a natural, unstrained way to give the α-polonium net, six-connected centers with trigonal-prismatic geometry can be assembled in an unstrained manner to give a simple 3D net (Figure 69a); the threefold axes of the individual trigonal-prismatic centers are parallel. $[Eu\{Ag(CN)_2\}_3(H_2O)_3]$[133] contains nine-coordinate Eu atoms around which three trigonally disposed water ligands occupy an "equatorial belt". Three N donors from $Ag(CN)_2^-$ bridging ligands above the belt and three others below it form the trigonal prism. What has not been previously recognized is that this structure involves threefold interpenetration (Figure 69b), and the individual nets have the connectivity shown in Figure 69a. Yet again, interaction between individual nets is apparent in the form of close Ag···Ag contacts.

4.4. Interpenetrating Nets Each Containing Two Types of Nodes with Different Connectivities

4.4.1. Interpenetrating Nets with Three- and Six-Connected Nodes

The series of isostructural "binary" metal–tcm compounds $[M(tcm)_2]$ ($tcm^- = C(CN)_3^-$; M = Cr, Mn, Co, Ni, Cu, Zn, Cd, Hg) consist of two rutile-related nets that interpenetrate in the manner shown in Figure 70.[28, 44, 134]

$[Cd(bipy)_2\{Ag(CN)_2\}_2]$ consists of two interpenetrating three, six-connected 3D nets that can be visualized in terms of square-grid sheets made up of Cd^{II} centers interconnected through approximately linear bridging $Ag(CN)_2^-$ ligands; bridging bipy ligands link the silver atoms of one sheet to the cadmium atoms of a neighboring sheet.[132] There are twice as many silver atoms present as cadmium atoms, and each

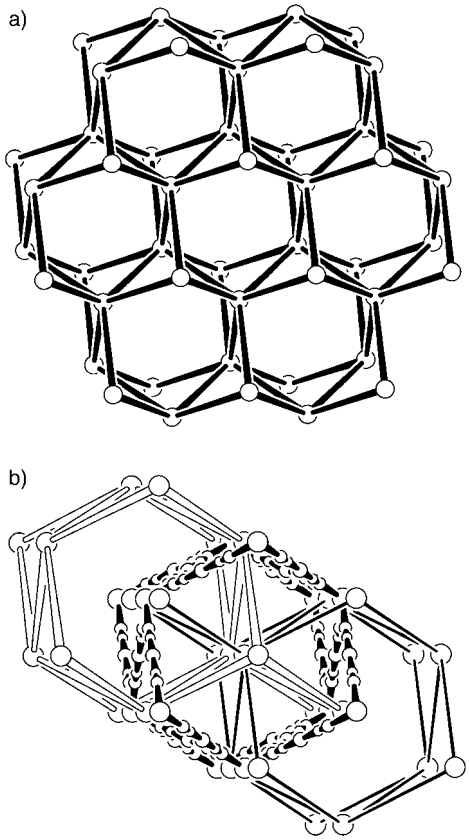

Figure 69. a) A simple six-connected 3D net formed by linking nodes with trigonal-prismatic geometry. The single nets in $[Eu\{Ag(CN)_2\}_3(H_2O)_3]$ have this topology. b) Three nets of the type shown in a) that interpenetrate in $[Eu\{Ag(CN)_2\}_3(H_2O)_3]$. The circles represent Eu atoms, and linear connections represent EuNCAgCNEu groups (shown in full in the central net).

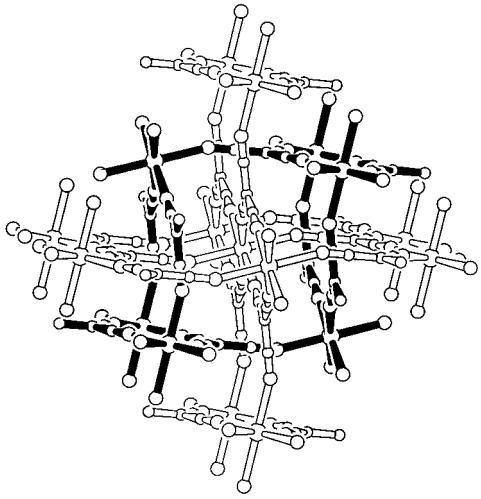

Figure 70. Two interpenetrating rutile-related nets in the structure of $[Hg\{C(CN)_3\}_2]$. The circles represent in order of decreasing size Hg, N, and C atoms.

silver atom is attached to one bipy ligandwhilst each cadmium atom is attached to two. The silver atoms thus become three-connected, and the cadmium atoms six-connected. Two 3D nets of this type then interpenetrate as shown in Figure 71.

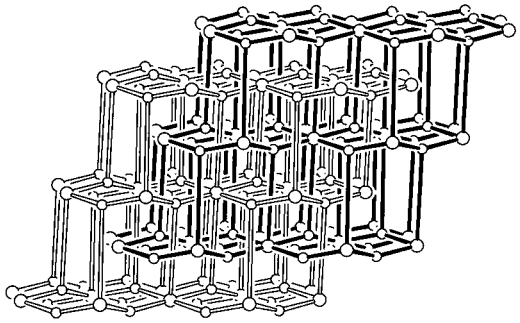

Figure 71. Two interpenetrating nets with three- and six-connected nodes in the structure of $[Cd(bipy)_2\{Ag(CN)_2\}_2]$. The larger circles represent Cd atoms, and the smaller circles Ag atoms. The long Cd···Ag connections (verticle here) are through bipy ligands.

4.4.2. Interpenetrating Nets with Three- and Five-Connected Nodes

Compounds [Ag(tcm)(L)] (L = pyrazine, 1,4-diazobicyclo-[2.2.2]octane (dabco), 4,4′-bipyridine) consist of planar hexagonal-grid [Ag(tcm)] sheets that are connected together into a 3D net through bridging ligands L that link silver atoms of adjacent sheets.[27, 28] The silver centers thereby become five-connected, and the central carbon atoms of the tcm molecules remain three-connected. Two such nets with three- and five-connected nodes then interpenetrate in the manner shown in Figure 72 with the example of the dabco compound.

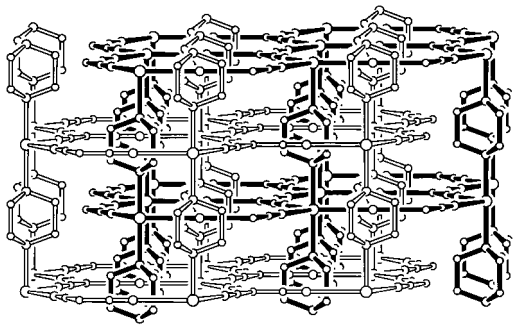

Figure 72. Two interpenetrating nets with three- and five-connected nodes in the structure of [Ag(tcm)(dabco)]. The circles represent in order of decreasing size Ag, N, and C atoms.

4.5. Interpenetrating Nets with Different Chemical Compositions

4.5.1. Interpenetrating Nets of the Same Topology

It is rather surprising that crystals will spontaneously assemble that consist of two independent and interpenetrating nets with the same topology and with exactly the same separation between nodes, but of different chemical composition. Nevertheless, examples do exist.

Crystals of composition $K_2[PdSe_{10}]$ consist of two interpenetrating diamond-related nets of different composition (Figure 73).[80] In both nets the four-connected centers are provided by Pd^{II} atoms in an essentially square-planar coordination environment of four anionic Se donors. In one

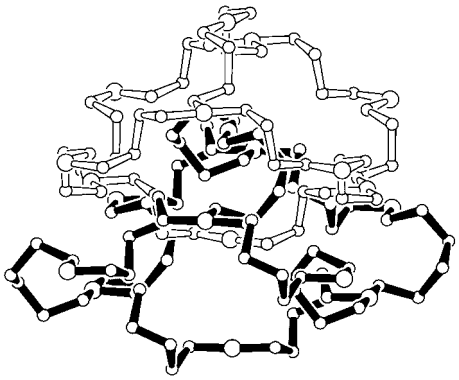

Figure 73. Two interpenetrating adamantane units from the two different diamond-related nets in the structure of $K_2[PdSe_{10}]$. In the net depicted in black, the Pd atoms are connected through Se_6^{2-} units. The large circles represent Pd atoms, and the small circles Se atoms.

net the metal centers are interconnected through Se_4^{2-} bridging ligands, and in the other the bridging ligands are Se_6^{2-}. Although the immediate coordination environment of the metal is square planar, the twisted character of the bridging ligands enables the metal centers to play the role of pseudo-tetrahedral four-connected node required for the diamond net. The same Pd···Pd separation within the two nets is achieved by the Se_6^{2-} ligand adopting a much more twisted conformation than the Se_4^{2-} ligand.

Some oxides of the pyrochlore type can be described in terms of two different interpenetrating diamondlike nets.[59, 135] $Hg_2Nb_2O_7$, which we use here to illustrate the general features of this type of interpenetration, can be viewed in terms of separate $[Hg_2^{II}O^{2+}]_n$ and $[Nb_2^{V}O_6^{2-}]_n$ nets. The mercury-based diamond net, is relatively simple: The tetrahedral nodes are provided by oxides and are linked through two-coordinate linear metal centers, much as in Cu_2O. The basic tetrahedral units from which the diamondlike $[Nb_2^{V}O_6^{2-}]_n$ net is constructed are "Nb_4O_6" cages of the sort shown in Figure 74a, which themselves are, interestingly, adamantane-like. Cages of this type are linked together through shared niobium centers; hence the composition of each cage strictly is $[(Nb_{1/2})_4O_6]^{2-}$. Each niobium center is bonded in an octahedral fashion to three oxygen atoms in one cage and three in its neighboring cage. Every cage is thus connected tetrahedrally to four others, and in this way the diamond net is built up. Figure 74b shows an adamantane unit of this diamond net, the four-connected nodes of which are located at the centers of the "Nb_4O_6" cages. The separation between these nodes is exactly the same as that between the oxide nodes of the $[Hg_2O^{2+}]_n$ net, which enables the two different nets to interpenetrate as shown in Figure 74b.

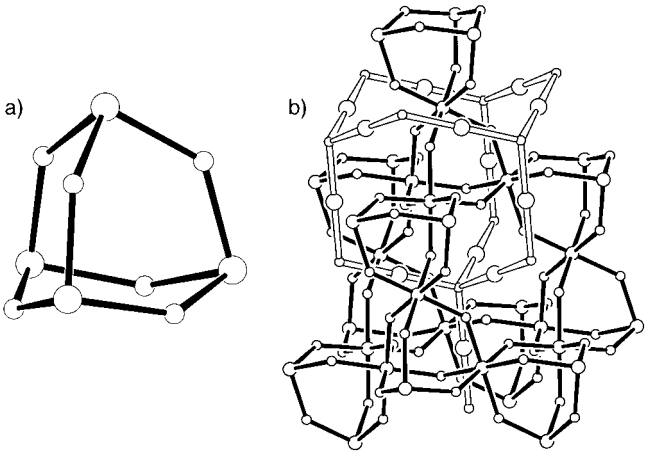

Figure 74. a) "Nb_4O_6" cages present in the pyrochlore structure of $Hg_2Nb_2O_7$. The large circles represent Nb atoms, and the small circles O atoms. b) Interpenetrating adamantane units of the $[Nb_2O_6^{2-}]_n$ (filled bonds) and $[Hg_2O^{2+}]_n$ nets (open bonds) in pyrochlore. The circles represent in order of decreasing size Hg, Nb, and O atoms.

$[Ag(hmta)](PF_6)(H_2O)$ (hmta = hexamethylenetetramine) contains two interpenetrating (10,3)-a nets.[136] One is a Ag/hmta coordination polymer in which the three-connected nodes are provided in an alternating fashion by three-coordinate silver atoms and hmta ligands which use only three of the four nitrogen atoms to form donor bonds to metal. The second (10,3)-a net, which is of the opposite handedness, consists of a hydrogen-bonded $PF_6^- \cdot H_2O$ system in which the PF_6^- ions act as the three-connected nodes.

As mentioned in Section 3.2.1, the structure of $[Cd(4\text{-ampy})_2\{Ag(CN)_2\}_2] \cdot [Cd(mea)(4\text{-ampy})\{Ag(CN)_2\}_2]_2$ contains two sets of (4,4) 2D nets displaying inclined interpenetration.[48] One set of sheets is a $[Cd(4\text{-ampy})_2\{Ag(CN)_2\}_2]$ coordination polymer, and the other is composed of linear coordination polymer chains cross-linked by hydrogen bonds.

4.5.2. Interpenetrating Nets of Different Topology

Crystals of composition $[H_{31}O_{14}][CdCu_2(CN)_7]$ contain a crystallographically well-defined anionic coordination polymer of composition $[CdCu_2^{I}(CN)_7]^{3-}$ which has the pyrites topology.[137] This is interpenetrated by a hydrogen-bonded network that is not as well defined of apparent composition $(H_3O^+)_3 + (H_2O)_{11}$ (some apparent O···O separations are unrealistically short, and thermal parameters are extremely large). Present in the coordination polymer net are $(CN)_3CuCNCu(CN)_3^{5-}$ units in which the CuCNCu moiety is essentially linear. Encircling each of these linear units in a rotaxane fashion are $(H_2O)_{12}$ rings (Figure 75). These rings

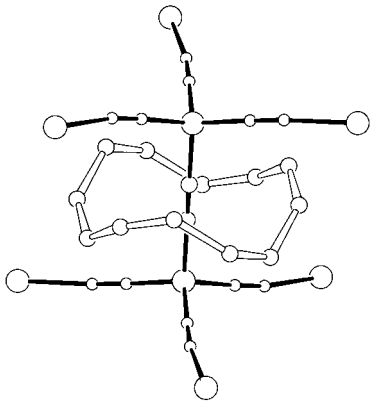

Figure 75. A $(H_2O)_{12}$ ring component of the $[H_{31}O_{14}^{3+}]_n$ 3D network encircling a $(CN)_3CuCNCu(CN)_3^{5-}$ component of the pyrites-like $[CdCu_2(CN)_7^{3-}]_n$ net in $[H_{31}O_{14}][CdCu(CN)_7]$. The circles represent in order of decreasing size Cd, O, and C/N atoms.

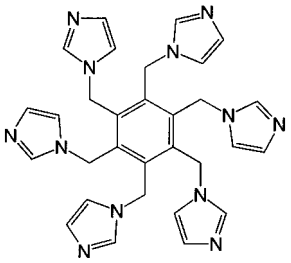

17

are hydrogen-bonded to others through intervening and ill-defined H_2O or H_3O^+ units to give a complicated 3D net.

Hexakis(imidazol-1-ylmethyl)-benzene (**17**) reacts with cadmium fluoride to give heavily hydrated crystals of composition $[Cd(\mathbf{17})F_2]\cdot 14\,H_2O$ which contain a single, rhombohedral α-polonium-related net (Figure 76a); the Cd^{II} centers are octahedrally coordinated by imidazole donors from six separate ligands **17**, and each ligand is bonded to six cadmium atoms.[138] Two types of hydrogen-bonded sheets of (6,3) topology, one consisting entirely of water molecules and the other of F^- ions and water molecules, interpenetrate the coordination polymer network (but not each other, because they are parallel) with their average planes perpendicular to the rhombohedral axis (Figure 76b).

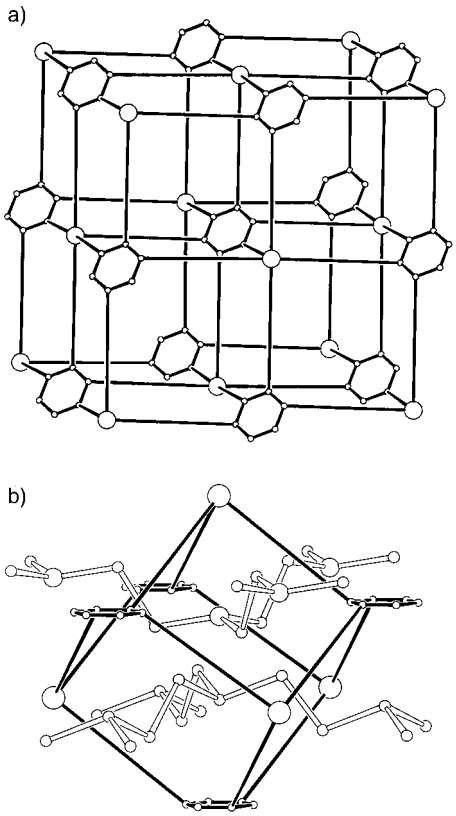

Figure 76. a) The rhombohedral $[Cd(\mathbf{17})^{2+}]_n$ α-polonium-related net in $[Cd(\mathbf{17})F_2]\cdot 14\,H_2O$. The small circles represent the C atoms of the central C_6 ring of **17**, and the large circles Cd atoms. Long connections between C and Cd are through the imidazolylmethyl arms of **17**. b) One rhombohedron of the $[Cd(\mathbf{17})^{2+}]_n$ α-polonium net with two different hydrogen-bonded sheets interpenetrating it. The circles represent in order of decreasing size Cd, F, O, and C atoms. Connections drawn with open lines represent hydrogen bonds.

The structure of $Bi_3GaSb_2O_{11}$ may be described in terms of three interpenetrating nets, one with NbO-like topology and two with diamondlike topology (Figure 77).[139] The NbO-like net consists of $(Ga_{1/3}Sb_{2/3})_4O_6$ clusters connected to each other through shared metal atoms. The four-connected node of the NbO net can thus be placed at the center of these clusters. The two diamondlike nets contain cubelike clusters of alternating bismuth and oxygen atoms of composition Bi_4O_4. These clusters are connected to one another through two-connected bismuth atoms coordinating to the tetrahedral oxygen atoms of the clusters. The nodes of the diamond nets are consequently at the centers of the cubelike clusters. There are interactions between the two-connected bismuth atoms of the diamondlike nets and the oxygen atoms of the NbO net; however, these Bi–O distances are significantly longer than those within the nets.

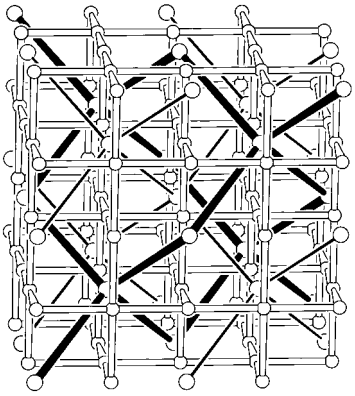

Figure 77. The three interpenetrating nets (one NbO-like and two diamond-related) in the structure of Bi_3GaSbO_{11}. One diamondlike net is shown with thick lines, and the other with thin lines. The NbO-like net is shown with open lines. The smaller circles represent the centers of $(Ga_{1/3}Sb_{2/3})_4O_6$ clusters, and the larger circles represent the centers of Bi_4O_4 clusters.

5. Summary and Outlook

There can be no doubt that many new framework solids will be created in the near future and that new forms of interpenetration will soon need to be added to those considered here. Useful properties and applications arising directly from the phenomenon of interpenetration remain to be discovered, but we suspect the area is ripe for such discoveries. The ordered juxtapositioning of components from independent networks cries out for exploitation, for example with regard to electronic interactions or secondary chemical reactions such as polymerization. Hoffmann et al. have proposed that a possible way to obtain materials harder than diamond is to use interpenetrating frameworks,[140] and a coordination polymer with metallike electrical conductivity consisting of seven interpenetrating diamondlike networks is thought to owe this property to the interpenetration.[83] It is interesting that one of the more promising systems generated in the quest for new magnetic materials is, coincidentally, interpenetrating.[51]

The degree to which nets we choose to regard as separate are truly independent is variable and debatable. Nevertheless, the approach adopted here of breaking down complicated interpenetrating structures into nets we choose to describe as "independent", even though significant interaction between

nets is clearly evident in some cases, remains a useful, powerful, and simplifying aid to understanding the structures.

There is a need for radical new theoretical work in two separate areas associated with interpenetrating networks. Our inability to predict the structure of a crystal given the components in the medium from which the crystal grows was referred to, unjustifiably in our opinion, as the "scandal" of crystal engineering as long ago as 1988[141] and remains as much a scandal today. This is a difficult problem, and, in the case of framework solids, simply predicting the connectivity of the net formed, which appears at present on purely empirical grounds to depend critically on moderately subtle and not easily modeled factors such as interactions with solvent molecules and the nature of counterions, seems almost intractable. Predicting the nature of interpenetration would appear to be even more difficult. We suspect that the empirical, experimental approach, provided it is based on sound chemical intuition and sensible design, will remain a very fruitful way forward for some considerable time to come.

The second area where theoretical input is required concerns the basic mathematical theory underlying the topology of 2D and 3D nets. Wells's compilation of nets[4] is extremely useful for synthetic chemists such as ourselves, but he did not attempt to conceal the fact that his derivations were intuitive, nonrigorous, and probably incomplete. Constructing a comprehensive theory of the topology of nets would be challenging; a theory of the *topology of interpenetration* would, we suspect, be even more testing.[142]

We are grateful to the Australian Research Council and The American Chemical Society Petroleum Research Fund for support, and to our colleagues Dr. Bernard Hoskins and Dr. Brendan Abrahams for many useful discussions.

Received: July 17, 1997 [A 244 IE]
German version: *Angew. Chem.* **1998**, *110*, 1558 – 1595

[1] R. Robson in *Comprehensive Supramolecular Chemistry, Vol. 6* (Eds.: J. L. Atwood, J. E. D. Davies, D. D. MacNicol, F. Vögtle, F. Toda, R. Bishop), Pergamon, Oxford, **1996**, pp. 733 – 755.

[2] Examples of noninterpenetrating coordination polymers: a) B. F. Abrahams, B. F. Hoskins, R. Robson, *J. Chem. Soc. Chem. Commun.* **1990**, 60 – 61; b) S. R. Batten, B. F. Hoskins, R. Robson, *Angew. Chem.* **1995**, *107*, 884 – 886; *Angew. Chem. Int. Ed. Engl.* **1995**, *34*, 820 – 822; c) B. F. Abrahams, B. F. Hoskins, J. Liu, R. Robson, *J. Am. Chem. Soc.* **1991**, *113*, 3045 – 3051; d) B. F. Abrahams, B. F. Hoskins, R. Robson, *ibid.* **1991**, *113*, 3606 – 3607; e) S. R. Batten, B. F. Hoskins, R. Robson, *Angew. Chem.* **1997**, *109*, 652 – 653; *Angew. Chem. Int. Ed. Engl.* **1997**, *36*, 636 – 637; f) B. F. Abrahams, M. J. Hardie, B. F. Hoskins, R. Robson, G. A. Williams, *J. Am. Chem. Soc.* **1992**, *114*, 10641 – 10643; g) B. F. Abrahams, M. J. Hardie, B. F. Hoskins, R. Robson, E. E. Sutherland, *J. Chem. Soc. Chem. Commun.* **1994**, 1049 – 1050; h) B. F. Abrahams, S. J. Egan, B. F. Hoskins, R. Robson, *Chem. Commun.* **1996**, 1099 – 1100; i) S. Subramanian, M. J. Zaworotko, *Angew. Chem.* **1995**, *107*, 2295 – 2297; *Angew. Chem. Int. Ed. Engl.* **1995**, *34*, 2127 – 2129; j) P. Losier, M. J. Zaworotko, *ibid.* **1996**, *108*, 2957 – 2960 and **1996**, *35*, 2779 – 2782; k) O. M. Yaghi, G. Li, H. Li, *Nature* **1995**, *378*, 703 – 706; l) L. Carlucci, G. Ciani, D. M. Proserpio, A. Sironi, *Angew. Chem.* **1995**, *107*, 2037 – 2040; *Angew. Chem. Int. Ed. Engl.* **1995**, *34*, 1895 – 1898; m) D. M. L. Goodgame, D. A. Katahira, S. Menzer, D. J. Williams, *Inorg. Chim. Acta* **1995**, *229*, 77 – 80; n) D. M. L. Goodgame, S. Menzer, A. T. Ross, D. J. Williams, *ibid.* **1996**, *251*, 141 – 149; o) O. M. Yaghi, Z. Sun, D. A. Richardson, T. L. Groy, *J. Am. Chem. Soc.* **1994**, *116*, 807 – 808; p) O. M. Yaghi, H. Li, T. L. Groy, *ibid.* **1996**, *118*, 9096 – 9101; q) O. M. Yaghi, C. E. Davis, G. Li, H. Li, *ibid.* **1997**, *119*, 2861 – 2868; r) L. Carlucci, G. Ciani, D. W. v. Gudenberg, D. M. Proserpio, A. Sironi, *Chem. Commun.* **1997**, 631 – 632; s) S. Kitagawa, M. Munakata, T. Tanimura, *Inorg. Chem.* **1992**, *31*, 1714 – 1717; t) S. Kawata, S. Kitagawa, M. Kondo, I. Furuchi, M. Munakata, *Angew. Chem.* **1994**, *106*, 1851 – 1854; *Angew. Chem. Int. Ed. Engl.* **1994**, *33*, 1759 – 1761; u) S. Kitagawa, T. Okubo, S. Kawata, M. Kondo, M. Katada, H. Kobayashi, *Inorg. Chem.* **1995**, *34*, 4790 – 4796; v) L. P. Wu, Y. Yamagiwa, T. Kuroda-Sowa, T. Kamikawa, M. Munakata, *Inorg. Chim. Acta* **1997**, *256*, 155 – 159; w) S. Decurtins, H. W. Schmalle, H. R. Oswald, A. Linden, J. Ensling, P. Gütlich, A. Hauser, *ibid.* **1994**, *216*, 65 – 73; x) T. Otieno, S. J. Rettig, R. C. Thompson, J. Trotter, *Can. J. Chem.* **1989**, *67*, 1964 – 1969; y) G. De Munno, R. Ruiz, F. Lloret, J. Faus, R. Sessoli, M. Julve, *Inorg. Chem.* **1995**, *34*, 408 – 411; z) C. L. Bowes, G. Ozin, *Adv. Mater.* **1996**, *8*, 13 – 28.

[3] Examples of noninterpenetrating hydrogen-bonded networks: a) C. B. Aakeroy, K. R. Seddon, *Chem. Soc. Rev.* **1993**, *22*, 397 – 407; b) O. Ermer, A. Eling, *J. Chem. Soc. Perkin Trans. 2* **1994**, 925 – 944; c) P. Brunet, M. Simard, J. D. Wuest, *J. Am. Chem. Soc.* **1997**, *119*, 2737 – 2738; d) D. S. Reddy, D. C. Craig, G. R. Desiraju, *J. Chem. Soc. Chem. Commun.* **1995**, 339 – 340; e) V. A. Russell, M. D. Ward, *Chem. Mater.* **1996**, *8*, 1654 – 1666; f) K. Kobayashi, K. Endo, Y. Aoyama, H. Masuda, *Tetrahedron Lett.* **1993**, *34*, 7929 – 7932; g) K. Endo, T. Sawaki, M. Koyanagi, K. Kobayashi, H. Masuda, Y. Aoyama, *J. Am. Chem. Soc.* **1995**, *117*, 8341 – 8352; h) M. Mitsumi, J. Toyoda, K. Nakasuji, *Inorg. Chem.* **1995**, *34*, 3367 – 3370; i) S. Subramanian, M. J. Zaworotko, *Coord. Chem. Rev.* **1994**, *137*, 357 – 401.

[4] a) A. F. Wells, *Three-dimensional Nets and Polyhedra*, Wiley-Interscience, New York, **1977**; b) *Further Studies of Three-dimensional Nets*, ACA Monograph No. 8, American Crystallographic Association, **1979**.

[5] While square-planar and tetrahedral centers are topologically identical and indistinguishable (i.e., four-connected), there are clear chemical reasons for treating them differently.

[6] B. F. Hoskins, R. Robson, *J. Am. Chem. Soc.* **1990**, *112*, 1546 – 1554.

[7] B. F. Hoskins, R. Robson, *J. Am. Chem. Soc.* **1989**, *111*, 5962 – 5964.

[8] M. J. Zaworotko, *Chem. Soc. Rev.* **1994**, *23*, 283 – 288.

[9] R. W. Gable, B. F. Hoskins, R. Robson, *J. Chem. Soc. Chem. Commun.* **1990**, 762 – 763.

[10] B. F. Abrahams, B. F. Hoskins, D. M. Michail, R. Robson, *Nature* **1994**, *369*, 727 – 729.

[11] B. F. Hoskins, R. Robson, N. V. Y. Scarlett, *J. Chem. Soc. Chem. Commun.* **1994**, 2025 – 2026.

[12] P. C. M. Duncan, D. M. L. Goodgame, S. Menzer, D. J. Williams, *Chem. Commun.* **1996**, 2127 – 2128.

[13] a) D. J. Duchamp, R. E. Marsh, *Acta Crystallogr. Sect. B* **1969**, *25*, 5 – 19; b) F. H. Herbstein, M. Kapon, G. M. Reisner, *ibid.* **1985**, *41*, 348 – 354; c) F. H. Herbstein, M. Kapon, G. M. Reisner, *Proc. R. Soc. Lond. A* **1981**, *376*, 301 – 318; d) F. H. Herbstein, *Isr. J. Chem.* **1968**, *6*, IVp; e) J. E. Davies, P. Finocchiaro, F. H. Herbstein in *Inclusion Compounds, Vol. 2* (Eds.: J. L. Atwood, J. E. D. Davies, D. D. MacNicol), Academic Press, London, **1984**, chap. 11; f) F. H. Herbstein, *Top. Curr. Chem.* **1987**, *140*, 108 – 139.

[14] D. Venkataraman, G. B. Gardner, S. Lee, J. S. Moore, *J. Am. Chem. Soc.* **1995**, *117*, 11600 – 11601.

[15] An early very significant insight into interpenetration and its relationship to clathration was presented in 1948 by Powell: H. M. Powell, *J. Chem. Soc.* **1948**, 61 – 73.

[16] a) L. H. Sperling, *Interpenetrating Polymer Networks and Related Materials*, Plenum, New York, **1981**; b) *Interpenetrating Polymer Networks* (Eds.: D. Klempner, L. H. Sperling, L. A. Utracki), American Chemical Society, Washington DC, **1994**.

[17] a) D. H. Busch in *Transition Metals in Supramolecular Chemistry* (Eds.: L. Fabbrizzi, A. Poggi), Kluwer, Dordrecht, **1994**, pp. 55 – 79; b) D. B. Amabilino, J. F. Stoddart, *Chem. Rev.* **1995**, *95*, 2725 – 2828.

[18] See, for example, a) E. C. Constable, *Tetrahedron* **1992**, *48*, 10013 – 10059; b) *Angew. Chem.* **1991**, *103*, 1482 – 1483; *Angew. Chem. Int. Ed. Engl.* **1991**, *30*, 1450 – 1451; c) C. Piguet, G. Bernardinelli, B. Bocquet, A. Quattropaini, A. F. Williams, *J. Am. Chem. Soc.* **1992**,

114, 7440 – 7451; d) J. M. Lehn, A. Rigault, *Angew. Chem.* **1988**, *100*, 1121 – 1122; *Angew. Chem. Int. Ed. Engl.* **1988**, *27*, 1095 – 1097; e) K. T. Potts, C. P. Horwitz, A. Fessak, M. Keshavarz-K, K. E. Nash, P. J. Toscano, *J. Am. Chem. Soc.* **1993**, *115*, 10444 – 10445.

[19] See, for example, a) C. J. Hawker, J. M. J. Frechet, *J. Am. Chem. Soc.* **1990**, *112*, 7638 – 7647; b) C. Hawker, J. M. J. Frechet, *J. Chem. Soc. Chem. Commun.* **1990**, 1010 – 1013; c) S. C. Zimmerman, F. Zheng, D. E. C. Reichert, S. V. Kolotuchin, *Science* **1996**, *271*, 1095 – 1098.

[20] See, for example, a) G. Schill, *Catenanes, Rotaxanes and Knots*, Academic Press, New York, **1971**; b) P. R. Ashton, R. A. Bissell, D. Philp, N. Spencer, J. F. Stoddart in *Supramolecular Chemistry* (Eds.: V. Balzani, L. De Cola), Kluwer, Dordrecht, **1992**, pp. 1 – 16; c) D. Philp, J. F. Stoddart, *Synlett* **1991**, 445 – 458; d) J.-C. Chambron, C. O. Dietrich-Buchecker, J.-P. Sauvage, *Top. Curr. Chem.*, **1993**, *165*, 131 – 162; e) J.-P. Sauvage, *Acc. Chem. Res.* **1990**, *23*, 319 – 327; f) C. O. Dietrich-Buchecker, J.-P. Sauvage in *Supramolecular Chemistry* (Eds.: V. Balzani, L. De Cola), Kluwer, Dordrecht, **1992**, pp. 259 – 277; g) *Bioorg. Chem. Front.* **1991**, *2*, 195 – 247; h) *Chem. Rev.* **1987**, *87*, 795 – 810; i) D. Philip, J. F. Stoddart, *Angew. Chem.* **1996**, *108*, 1242 – 1286; *Angew. Chem. Int. Ed. Engl.* **1996**, *35*, 1154 – 1196; j) M. Fujita, F. Ibukuro, K. Yamaguchi, K. Ogura, *J. Am. Chem. Soc.* **1995**, *117*, 4175 – 4176; k) S. Ottens-Hildebrandt, S. Meier, W. Schmidt, F. Vögtle, *Angew. Chem.* **1994**, *106*, 1818; *Angew. Chem. Int. Ed. Engl.* **1994**, *33*, 1767 – 1770, and references therein; l) F. Vögtle, T. Dunnwald, T. Schmidt, *Acc. Chem. Res.* **1996**, *29*, 451 – 460; m) M. J. Gunter, M. R. Johnston, *J. Chem. Soc. Chem. Commun.* **1994**, 829 – 830; n) Y. Zhang, N. C. Seeman, *J. Am. Chem. Soc.* **1994**, *116*, 1661 – 1669; o) R. A. Bissell, E. Cordova, A. E. Kaifer, J. F. Stoddart, *Nature* **1994**, *369*, 133 – 137; p) P. L. Anelli, P. R. Ashton, R. Ballardini, V. Balzani, M. Delgado, M. T. Gandolfi, T. T. Goodnow, A. E. Kaifer, D. Philp, M. Pietraszkiewicz, L. Prodi, M. V. Reddington, A. M. Z. Slawin, N. Spencer, J. F. Stoddart, C. Vicent, D. J. Williams, *J. Am. Chem. Soc.* **1992**, *114*, 193 – 218; q) D. B. Amabilino, P. R. Ashton, A. S. Reder, N. Spencer, J. F. Stoddart, *Angew. Chem.* **1994**, *106*, 1316 – 1319; *Angew. Chem. Int. Ed. Engl.* **1994**, *33*, 1286 – 1290.

[21] H. S. Zhdanov, *C. R. Acad. Sci. URSS* **1941**, *31*, 352 – 354.

[22] T. Kitazawa, S. Nishikiori, R. Kuroda, T. Iwamoto, *J. Chem. Soc. Dalton Trans.* **1994**, 1029 – 1036.

[23] P. M. Van Calcar, M. M. Olmstead, A. L. Balch, *J. Chem. Soc. Chem. Commun.* **1995**, 1773 – 1774.

[24] M. Fujita, Y. J. Kwon, O. Sasaki, K. Yamaguchi, K. Ogura, *J. Am. Chem. Soc.* **1995**, *117*, 7287 – 7288.

[25] B. F. Hoskins, R. Robson, D. A. Slizys, *J. Am. Chem. Soc.* **1997**, *119*, 2952 – 2953.

[26] J. Konnert, D. Britton, *Inorg. Chem.* **1966**, *5*, 1193 – 1196.

[27] S. R. Batten, B. F. Hoskins, R. Robson, *New. J. Chem.* **1998**, *22*, 173 – 175.

[28] S. R. Batten, B. F. Hoskins, R. Robson, unpublished results.

[29] Y. M. Chow, D. Britton, *Acta Crystallogr. Sect. B* **1974**, *30*, 1117 – 1118.

[30] M. Schwarten, J. Chomic, J. Cernak, D. Babel, *Z. Anorg. Allg. Chem.* **1996**, *622*, 1449 – 1456.

[31] L. Carlucci, G. Ciani, D. M. Proserpio, A. Sironi, *Angew. Chem.* **1996**, *108*, 1170 – 1172; *Angew. Chem. Int. Ed. Engl.* **1996**, *35*, 1088 – 1090.

[32] a) G. Saito, H. Yamochi, T. Nakamura, T. Komatsu, N. Matsukawa, T. Inoue, H. Ito, T. Ishiguro, M. Kusunoki, K. Sakaguchi, T. Mori, *Synth. Met.* **1993**, *55 – 57*, 2883 – 2890; b) T. Komatsu, H. Sato, N. Matsukawa, T. Nakamura, H. Yamochi, G. Saito, M. Kusunoki, K. Sakaguchi, S. Kagoshima, *ibid.* **1995**, *70*, 779 – 780; c) T. Komatsu, H. Sato, T. Nakamura, N. Matsukawa, H. Yamochi, G. Saito, M. Kusunoki, K. Sakaguchi, S. Kagoshima, *Bull. Chem. Soc. Jpn.* **1995**, *68*, 2233 – 2244.

[33] B. F. Hoskins, R. Robson, D. A. Slizys, *Angew. Chem.* **1997**, *109*, 2430 – 2432; *Angew. Chem. Int. Ed. Engl.* **1997**, *36*, 2336 – 2338.

[34] T. Soma, T. Iwamoto, *Chem. Lett.* **1994**, 821 – 824.

[35] S. B. Copp, S. Subramanian, M. J. Zaworotko, *Angew. Chem.* **1993**, *105*, 755 – 758; *Angew. Chem. Int. Ed. Engl.* **1993**, *32*, 706 – 709.

[36] a) C. Glidewell, G. Ferguson, *Acta Crystallogr. Sect. C* **1996**, *52*, 2528 – 2530; b) C. Davies, R. F. Langler, C. V. K. Sharma, M. J. Zaworotko, *Chem. Commun.* **1997**, 567 – 568.

[37] D. M. L. Goodgame, S. Menzer, A. M. Smith, D. J. Williams, *Angew. Chem.* **1995**, *107*, 605 – 607; *Angew. Chem. Int. Ed. Engl.* **1995**, *34*, 574 – 575.

[38] V. H. Thurn, H. Krebs, *Acta Crystallogr. Sect. B* **1969**, *25*, 125 – 135.

[39] C. V. K. Sharma, M. J. Zaworotko, *Chem. Commun.* **1996**, 2655 – 2656.

[40] A. Zafar, J. Yang, S. J. Geib, A. D. Hamilton, *Tetrahedron Lett.* **1996**, *37*, 2327 – 2330.

[41] Y. Aoyama, K. Endo, T. Anzai, Y. Yamaguchi, T. Sawaki, K. Kobayashi, N. Kanehisa, H. Hashimoto, Y. Kai, H. Masuda, *J. Am. Chem. Soc.* **1996**, *118*, 5562 – 5571.

[42] D. Venkataraman, S. Lee, J. S. Moore, P. Zhang, K. A. Hirsch, G. B. Gardner, A. C. Covey, C. L. Prentice, *Chem. Mater.* **1996**, *8*, 2030 – 2040.

[43] R. W. Gable, B. F. Hoskins, R. Robson, *J. Chem. Soc. Chem. Commun.* **1990**, 1677 – 1678.

[44] R. Robson, B. F. Abrahams, S. R. Batten, R. W. Gable, B. F. Hoskins, J. Liu in *Supramolecular Architecture: Synthetic Control in Thin Films and Solids* (Ed.: T. Bein), American Chemical Society, Washington DC, **1992**, pp. 256 – 273.

[45] J. A. Real, E. Andres, M. C. Munoz, M. Julve, T. Granier, A. Bousseksou, F. Varret, *Science* **1995**, *268*, 265 – 267.

[46] B. F. Hoskins, R. Robson, E. E. Sutherland, unpublished results.

[47] T. Soma, T. Iwamoto, *Chem. Lett.* **1995**, 271 – 272.

[48] T. Soma, T. Iwamoto, *Acta Crystallogr. Sect. C* **1996**, *52*, 1200 – 1203.

[49] a) T. Soma, T. Iwamoto, *Mol. Cryst. Liq. Cryst.* **1996**, *276*, 19 – 24; b) T. Soma, T. Iwamoto, *J. Inclusion Phenom. Mol. Recognit. Chem.* **1996**, *26*, 161 – 173.

[50] L. R. MacGillivray, S. Subramanian, M. J. Zaworotko, *J. Chem. Soc. Chem. Commun.* **1994**, 1325 – 1326.

[51] a) H. O. Stumpf, L. Ouahab, Y. Pei, D. Grandjean, O. Kahn, *Science* **1993**, *261*, 447 – 449; b) H. O. Stumpf, L. Ouahab, Y. Pei, P. Bergerat, O. Kahn, *J. Am. Chem. Soc.* **1994**, *116*, 3866 – 3874.

[52] D. Whang, K. Kim, *J. Am. Chem. Soc.* **1997**, *119*, 451 – 452.

[53] O. M. Yaghi, G. Li, *Angew. Chem.* **1995**, *107*, 232 – 234; *Angew. Chem. Int. Ed. Engl.* **1995**, *34*, 207 – 209.

[54] S. R. Batten, J. C. Jeffery, M. D. Ward, unpublished results.

[55] M. A. Brook, R. Faggiani, C. J. L. Lock, D. Seebach, *Acta Cryst. Sect. C* **1988**, *44*, 1981 – 1984.

[56] L. Carlucci, G. Ciani, D. M. Proserpio, A. Sironi, *Chem. Commun.* **1996**, 1393 – 1394.

[57] B. F. Abrahams, S. R. Batten, H. Hamit, B. F. Hoskins, R. Robson, *Chem. Commun.* **1996**, 1313 – 1314.

[58] a) K. Mereiter, J. Zemann, A. W. Hewat, *Am. Miner.* **1992**, *77*, 839 – 842; b) K. Mereiter, J. Zemann, *Tschermaks Miner. Petrogr. Mitt.* **1976**, *23*, 105 – 115.

[59] A. F. Wells, *Structural Inorganic Chemistry*, 5th ed., Oxford University Press, **1983**.

[60] Y. Grin, U. Wedig, H. G. von Schnering, *Angew. Chem.* **1995**, *107*, 1318 – 1320; *Angew. Chem. Int. Ed. Engl.* **1995**, *34*, 1204 – 1206, and references therein

[61] E. Cannillo, F. Mazzi, G. Rossi, *Acta Crystallogr.* **1966**, *21*, 200 – 208.

[62] L. Carlucci, G. Ciani, D. M. Proserpio, A. Sironi, *J. Am. Chem. Soc.* **1995**, *117*, 4562 – 4569.

[63] P. Fragnaud, M. Evain, E. Prouzet, R. Brec, *J. Solid State Chem.* **1993**, *102*, 390 – 399.

[64] a) F. Robinson, M. J. Zaworotko, *J. Chem. Soc. Chem. Commun.* **1995**, 2413 – 2414; b) O. M. Yaghi, H. Li, *J. Am. Chem. Soc.* **1996**, *118*, 295 – 296.

[65] a) G. B. Gardner, D. Venkataraman, J. S. Moore, S. Lee, *Nature* **1995**, *374*, 792 – 795; b) G. B. Gardner, Y.-H. Kiang, S. Lee, A. Asgaonkar, D. Venkataraman, *J. Am. Chem. Soc.* **1996**, *118*, 6946 – 6953.

[66] O. M. Yaghi, H. Li, *J. Am. Chem. Soc.* **1995**, *117*, 10401 – 10402.

[67] X. Cieren, J. Angenault, J.-C. Courtier, S. Jaulmes, M. Quarton, F. Robert, *J. Solid State Chem.* **1996**, *121*, 230 – 235.

[68] K. A. Hirsch, D. Venkataraman, S. R. Wilson, J. S. Moore, S. Lee, *J. Chem. Soc. Chem. Commun.* **1995**, 2199 – 2200. Moore et al. recently proposed a packing model for interpenetrating diamond-related structures: K. A. Hirsch, S. C. Wilson, J. S. Moore, *Chem. Eur. J.* **1997**, *3*, 765 – 771.

[69] O. Ermer, *J. Am. Chem. Soc.* **1988**, *110*, 3747 – 3754.

[70] O. Ermer, L. Lindenberg, *Helv. Chim. Acta* **1988**, *71*, 1084 – 1093.

[71] O. Ermer, L. Lindenberg, *Helv. Chim. Acta* **1991**, *74*, 825 – 877.

[72] X. Wang, M. Simard, J. D. Wuest, *J. Am. Chem. Soc.* **1994**, *116*, 12119 – 12120.

[73] D. Su, X. Wang, P. Deschatelets, L. Vaillancourt, M. Simard, J. D. Wuest, *Polymer Prepr.* **1995**, *36*, 554 – 555.
[74] M. Simard, D. Su, J. D. Wuest, *J. Am. Chem. Soc.* **1991**, *113*, 4696 – 4698.
[75] D. Su, X. Wang, M. Simard, J. D. Wuest, *Supramol. Chem.* **1995**, *6*, 171 – 178.
[76] H. S. Zhdanov, *C. R. Acad. Sci. URSS* **1941**, *31*, 352 – 354.
[77] a) T. Kitazawa, S. Nishikiori, R. Kuroda, T. Iwamoto, *Chem. Lett.* **1988**, 1729 – 1732; b) T. Kitazawa, S. Nishikiori, A. Yamagishi, R. Kuroda, T. Iwamoto, *J. Chem. Soc. Chem. Commun.* **1992**, 413 – 415; c) T. Iwamoto in *Chemistry of Microporous Crystals* (Eds.: T. Inui, S. Namba, T. Tatsumi), Kodansha-Elsevier, Tokyo, **1991**, pp. 3 – 10; d) T. Iwamoto in *Inclusion Compounds*, *Vol. 5* (Eds.: J. L. Atwood, J. E. D. Davies, D. D. MacNicol), Oxford University Press, Oxford, **1991**, p. 177; e) S. Nishikiori, C. I. Ratcliffe, J. A. Ripmeester, *Can. J. Chem.* **1990**, *68*, 2270 – 2273; f) T. Kitazawa, T. Kikuyama, M. Takeda, T. Iwamoto, *J. Chem. Soc. Dalton Trans.* **1995**, 3715 – 3720; g) E. Ruiz, S. Alvarez, *Inorg. Chem.* **1995**, *34*, 5845 – 5851.
[78] S. O. H. Gutschke, A. M. Z. Slawin, P. T. Wood, *J. Chem. Soc. Chem. Commun.* **1995**, 2197 – 2198.
[79] a) B. F. Abrahams, J. Coleiro, B. F. Hoskins, R. Robson, *Chem. Commun.* **1996**, 603 – 604; b) B. F. Abrahams, J. Coleiro, B. F. Hoskins, R. Robson, unpublished results.
[80] K. W. Kim, M. G. Kanatzidis, *J. Am. Chem. Soc.* **1992**, *114*, 4878 – 4883.
[81] a) D. B. Alward, D. J. Kinning, E. L. Thomas, L. J. Fetters, *Macromolecules* **1986**, *19*, 215 – 224; b) H. Hasegawa, H. Tanaka, K. Yamasaki, T. Hashimoto, *ibid.* **1987**, *20*, 1651 – 1662; c) D. M. Anderson, E. L. Thomas, *ibid.* **1988**, *21*, 3221 – 3230; d) E. L. Thomas, D. B. Alward, D. J. Kinning, D. C. Martin, D. L. Handlin, Jr., L. J. Fetters, *ibid.* **1986**, *19*, 2197 – 2202; e) E. L. Thomas, D. M. Anderson, C. S. Henkee, D. Hoffman, *Nature* **1988**, *334*, 598 – 601; f) Y. Mogi, K. Mori, Y. Matsushita, Y. Noda, *Macromolecules* **1992**, *25*, 5412 – 5415; g) Y. Mogi, H. Kotsuji, Y. Kaneko, K. Mori, Y. Matsushita, I. Noda, *ibid.* **1992**, *25*, 5408 – 5411; h) Y. Matsushita, M. Tamura, I. Noda, *ibid.* **1994**, *27*, 3680 – 3682.
[82] W. Longley, T. J. McIntosh, *Nature* **1983**, *303*, 612 – 614.
[83] a) O. Ermer, *Adv. Mater.* **1991**, *3*, 608 – 611; b) K. Sinzger, S. Hünig, M. Jopp, D. Bauer, W. Bietsch, J. U. von Schütz, H. C. Wulf, R. K. Kremer, T. Metzenthin, R. Bau, S. I. Khan, A. Lindbaum, C. L. Lengauer, E. Tillmanns, *J. Am. Chem. Soc.* **1993**, *115*, 7696 – 7705; c) A. Aumüller, P. Erk, G. Klebe, S. Hünig, J. U. von Schütz, H.-P. Werner, *Angew. Chem.* **1986**, *98*, 759 – 761; *Angew. Chem. Int. Ed. Engl.* **1986**, *25*, 740 – 741; d) R. Kato, H. Kobayashi, A. Kobayashi, T. Mori, H. Inokuchi, *Chem. Lett.* **1987**, 1579 – 1582; e) R. Kato, H. Kobayashi, A. Kobayashi, *J. Am. Chem. Soc.* **1989**, *111*, 5224 – 5232; f) A. Kobayashi, R. Kato, H. Kobayashi, T. Mori, H. Inokuchi, *Solid State Commun.* **1987**, *64*, 45 – 51; g) S. Hünig, A. Aumüller, P. Erk, H. Meixner, J. U. von Schütz, H.-J. Gross, U. Langohr, H.-P. Werner, H. C. Wolf, C. Burschka, G. Klebe, K. Peters, H. G. von Schnering, *Synth. Met.* **1988**, *27*, B181 – B188; h) R. Kato, H. Kobayashi, A. Kobayashi, T. Mori, H. Inokuchi, *ibid.* **1988**, *27*, B263 – B268; i) A. Kobayashi, T. Mori, H. Inokuchi, R. Kato, H. Kobayashi, *ibid.* **1988**, *27*, B275 – B280; j) A. Aumüller, P. Erk, S. Hünig, J.-U. von Schütz, H. P. Werner, H. C. Wolf, G. Klebe, *Mol. Cryst. Liq. Cryst.* **1988**, *156*, 215 – 221; see also k) S. Hünig, *J. Mater. Chem.* **1995**, *5*, 1469 – 1479; l) S. Hünig, P. Erk, *Adv. Mater.* **1991**, *3*, 225 – 236; m) S. Hünig, *Pure Appl. Chem.* **1990**, *62*, 395 – 406.
[84] P. Niggli, *Z. Kristallogr.* **1922**, *57*, 253.
[85] R. W. G. Wyckoff, *Crystal Structures*, *Vol. 1*, 2nd ed., Wiley, New York, **1963**.
[86] G. J. Kruger, E. C. Reynhardt, *Acta Crystallogr. Sect. B* **1978**, *34*, 259 – 261.
[87] O. Ermer, A. Eling, *Angew. Chem.* **1988**, *100*, 856; *Angew. Chem. Int. Ed. Engl.* **1988**, *27*, 829 – 833.
[88] a) J. Krogh-Moe, *Acta Crystallogr.* **1962**, *15*, 190 – 193; b) J. Krogh-Moe, *Acta Crystallogr. Sect. B* **1968**, *24*, 179 – 181; c) M. Natarajan, R. Faggiani, I. D. Brown, *Cryst. Struct. Commun.* **1979**, *8*, 367 – 370; d) H. Bartl, W. Schuckmann, *Neues Jahrb. Miner. Monatsh.* **1966**, 142 – 148; e) E. Ecker, Dissertation, Technische Hochschule Karlsruhe, **1966**; f) M. Martinez-Ripoll, S. Martinez-Carrera, S. Garcia-Blanco, *Acta Crystallogr. Sect. B* **1971**, *27*, 672 – 677; f) M. Ihara, J. Krogh-Moe, *Acta Crystallogr.* **1966**, *20*, 132 – 134; g) J. Krogh-Moe, *Acta Crystallogr. Sect. B* **1974**, *30*, 747 – 752; h) *Acta Crystallogr.* **1965**, *18*, 77 – 81; i) A. Hyman, A. Perloff, F. Mauer, S. Block, *ibid.* **1967**, *22*, 815 – 821; j) J. Krough-Moe, *Acta Crystallogr. Sect. B* **1969**, *25*, 2153 – 2154; k) *Acta Crystallogr.* **1965**, *18*, 1088 – 1089; l) *Acta Crystallogr. Sect. B* **1972**, *28*, 168 – 172; m) *Ark. Kemi* **1959**, *14*, 439 – 448; n) M. Touboul, *C.R. Acad. Sci. Ser. C* **1973**, *277*, 1025 – 1027; o) J. Krogh-Moe, M. Ihara, *Acta Crystallogr.* **1967**, *23*, 427 – 430; p) J. Krogh-Moe, *Ark. Kemi* **1959**, *14*, 451 – 459.
[89] a) B. Kamb, B. L. Davis, *Proc. Natl. Acad. Sci. USA* **1964**, *52*, 1433 – 1439; b) A. J. Brown, E. Whalley, *J. Chem. Phys.* **1966**, *45*, 4360 – 4361; c) E. Whalley, D. W. Davidson, J. B. R. Heath, *ibid.* **1966**, *45*, 3976 – 3982; d) C. Weir, S. Block, G. Piermarini, *J. Res. Natl. Bur. St. Ser. C* **1965**, *69*, 275; e) B. Kamb, *J. Chem. Phys.* **1965**, *43*, 3917 – 3924; f) J. D. Jorgensen, T. G. Worlton, *ibid.* **1985**, *83*, 329 – 333.
[90] J. B. Parise, Y. Ko, *Chem. Mater.* **1994**, *6*, 718 – 720.
[91] R. Riedel, A. Greiner, G. Miehe, W. Dressler, H. Fuess, J. Bill, F. Aldinger, *Angew. Chem.* **1997**, *109*, 657 – 660; *Angew. Chem. Int. Ed. Engl.* **1997**, *36*, 603 – 606.
[92] D. S. Reddy, D. C. Craig, A. D. Rae, G. R. Desiraju, *J. Chem. Soc. Chem. Commun.* **1993**, 1737 – 1739.
[93] a) S. B. Copp, S. Subramanian, M. J. Zaworotko, *J. Am. Chem. Soc.* **1992**, *114*, 8719 – 8720; b) *J. Chem. Soc. Chem. Commun.* **1993**, 1078 – 1079; c) M. J. Zaworotko, S. Subramanian, L. R. MacGillivray, *Mater. Res. Soc. Symp. Proc.* **1994**, *328*, 107 – 112; d) S. B. Copp, K. T. Holman, J. O. S. Sangster, S. Subramanian, M. J. Zaworotko, *J. Chem. Soc. Dalton Trans.* **1995**, 2233 – 2243.
[94] I. G. Dance in *Perspectives in Coordination Chemistry* (Eds.: A. F. Williams, C. Floriani, A. Merbach), Helvetica Chimica Acta, Basel, Schweiz, **1992**, pp. 165 – 181.
[95] T. Vossmeyer, G. Reck, L. Katsikas, E. T. K. Haupt, B. Schulz, H. Weller, *Science* **1995**, *267*, 1476 – 1479.
[96] B. F. Hoskins, J. Liu, R. Robson, unpublished results.
[97] a) S. Nishikiori, T. Iwamoto, Y. Yoshino, *Chem. Lett.* **1979**, 1509 – 1512; b) S. Nishikiori, T. Iwamoto, *J. Incl. Phenom.* **1985**, *3*, 283 – 295.
[98] F. Hiltmann, P. zum Hebel, A. Hammerschmidt, B. Krebs, *Z. Anorg. Allg. Chem.* **1993**, *619*, 293 – 302.
[99] O. Ermer, L. Lindenberg, *Chem. Ber.* **1990**, *123*, 1111 – 1118.
[100] B. F. Hoskins, A. Liang, R. Robson, unpublished results.
[101] D. T. Cromer, A. C. Larson, *Acta Crystallogr. Sect. B* **1972**, *28*, 1052 – 1058.
[102] A. Michaelides, V. Kiritsis, S. Skoulika, A. Aubry, *Angew. Chem.* **1993**, *105*, 1525 – 1526; *Angew. Chem. Int. Ed. Engl.* **1993**, *32*, 1495 – 1497. The three independent diamondlike nets in the original report appeared to interpenetrate in an unusual manner, but it became clear when we replotted the data that the interpenetration is normal.
[103] H. Yuge, S. Nishikiori, T. Iwamoto, *Acta Crystallogr. Sect. C* **1996**, *52*, 575 – 578.
[104] T. Kuroda-Sowa, M. Yamamoto, M. Munakata, M. Seto, M. Maekawa, *Chem. Lett.* **1996**, 349 – 350.
[105] M. Munakata, L. P. Wu, M. Yamamoto, T. Kuroda-Sowa, M. Maekawa, *J. Am. Chem. Soc.* **1996**, *118*, 3117 – 3124.
[106] O. M. Yaghi, D. A. Richardson, G. Li, C. E. Davis, T. L. Groy, *Mater. Res. Soc. Symp. Proc. (Adv. in Porous Materials)* **1993**, *371*, 15 – 19.
[107] L. Carlucci, G. Ciani, D. M. Proserpio, A. Sironi, *J. Chem. Soc. Chem. Commun.* **1994**, 2755 – 2756.
[108] A. J. Blake, N. R. Champness, S. S. M. Chung, W.-S. Li, M. Schroder, *Chem. Commun.* **1997**, 1005 – 1006.
[109] P.-R. Wei, B.-M. Wu, W.-P. Leung, T. C. W. Mak, *Polyhedron* **1996**, *15*, 4041 – 4046. The structure was originally reported as two interpenetrating nets, however reexamination of the structure by ourselves revealed it to contain six interpenetrating diamondlike nets.
[110] Y. Kinoshita, I. Matsubara, T. Higuchi, Y. Saito, *Bull. Chem. Soc. Jpn.* **1959**, *32*, 1221 – 1226.
[111] B. F. Hoskins, R. Robson, N. V. Y. Scarlett, *Angew. Chem.* **1995**, *107*, 1317 – 1318; *Angew. Chem. Int. Ed. Engl.* **1995**, *34*, 1203 – 1204.
[112] S. C. Abrahams, L. E. Zyontz, J. L. Bernstein, *J. Chem. Phys.* **1982**, *76*, 5458 – 5462.
[113] N. M. Stainton, K. D. M. Harris, R. A. Howie, *J. Chem. Soc. Chem. Commun.* **1991**, 1781 – 1784.
[114] B. F. Hoskins, N. V. Y. Scarlett, R. Robson, unpublished results.
[115] L. Shields, *J. Chem. Soc. Faraday Trans.* **1985**, *81*, 1 – 9.

[116] a) S. C. Hawkins, R. Bishop, I. G. Dance, T. Lipari, D. C. Craig, M. L. Scudder, *J. Chem. Soc. Perkin Trans. 2* **1993**, 1729; b) R. Bishop, I. G. Dance, S. C. Hawkins, *J. Chem. Soc. Chem. Commun.* **1983**, 889.
[117] H. Schäfer, H.-G. Schnering, K.-J. Niehues, H. G. Nieder-Vahrenholz, *J. Less-Common Met.* **1965**, *9*, 95 – 104.
[118] J. Zhang, J. D. Corbett, *Inorg. Chem.* **1991**, *30*, 431 – 435.
[119] F. Böttcher, A. Simon, R. K. Kremer, H. Buchkremer-Hermanns, J. K. Cockcroft, *Z. Anorg. Allg. Chem.* **1991**, *589 – 599*, 25 – 44.
[120] A. Simon, F. Böttcher, J. K. Cockcroft, *Angew. Chem.* **1991**, *103*, 79 – 80; *Angew. Chem. Int. Ed. Engl.* **1991**, *30*, 101 – 102.
[121] B. F. Abrahams, S. R. Batten, H. Hamit, B. F. Hoskins, R. Robson, *Angew. Chem.* **1996**, *108*, 1794 – 1795; *Angew. Chem. Int. Ed. Engl.* **1996**, *35*, 1690 – 1692.
[122] S. R. Batten, B. F. Hoskins, R. Robson, *J. Am. Chem. Soc.* **1995**, *117*, 5385 – 5386.
[123] B. Kamb, *Science* **1965**, *150*, 205 – 209.
[124] P. G. Desmartin, A. F. Williams, G. Bernardinelli, *New J. Chem.* **1995**, *19*, 1109 – 1112.
[125] P. C. M. Duncan, D. M. L. Goodgame, S. Menzer, D. J. Williams, *Chem. Commun.* **1996**, 2127 – 2128.
[126] a) D. E. Palin, H. M. Powell, *J. Chem. Soc.* **1947**, 208 – 221; b) H. M. Powell in *Non-Stoichiometric Compounds* (Ed.: L. Mandelcorn), Academic Press, New York, **1964**, chap. 7, p. 438; c) D. D. MacNicol in *Inclusion Compounds, Vol. 2* (Eds.: J. L. Atwood, J. E. D. Davies, D. D. MacNicol), Academic Press, London, **1984**, chap. 1, and references therein; d) T. C. W. Mak, J. S. Tse, C.-S. Tse, K.-S. Lee, Y.-H. Chong, *J. Chem. Soc. Perkin Trans. 2* **1976**, 1169 – 1172; e) J. C. A. Boeyens, J. A. Pretorius, *Acta Crystallogr. Sect. B* **1977**, *33*, 2120 – 2124; f) T. C. Mak, K.-A. Lee, *ibid.* **1978**, *34*, 3631 – 3634; g) H. M. Powell, *J. Chem. Soc.* **1950**, 300 – 301.
[127] a) L. Pauling, P. Pauling, *Proc. Natl. Acad. Sci. USA* **1968**, *60*, 362 – 367; see also b) A. Ludi, H. U. Gudel, *Helv. Chim. Acta* **1968**, *51*, 1762 – 1765; c) H. U. Gudel, A. Ludi, P. Fischer, *J. Chem. Phys.* **1972**, *56*, 674 – 675; d) H. U. Gudel, A. Ludi, P. Fischer, W. Halg, *ibid.* **1970**, *53*, 1917 – 1923; e) H. U. Gudel, A. Ludi, H. Burki, *Helv. Chim. Acta* **1968**, *51*, 1383 – 1389; f) A. Ludi, H. U. Gudel, V. Dvorak, *ibid.* **1967**, *50*, 2035 – 2039.
[128] A. D. Kirk, H. L. Schlafer, A. Ludi, *Can. J. Chem.* **1970**, *48*, 1065 – 1072.
[129] R. Haser, C. E. de Broin, M. Pierrot, *Acta Crystallogr. Sect. B* **1972**, *28*, 2530 – 2537.
[130] S. C. Abrahams, J. L. Bernstein, R. Liminga, *J. Chem. Phys.* **1980**, *73*, 4585 – 4590.
[131] B. F. Hoskins, R. Robson, D. A. Slizys, unpublished results.
[132] T. Soma, H. Yuge, T. Iwamoto, *Angew. Chem.* **1994**, *106*, 1746 – 1748; *Angew. Chem. Int. Ed. Engl.* **1994**, *33*, 1665 – 1666.
[133] Z. Assefa, R. J. Staples, J. P. Fackler Jr., *Acta Crystallogr. Sect. C* **1995**, *51*, 2527 – 2529.
[134] S. R. Batten, B. F. Hoskins, R. Robson, *J. Chem. Soc. Chem. Commun.* **1991**, 445 – 447. An earlier, incomplete investigation of the structure of $Cu(tcm)_2$ in which the interpenetration was not recognized was reported: C. Biondi, M. Bonamico, L. Torelli, A. Vaciago, *J. Chem. Soc. Chem. Commun.* **1965**, 191 – 192.
[135] A. W. Sleight, *Inorg. Chem.* **1968**, *7*, 1704 – 1708.
[136] L. Carlucci, G. Ciani, D. M. Proserpio, A. Sironi, *J. Am. Chem. Soc.* **1995**, *117*, 12861 – 12862.
[137] S. Nishikiori, T. Iwamoto, *J. Chem. Soc. Chem. Commun.* **1993**, 1555 – 1556.
[138] B. F. Hoskins, R. Robson, D. A. Slizys, *Angew. Chem.* **1997**, *109*, 2861 – 2863; *Angew. Chem. Int. Ed. Engl.* **1997**, *36*, 2752 – 2755.
[139] A. W. Sleight, R. J. Bouchard, *Inorg. Chem.* **1973**, *12*, 2314 – 2316.
[140] D. M. Proserpio, R. Hoffmann, P. Preuss, *J. Am. Chem. Soc.* **1994**, *116*, 9634 – 9637.
[141] J. Maddox, *Nature* **1988**, *335*, 201.
[142] Since submission of this review we have become aware of a number of other very recent structures which contain interpenetrating nets: a) $[Zn(H_2O)_4(bipy)](NO_3)_2 \cdot bipy$: two interpenetrating hydrogen-bonded α-polonium nets (L. Carlucci, G. Ciani, D. M. Proserpio, A. Sironi, *Chem. Commun.* **1997**, 1801 – 1803); b) $K_2[Cd(H_2O)\text{-}Cu_4(CN)_8] \cdot 1.5\,H_2O$: two interpenetrating, enantiomeric 3D nets with three- and four-connected nodes (S. Nishikiori, *J. Coord. Chem.* **1996**, *37*, 23 – 38); c) $[Cd(1,3\text{-bppn})_2\{Ag(CN)_2\}_2]$ (1,3-bppn = 1,3-bis(4-pyridyl)-propane): two interpenetrating 3D nets with a topology identical to that of the bipy analogue described in Section 4.4.1 (T. Soma, T. Iwamoto, *Acta Crystallogr. Sect. C* **1997**, *53*, 1819 – 1821); d) $[Ag(3,3'\text{-dcpa})_2]XF_6$ (X = P, As, Sb; 3,3′-dcpa = 3,3′-dicyanodiphenylacetylene): twofold parallel interpenetrating (4,4) sheets with a topology identical to that shown in Figure 18; $[Ag(3,3'\text{-dcpa})_2]ClO_4 \cdot H_2O$: eight interpenetrating diamondlike nets (K. A. Hirsch, S. R. Wilson, J. S. Moore, *Inorg. Chem.* **1997**, *36*, 2960 – 2968); e) $(NH_4)\{N(NO_2)_2\}$: two interpenetrating hydrogen-bonded 3D nets with three- and four-connected nodes (R. Gilardi, J. Flippen-Anderson, C. George, R. J. Butcher, *J. Am. Chem. Soc.* **1997**, *119*, 9411 – 9416); f) $MGa(CN)_4$ (M = Li, Cu) (L. C. Brousseau, D. Williams, J. Kouvetakis, M. O'Keeffe, *J. Am. Chem. Soc.* **1997**, *119*, 6292 – 6296) and $Li[Co(CO)_4]$ (P. Klufers, *Z. Kristallogr.* **1984**, *167*, 275 – 286); these compounds are amorphous with $Zn(CN)_2$ (which has recently been examined with neutron diffraction: D. J. Williams, D. E. Partin, F. J. Lincoln, J. Kouvetakis, M. O'Keeffe, *J. Solid State Chem.* **1997**, *134*, 164 – 169); g) $[Cu(dmtpn)_2](X)(dmtpn)(THF)$ (dmtpn = 2,5-dimethylterephthalonitrile; $X = BF_4^-$, ClO_4^-): three interpenetrating diamondlike nets (T. Kuroda-Sowa, T. Horino, M. Yamamoto, Y. Ohno, M. Maekawa, M. Munakata, *Inorg. Chem.* **1997**, *36*, 6382 – 6389); h) $(Me_3Sn)_3Rh(SCN)_6$: three interpenetrating α-polonium-related nets (E. Siebel, R. D. Fischer, *Chem. Eur. J.* **1997**, *3*, 1987 – 1991); i) $[Cu(3,3'\text{-bipy})_2](X)$ ($X = BF_4^-$, PF_6^-): doubly interpenetrating diamond-like nets (S. Lopez, M. Kahraman, M. Harmata, S. W. Keller, *Inorg. Chem.* **1997**, *36*, 6138 – 6140); j) $[(CH_3)_2NH_2]_6In_{10}S_{18}$: two interpenetrating diamond-like nets in which $[In_{10}S_{20}]^{10-}$ clusters act as the tetrahedral nodes (C. L. Cahill, Y. Ko, J. B. Parise, *Chem. Mater.* **1998**, *10*, 19 – 21); k) $[Ni_3(btc)_2(py)_6(eg)_6] \cdot x\,eg \cdot y\,H_2O$ (btc = benzene-1,3,5-tricarboxylate, py = pyridine, eg = ethylene glycol): four interpenetrating (10,3)-a nets of the same handedness (C. J. Kepert, M. J. Rosseinsky, *Chem. Commun.* **1998**, 31 – 32); l) $[Cu_2(MeCN)_2(L)_3](PF_6)_2$ (L = 1,4-bis(4-pyridyl)butadiyne): 1D ladderlike chains which interpenetrate in a side-by-side fashion (which is topologically different to the examples of 1D interpenetration described in Section 2) to give 2D sheets (A. J. Blake, N. R. Champness, A. Khlobystov, D. A. Lemenovskii, W.-S. Li, M. Schroder, *Chem. Commun.* **1997**, 2027 – 2028); each ladder is interpenetrated by four others; m) The remarkable structure of $[AgL_2]SbF_6$ (L = 3-cyanophenyl 4-cyanobenzoate) displays both 2D inclined and parallel interpenetration simultaneously: layers of 2D parallel twofold interpenetrating (4,4) sheets interpenetrate each other in an inclined fashion (K. A. Hirsch, S. R. Wilson, J. S. Moore, *Chem. Commun.* **1998**, 13 – 14). n) The 1:1 adduct of hexamethylenetetramine and 1,1,1-tris(4-hydroxyphenyl)ethane contains hydrogen-bonded (6,3) nets which show twofold 2D parallel interpenetration analogous to that of [Ag(tcm)]; however, the nets are cross-linked through C–H···O bonds (P. J. Coupar, G. Ferguson, C. Glidewell, P. R. Meehan, *Acta Crystallogr. Sect. C* **1997**, *53*, 1978 – 1980). When 1,1,3-tris(2-methyl-4-hydroxy-5-*tert*-butylphenyl)butane is used in place of 1,1,1-tris(4-hydroxyphenyl)ethane, the (6,3) sheets do not interpenetrate owing to the larger steric bulk (P. R. Meehan, R. M. Gregson, C. Glidewell, G. Ferguson, *Acta Crystallogr. Sect. C* **1997**, *53*, 1637 – 1640). o) $Fe(C_5H_4COC_6H_4OH)_2$: hydrogen-bonded (6,3) sheets displaying 2D inclined interpenetration analogous to that shown in Figure 32a (A. C. Benyei, C. Glidewell, P. Lightfoot, B. J. L. Royles, D. M. Smith, *J. Organomet. Chem.* **1997**, *539*, 177 – 186); p) Co(4,4′-dipyridyl sulfide)$_2$Cl$_2$: twofold 2D parallel interpenetrating (4,4) sheets of a motif unrelated to those discussed in the main text (O.-S. Jung, S. H. Park, D. C. Kim, K. M. Kim, *Inorg. Chem.* **1998**, *37*, 610 – 611); q) $[Ag_2Si(p\text{-}C_6H_5CN)_4](OTf)_2 \cdot 2\,C_6H_6$ (Tf = CF_3SO_2): four interpenetrating 3D nets with three- and four-connected nodes (related to the individual nets of $[Ag(tcm)(L)_{1/2}]$ (L = phenazine); see Section 3.1.1) which are cross-linked into a single, self-penetrating 3D net through close Ag – Ag interactions. $[Ag_3\{Si(p\text{-}C_6H_5CN)_4\}_2](PF_6)_3 \cdot 1.6\,THF \cdot 0.5\,C_6H_6 \cdot CH_2Cl_2$ contains 2D double layers displaying 2D parallel interpenetration. Each double layer is interpenetrated by four other double layers so that an overall 3D structure results, rather than the normal 2D structure. This is a result of average planes of the double layers being parallel but not coincident (F.-Q. Liu, T. D. Tilley, *Inorg. Chem.* **1997**, *36*, 5090 – 5096). r) While we have tried to make this review as comprehensive as possible, either of the authors would appreciate hearing about any other interpenetrating structures known.